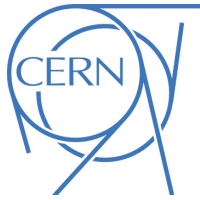


EUROPEAN ORGANISATION FOR NUCLEAR RESEARCH (CERN)



Phys. Rev. C. 100 (2019) 064901
 DOI: [10.1103/PhysRevC.100.064901](https://doi.org/10.1103/PhysRevC.100.064901)



CERN-EP-2019-158
 August 26, 2020

Measurement of angular and momentum distributions of charged particles within and around jets in Pb+Pb and pp collisions at $\sqrt{s_{\text{NN}}} = 5.02$ TeV with the ATLAS detector

The ATLAS Collaboration

Studies of the fragmentation of jets into charged particles in heavy-ion collisions can provide information about the mechanism of jet-quenching by the hot and dense QCD matter created in such collisions, the quark-gluon plasma. This paper presents a measurement of the angular distribution of charged particles around the jet axis in $\sqrt{s_{\text{NN}}} = 5.02$ TeV Pb+Pb and pp collisions, using the ATLAS detector at the LHC. The Pb+Pb and pp data sets have integrated luminosities of 0.49 nb^{-1} and 25 pb^{-1} , respectively. The measurement is performed for jets reconstructed with the anti- k_t algorithm with radius parameter $R = 0.4$ and is extended to an angular distance of $r = 0.8$ from the jet axis. Results are presented as a function of Pb+Pb collision centrality and distance from the jet axis for charged particles with transverse momenta in the 1–63 GeV range, matched to jets with transverse momenta in the 126–316 GeV range and an absolute value of jet rapidity of less than 1.7. Modifications to the measured distributions are quantified by taking a ratio to the measurements in pp collisions. Yields of charged particles with transverse momenta below 4 GeV are observed to be increasingly enhanced as a function of angular distance from the jet axis, reaching a maximum at $r = 0.6$. Charged particles with transverse momenta above 4 GeV have an enhanced yield in Pb+Pb collisions in the jet core for angular distances up to $r = 0.05$ from the jet axis, with a suppression at larger distances.

© 2020 CERN for the benefit of the ATLAS Collaboration.

Reproduction of this article or parts of it is allowed as specified in the CC-BY-4.0 license.

1 Introduction

Ultra-relativistic nuclear collisions at the Large Hadron Collider (LHC) produce hot, dense matter called a quark–gluon plasma, QGP (see Refs. [1, 2] for recent reviews). Jets from hard-scattering processes in these collisions traverse and interact with the QGP, losing energy via a process called jet-quenching. The rates and characteristics of these jets in heavy-ion collisions can be compared with the same quantities in pp collisions, where the production of a QGP is not expected. This comparison can provide information about the properties of the QGP and how it interacts with partons from the hard scatter.

Jets with large transverse momenta, p_T^{jet} , in central lead–lead (Pb+Pb) collisions at the LHC are measured at approximately half the rates in pp collisions when the nuclear overlap function of Pb+Pb collisions is taken into account [3–7]. Similarly, back-to-back dijet [8–10] and photon–jet pairs [11, 12] are observed to have less-balanced transverse momenta in Pb+Pb collisions compared to pp collisions. These observations suggest that some of the energy from the hard-scattered parton may be transferred outside of the jet through its interaction with the QGP medium.

Complementary measurements look at how the structure of jets in Pb+Pb collisions is modified relative to that in pp collisions. Previous measurements have shown a broadening of jets in Pb+Pb [13–16], as well as an excess of low- and high-momentum charged-particles and a depletion of intermediate-momentum charged-particles associated with these jets [17–20]. Particles carrying a large fraction of the jet momentum are generally closely aligned with the jet axis, whereas low-momentum particles are observed to have a much broader angular distribution extending outside the jet [9, 21–24]. These observations suggest that the energy lost via jet-quenching is being transferred to soft particles around the jet axis via soft gluon emission [25–31]. Measurements of yields of these particles as a function of transverse momentum, p_T , and angular distance between the particle and the jet axis have the potential to provide further insight into the structure of jets in the QGP, as well as provide information about how the medium is affected by the presence of the jet.

This paper presents charged-particle p_T distributions at a distance r around the jet axis¹ that have been corrected for detector effects. The measured yields are defined as:

$$D(p_T, r) = \frac{1}{N_{\text{jet}}} \frac{1}{2\pi r dr} \frac{dn_{\text{ch}}(p_T, r)}{dp_T},$$

where N_{jet} is the number of jets in consideration and $n_{\text{ch}}(p_T, r)$ is the number of charged particles with a given p_T at a distance r from the jet axis. The ratios of the charged-particle yields measured in Pb+Pb and pp collisions,

$$R_{D(p_T, r)} = \frac{D(p_T, r)_{\text{Pb+Pb}}}{D(p_T, r)_{pp}},$$

¹ ATLAS uses a right-handed coordinate system with its origin at the nominal interaction point (IP) in the center of the detector, and the z -axis along the beam pipe. The x -axis points from the IP to the center of the LHC ring, and the y -axis points upward. Cylindrical coordinates (r, ϕ) are used in the transverse plane, ϕ being the azimuthal angle around the z -axis. The pseudorapidity is defined in terms of the polar angle θ as $\eta = -\ln \tan(\theta/2)$. The rapidity is defined as $y = 0.5 \ln[(E + p_z)/(E - p_z)]$ where E and p_z are the energy and z -component of the momentum along the beam direction respectively. Transverse momentum and transverse energy are defined as $p_T = p \sin \theta$ and $E_T = E \sin \theta$, respectively. The angular distance between two objects, r , with relative differences $\Delta\eta$ and $\Delta\phi$ in pseudorapidity and azimuth, respectively, is given by $\sqrt{(\Delta\eta)^2 + (\Delta\phi)^2}$.

quantify the modifications of the yields due to the QGP medium. Furthermore, the differences between the $D(p_T, r)$ distributions in Pb+Pb and pp collisions,

$$\Delta D(p_T, r) = D(p_T, r)_{\text{Pb+Pb}} - D(p_T, r)_{pp},$$

allow the absolute differences in charged-particle yields between the two collision systems to be measured.

2 ATLAS detector

The measurements presented here are performed using the ATLAS [32] calorimeter, inner detector, trigger, and data acquisition systems.

The calorimeter system consists of a sampling liquid-argon (LAr) electromagnetic (EM) calorimeter covering $|\eta| < 3.2$, a steel–scintillator sampling hadronic calorimeter covering $|\eta| < 1.7$, LAr hadronic calorimeters covering $1.5 < |\eta| < 3.2$, and two LAr forward calorimeters (FCal) covering $3.1 < |\eta| < 4.9$.

The EM calorimeters are segmented longitudinally in shower depth into three layers with an additional presampler layer. They have segmentation that varies with layer and pseudorapidity. The hadronic calorimeters have three sampling layers longitudinal in shower depth.

The inner detector measures charged particles within the pseudorapidity interval $|\eta| < 2.5$ using a combination of silicon pixel detectors, silicon microstrip detectors (SCT), and a straw-tube transition radiation tracker (TRT), all immersed in a 2 T axial magnetic field. Each of the three detectors is composed of a barrel and two symmetric endcap sections. The pixel detector is composed of four layers, including the insertable B-layer [33, 34] added in 2014. The SCT barrel section contains four layers of modules with sensors on both sides, and each endcap consists of nine layers of double-sided modules with radial strips. The TRT contains layers of staggered straws interleaved with the transition radiation material.

The zero-degree calorimeters (ZDCs) are located symmetrically at $z = \pm 140$ m and cover $|\eta| > 8.3$. The ZDCs use tungsten plates as absorbers, and quartz rods sandwiched between the tungsten plates as the active medium. In Pb+Pb collisions the ZDCs primarily measure ‘spectator’ neutrons. These are neutrons that do not interact hadronically when the incident nuclei collide. A ZDC coincidence trigger is implemented by requiring the pulse height from both ZDCs to be above a threshold that accepts the signal corresponding to the energy deposition from a single neutron.

This analysis uses the same trigger setup used in Ref. [20] and is briefly described below. A two-level trigger system was used to select the Pb+Pb and pp collisions. The first level, L1, is based on custom electronics, while the second level, the high-level trigger (HLT), is based on software [35]. Minimum-bias (MB) events were recorded using a logical OR of two triggers: 1) a total-energy L1 trigger selecting more-central collisions; 2) a ZDC coincidence trigger at L1 and a veto on the total-energy trigger, with the additional requirement of at least one track in the HLT, selecting peripheral collisions. The total-energy trigger required the total transverse energy measured in the calorimeter system to be greater than 50 GeV. Jet events were selected by the HLT, seeded by a jet identified by the L1 jet trigger in pp collisions or by the total-energy trigger with a threshold of 50 GeV in Pb+Pb collisions. The L1 jet trigger utilized in pp collisions required a jet with transverse momentum greater than 20 GeV. The HLT jet trigger uses a jet reconstruction procedure similar to that in the offline analysis as discussed in Section 4. It selected events containing jets with a transverse energy of at least 75 GeV in Pb+Pb collisions and at least 85 GeV

in pp collisions. The measurement is performed in the jet transverse momentum range where the trigger efficiencies are greater than 99%.

3 Data sets and event selection

The Pb+Pb and pp data used in this analysis were recorded in 2015. The data samples consist of 25 pb^{-1} of $\sqrt{s} = 5.02 \text{ TeV}$ pp and 0.49 nb^{-1} of $\sqrt{s_{\text{NN}}} = 5.02 \text{ TeV}$ Pb+Pb data. In both samples, events are required to have a reconstructed vertex within 150 mm of the nominal IP along the beam axis. Events with multiple interactions in the same bunch crossing are referred to as pileup. This is negligible in the Pb+Pb data, and the pp data was collected in low-pileup mode. The average number of interactions per bunch crossing in the pp collisions ranged from 0.6 to 1.3. Only events taken during stable beam conditions and satisfying detector and data-quality requirements that include the detector subsystems being in normal operating condition are considered.

In Pb+Pb collisions, the event centrality reflects the overlap area of the two colliding nuclei and is characterized by $\Sigma E_{\text{T}}^{\text{FCal}}$, the total transverse energy deposited in the FCal [36]. The six centrality intervals used in this analysis are defined according to successive percentiles of the $\Sigma E_{\text{T}}^{\text{FCal}}$ distribution obtained in MB collisions, ordered from the most-central (highest $\Sigma E_{\text{T}}^{\text{FCal}}$) to the most-peripheral (lowest $\Sigma E_{\text{T}}^{\text{FCal}}$) collisions: 0–10%, 10–20%, 20–30%, 30–40%, 40–60%, 60–80%.

The pp Monte Carlo (MC) sample consists of 1.8×10^7 5.02 TeV hard-scattering dijet pp events generated with PowHEG+PYTHIA8 [37–41] using the A14 tune of parameter values [42] and the NNPDF23LO PDF set [43]. The Pb+Pb MC sample was generated by overlaying an additional sample of MB Pb+Pb data events onto a separate set of 1.8×10^7 5.02 TeV hard-scattering dijet pp events generated with the same tune and PDFs as the pp MC sample. This ‘MC overlay’ sample was reweighted on an event-by-event basis such that it has the same centrality distribution as the jet-triggered data sample. Another sample of MB Pb+Pb events was generated using HIJING (version 1.38b) [44] and was only used to evaluate the track reconstruction performance. The detector response in all MC samples was simulated using GEANT4 [45, 46]. These MC samples are used to evaluate the performance of the detector and analysis procedure and correct the measured distributions for detector effects.

4 Jet and track selection

The jet reconstruction procedure is identical to that used in Ref. [7]. The anti- k_t algorithm [47, 48] is first run in four-momentum recombination mode on $\Delta\eta \times \Delta\phi = 0.1 \times 0.1$ calorimeter towers with two anti- k_t radius parameter values ($R = 0.2$ and $R = 0.4$). The energies in the towers are obtained by summing the energies of calorimeter cells at the electromagnetic energy scale. Then, an iterative procedure is used to estimate the η -dependent underlying event (UE) transverse energy density, while excluding the regions populated by jets. The estimate of the UE contribution is performed on an event-by-event basis. Furthermore, the background in Pb+Pb collisions is modulated to account for the azimuthal anisotropy in particle production [49]. The modulation includes the contributions of the second-, third-, and fourth-order azimuthal anisotropy harmonics. The UE transverse energy is subtracted from calorimeter towers included in the jet and the four-momentum of the jet is updated accordingly. Then, a jet η - and p_{T} -dependent correction factor to the $p_{\text{T}}^{\text{jet}}$ derived from the pp MC sample is applied to correct for the calorimeter energy response [50]. The same calibration factors are applied in both the pp and Pb+Pb collisions. An additional

correction based on *in situ* studies of jets recoiling against photons, Z bosons, and jets in other regions of the calorimeter is applied [51]. The same jet reconstruction procedure without the azimuthal modulation of the UE is also applied to pp collisions. The UE subtraction in pp collisions removes the pileup contribution to the jet. In this analysis, jets are required to have p_T^{jet} in the 126–316 GeV range, with rapidity $|\eta^{\text{jet}}| < 1.7$. The p_T^{jet} requirement is chosen in order to exclude the contribution of ‘UE jets’ generated by fluctuations in the UE, while the rapidity requirement is based on the acceptance of the tracking system. To prevent nearby jets from distorting the measurement of $D(p_T, r)$ distributions, jets are rejected if there is a neighboring jet with higher p_T^{jet} within an angular distance of $\Delta R = 1.0$. This isolation requirement removes approximately 0.01% of jets. Additionally, generator-level jets are reconstructed by applying the anti- k_t algorithm with radius parameter $R = 0.4$ to stable final-state particles from MC generators. These particles are required to have a lifetime of $\tau > 0.3 \times 10^{-10}$ s and do not include muons, neutrinos, and particles from pileup activity.

Charged-particle tracks in Pb+Pb collisions are reconstructed from hits in the inner detector using the track reconstruction algorithm that was optimized for the high hit density in heavy-ion collisions [52]. Tracks used in this analysis have $|\eta| < 2.5$ and are required to have at least 9 (11) total hits in the silicon detectors for charged particles with pseudorapidity $|\eta^{\text{ch}}| \leq 1.65$ ($|\eta^{\text{ch}}| > 1.65$). At least one hit is required in one of the two innermost pixel layers. If the track trajectory passes through an active module in the innermost layer, then a hit in this layer is required. Additionally, a track must have no more than two holes in the pixel and SCT detectors together, where a hole is defined by the absence of a hit predicted by the track trajectory. All charged-particle tracks used in this analysis are required to have reconstructed transverse momentum $p_T^{\text{ch}} > 1.0$ GeV. In order to suppress the contribution from secondary particles,² the distance of closest approach of the track to the primary vertex is required to be less than a value that varies from 0.45 mm at $p_T^{\text{ch}} = 4$ GeV to 0.2 mm at $p_T^{\text{ch}} = 20$ GeV in the transverse plane and less than 1.0 mm in the longitudinal direction. The primary vertex is determined using vertex finding and fitting algorithms described in Ref. [53]. The precision is better than $20\mu\text{m}$ in the transverse plane in peripheral collisions and improves inversely proportional to the square root of the number of reconstructed primary tracks in central collisions.

The efficiency, ε , for reconstructing charged particles in Pb+Pb and pp collisions is determined using the MC samples described above. It is evaluated as a function of the generator-level primary particle transverse momentum, p_T^{truth} , and pseudorapidity, η^{truth} , by matching tracks to generator-level primary particles [46]. In both collision systems the efficiency increases slowly with p_T^{truth} and is seen to be independent of p_T^{jet} in the measurement’s phase space. For Pb+Pb collisions, the efficiency for $|\eta| < 0.3$ is $\sim 80\%$ at 1 GeV and rises to $\sim 85\%$ at 10 GeV. For $1.0 < |\eta| < 2.0$, the efficiency is $\sim 67\%$ to $\sim 72\%$ over the same p_T range, with the variation in efficiency between the most-central and most-peripheral Pb+Pb collisions being approximately 3% in both η ranges. For pp collisions, the efficiency for $|\eta| < 0.3$ is $\sim 85\%$ at 1 GeV, and rises to $\sim 88\%$ at 10 GeV, remaining relatively constant thereafter. For $1.0 < |\eta| < 2.0$, the efficiency is $\sim 82\%$ to $\sim 86\%$ over the same p_T range. Further details about the tracking efficiency can be found in Ref. [19].

The contribution of reconstructed tracks that cannot be matched to a generated primary particle in the pp MC samples is less than 2% in the entire p_T^{ch} range under study in both the pp and Pb+Pb collisions. This contribution includes fakes and secondaries, where fakes originate from randomly matched hits in the

² Primary particles are defined as particles with a mean lifetime $\tau > 0.3 \times 10^{-10}$ s either directly produced in pp interactions or from subsequent decays of particles with a shorter lifetime. All other particles are considered to be secondary.

detector layers that do not correspond to the passage of charged particles. Both of these contributions are corrected for as described in the next section.

5 Analysis procedure

The analysis procedure is similar to that in Ref. [20], except it is also performed differentially in r . Measured tracks are considered to be associated with a reconstructed jet if their angular distance from the jet axis is less than 0.8. Their multiplicity distribution is given by:

$$\frac{d^2 n_{\text{ch}}^{\text{meas}}(p_T^{\text{ch}}, r)}{dp_T^{\text{ch}} dr} = \frac{1}{\varepsilon(p_T^{\text{ch}}, \eta^{\text{ch}})} \frac{\Delta n_{\text{ch}}(p_T^{\text{ch}}, r)}{\Delta p_T^{\text{ch}} \Delta r}$$

where $\Delta n_{\text{ch}}(p_T^{\text{ch}}, r)$ represents the number of tracks within a given Δp_T^{ch} and Δr range. The efficiency correction is applied as a $1/\varepsilon(p_T^{\text{ch}}, \eta^{\text{ch}})$ weight on a track-by-track basis, assuming $p_T^{\text{ch}} = p_T^{\text{truth}}$. While that assumption is not strictly valid, the efficiency varies sufficiently slowly with p_T^{truth} that the error introduced by this assumption is less than 1%, and is further corrected for by the Bayesian unfolding procedure described later in this section.

The measured track yields need to be corrected for the contributions from the UE, fake tracks, and secondary particles. In pp collisions, the UE contribution from hard scatterings not associated with jet production is negligible. The contributions from fake tracks and secondary charged particles are estimated from MC samples and subtracted. This procedure is similar to that applied in previous measurements [20, 54].

For Pb+Pb collisions, contributions from the UE, fake tracks, and secondary particles are estimated together in a two-step process: first, the MC overlay sample is used to generate η^{jet} vs. ϕ^{jet} maps of the average number of charged particles in a given annulus around a reconstructed jet. This is done for charged particles without an associated generated primary particle and as a function of p_T^{jet} , η^{jet} , ϕ^{jet} , $\Delta\Psi_{\text{jet}}$, r , p_T^{ch} , and centrality. Here $\Delta\Psi_{\text{jet}}$ is the azimuthal angle between the jet and the second-order event plane Ψ_2 and is given by $\Delta\Psi_{\text{jet}} = \phi^{\text{jet}} - \Psi_2$.³ In the second step, the η^{jet} vs. ϕ^{jet} maps are used to construct the UE distribution in the data as a function of p_T^{jet} , η^{jet} , ϕ^{jet} , $\Delta\Psi_{\text{jet}}$, and centrality. This distribution includes fakes and tracks from secondary particles, and is given by $d^2 n_{\text{ch}}^{\text{UE+Fake}}(p_T^{\text{ch}}, r)/dp_T^{\text{ch}} dr$. The yields decrease with decreasing collision centrality, increasing p_T^{ch} , and increasing $\Delta\Psi_2$. The subtracted distributions are then given by:

$$\frac{d^2 n_{\text{ch}}^{\text{sub}}(p_T^{\text{ch}}, r)}{dp_T^{\text{ch}} dr} = \frac{d^2 n_{\text{ch}}^{\text{meas}}(p_T^{\text{ch}}, r)}{dp_T^{\text{ch}} dr} - \frac{d^2 n_{\text{ch}}^{\text{UE+Fake}}(p_T^{\text{ch}}, r)}{dp_T^{\text{ch}} dr}.$$

Figure 1 shows the ratio of the charged-particle distributions before and after the subtraction of the UE, fake tracks, and secondaries, as a function of r for different p_T^{ch} intervals and $126 < p_T^{\text{jet}} < 158$ GeV for six centrality selections. The largest UE contribution is for 1.0 GeV charged particles at large values of r in

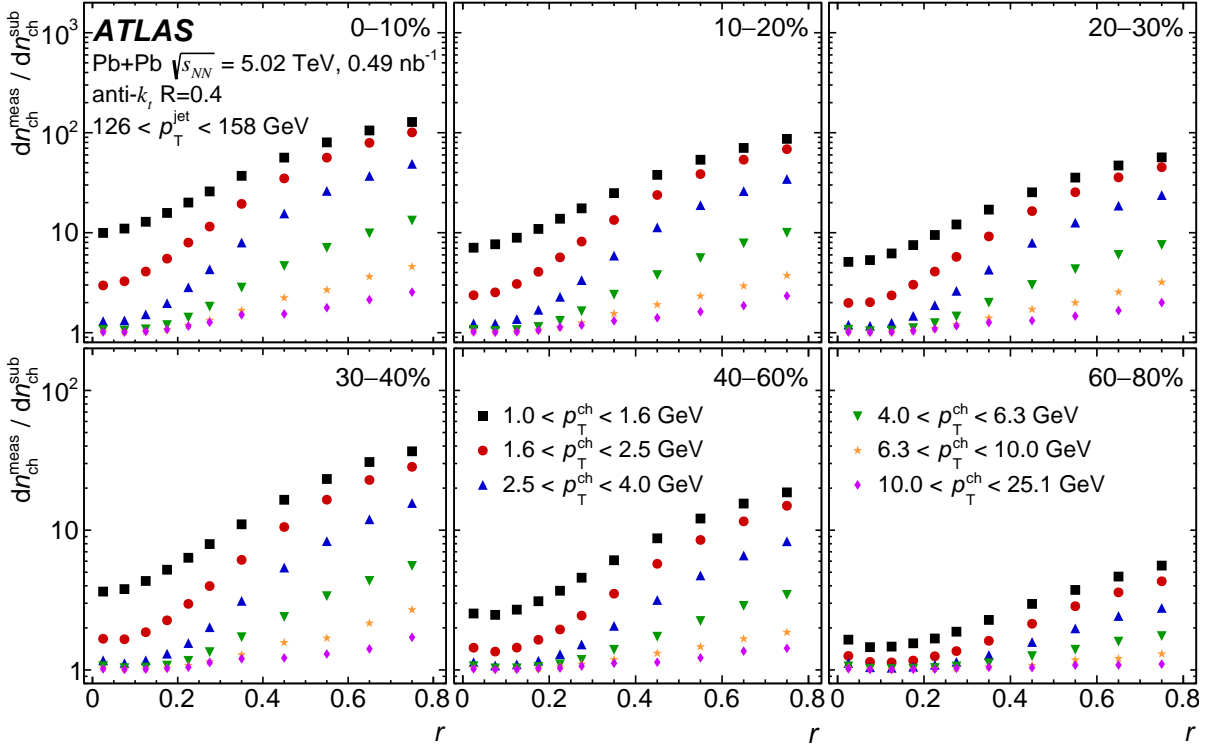


Figure 1: Ratio of the measured charged-particle distributions to those after the subtraction of the UE, fake tracks, and secondaries as a function of r for different p_T^{ch} intervals for p_T^{jet} in the range 126–158 GeV. The different panels represent the six centrality selections.

central collisions, with the background-to-signal ratio being approximately 100 and slowly decreasing with increasing p_T^{jet} . It rapidly decreases for more-peripheral collisions, larger p_T^{ch} , and smaller r .

To remove the effects of bin migration due to the jet energy and track momentum resolution, the subtracted $d^2n_{\text{ch}}^{\text{sub}}/dp_T^{\text{ch}} dr$ distributions are corrected by a two-dimensional Bayesian unfolding [55] in p_T^{ch} and p_T^{jet} as implemented in the RooUnfold package [56]. Two-dimensional unfolding is used because the calorimetric jet energy response depends on the fragmentation pattern of the jet [57]. Four-dimensional response matrices are created from the pp and Pb+Pb MC samples using the generator-level and reconstructed p_T^{jet} and the generator-level and reconstructed charged-particle p_T^{ch} . They are corrected for tracking efficiencies and are evaluated in bins of r and centrality. The Bayesian procedure requires a choice in the number of iterations. Additional iterations reduce the sensitivity to the choice of prior, but may amplify statistical fluctuations in the distributions. After four iterations the charged-particle distributions are found to be stable within 2–4% for both the Pb+Pb and pp data. A separate one-dimensional Bayesian unfolding is used to correct the measured p_T^{jet} spectra that are used to normalize the unfolded charged-particle distributions. The response matrices for both the one- and two-dimensional unfolding are reweighted such that the $D(p_T, r)$ and p_T^{jet} distributions match the shapes of the corresponding quantities in the reconstructed data.

An independent bin-by-bin unfolding procedure is used to correct for migrations originating from the jet and track angular resolutions. Two corresponding $D(p_T, r)$ distributions are evaluated in MC samples, one

³ The second-order event plane angle Ψ_2 is determined on an event-by-event basis by a standard method using the ϕ variation of transverse energy in the FCal [49].

using generator-level jets and primary particles, and the other using reconstructed jets and charged particles with their reconstructed p_T replaced by generator-level transverse momentum, p_T^{truth} . The ratio of these two MC distributions provides a correction factor which is then applied to the data. These factors are at the level of approximately 5% with variations up to 15% for particles with $p_T > 4 \text{ GeV}$, particularly near the edge of the jet. For 126–158 GeV jets in Pb+Pb collisions, the full unfolding correction is 8–14% (4–7%) for 1 GeV (6 GeV) tracks, depending on centrality.

The final particle-level corrected distributions, normalized by the area of the annulus being studied, are defined as:

$$D(p_T, r) = \frac{1}{N_{\text{jet}}^{\text{unfolded}}} \frac{1}{2\pi r dr} \frac{dn_{\text{ch}}^{\text{unfolded}}(p_T^{\text{ch}}, r)}{dp_T},$$

where $N_{\text{jet}}^{\text{unfolded}}$ is the unfolded number of jets in a given p_T^{jet} interval, and $n_{\text{ch}}^{\text{unfolded}}$ is the unfolded yield of charged particles with a given p_T matched to a jet with given p_T^{jet} , at a distance r .

The performance of the full analysis procedure is validated in the MC samples by comparing the fully corrected charged-particle distributions to the generator-level distributions. Good recovery of the generator-level distributions (closure) is observed, with a variation of less than 4% for charged particles with $p_T < 10 \text{ GeV}$ in both the pp and Pb+Pb collision systems. The non-closure is taken as an additional systematic uncertainty as discussed in Section 6. One important effect is that adding or removing particles carrying a large fraction of the jet momentum near the edge of the jet can significantly alter its reconstructed momentum and direction; this instability contributes to the non-closure mentioned above for particles with $p_T > 10 \text{ GeV}$ in jets with $p_T^{\text{jet}} < 200 \text{ GeV}$. Results are presented only where the non-closure in the pp MC sample is less than 5%.

6 Systematic uncertainties

The following sources of systematic uncertainty are considered: the jet energy scale (JES), the jet energy resolution (JER), the sensitivity of the unfolding to the prior, the UE contribution, the residual non-closure of the analysis procedure, and tracking-related uncertainties. For each variation accounting for a source of systematic uncertainty, the $D(p_T, r)$ distributions along with their ratios and differences are re-evaluated. The difference between the varied and nominal distributions is used as an estimate of the uncertainty.

The systematic uncertainty associated with the JES in Pb+Pb collisions is due to jets having a different structure and possibly a different detector response that is not modeled by the MC simulation. It is composed of two parts: a centrality-independent baseline component and a centrality-dependent component. Only the centrality-independent baseline component is used in pp collisions; it is determined from *in situ* studies of the calorimeter response [50, 57, 58] and the relative energy scale difference between the jet reconstruction procedures in heavy-ion [58] and pp collisions [50]. The centrality-dependent uncertainty reflects a modification of parton showers by the Pb+Pb environment. It is evaluated by comparing the ratio of the transverse momentum of calorimeter jets to the vectorial sum of the transverse momentum of charged particles within these jet in data and MC events. More details on this procedure can be found in Ref. [7]. The size of the centrality-dependent uncertainty in the JES reaches 0.5% in the most-central collisions. Each component that contributes to the JES uncertainty is varied separately by ± 1 standard

deviation for each interval in p_T^{jet} , and the response matrix is recomputed accordingly. The data are then unfolded with the modified matrices. The resulting uncertainty from the JES increases with increasing charged-particle p_T at fixed p_T^{jet} and decreases with increasing p_T^{jet} , and is at the level of 2–4%.

The uncertainty in the $D(p_T, r)$ distributions due to the JER is evaluated by repeating the unfolding procedure with modified response matrices, where an additional contribution is added to the resolution of the reconstructed p_T^{jet} using a Gaussian smearing procedure. The smearing factor is evaluated using an *in situ* technique in 13 TeV pp data that involves studies of dijet energy balance [59, 60]. An additional uncertainty is included to account for differences between the tower-based heavy-ion jet reconstruction and that used in analyses of 13 TeV pp data [50, 58]. The resulting uncertainty from the JER is symmetrized to account for negative variations of the JER. The size of the resulting uncertainty in the $D(p_T, r)$ distributions due to the JER typically reaches 4–5% for the highest charged-particle p_T intervals and decreases to 2–3% with decreasing charged-particle p_T at fixed p_T^{jet} .

The uncertainties related to track reconstruction and selection originate from several sources. Uncertainties related to the detector material description in simulation and the track transverse momentum resolution are obtained from studies in data and simulation described in Ref. [61]. The sensitivity of the tracking efficiency to the description of the inactive material in the MC samples is evaluated by varying the material description. This resulting uncertainty in the track reconstruction efficiency is between 0.5% and 2% in the track p_T range used in the analysis. The systematic uncertainty associated with the rate of fakes and secondary tracks is 30% in both collision systems [61]. The contamination of the $n_{\text{ch}}^{\text{sub}}$ from fakes and secondary tracks is approximately 20% in the jet core for tracks with $1 < p_T < 1.6$ GeV. It rapidly decreases as a function of p_T and r and is less than 2% at larger distances from the jet axis. The resulting uncertainty in the $D(p_T, r)$ distributions is at most $\sim 7\%$ in the jet core and decreases as a function of p_T and r . An additional uncertainty takes into account a possible residual misalignment of the tracking detectors in pp and Pb+Pb data-taking. The resulting uncertainties in the $D(p_T, r)$ distributions are typically less than 0.1%. An additional uncertainty in the tracking efficiency due to the high local track density in the core of jets is 0.4% [62] for all p_T^{jet} ranges in this analysis. The uncertainty due to the track selection is evaluated by repeating the analysis with an additional 3σ requirement on the significance of the distance of closest approach of the track to the primary vertex. This uncertainty affects the track reconstruction efficiencies, track momentum resolution, and rate of fake tracks. The resulting uncertainty typically varies between 1% and 2%. Finally, the track-to-particle matching requirements are varied. This variation affects the track reconstruction efficiency, track momentum resolution, and rate of fake tracks. The resulting systematic uncertainty is $\leq 0.1\%$ for the $D(p_T, r)$ distributions. All track-related systematic uncertainties are added in quadrature and presented as the total tracking uncertainty.

The systematic uncertainty associated with the UE subtraction has two components: the limited number of charged particles associated with a jet without a corresponding generator particle in the Pb+Pb MC overlay sample, and a comparison with the result of an alternative UE estimation using the cone method. The cone method uses jet-triggered events to estimate the background and is adapted from Refs. [19, 20]. A regular grid of nine cones of size $\Delta R = 0.8$ is used to cover the inner-detector region. Cones are excluded if the angular distance to any reconstructed jet in the event with $p_T^{\text{jet}} > 90$ GeV is less than 1.6 or if they contain a charged particle with $p_T > 10$ GeV. This exclusion reduces biases from any hard processes. The resulting UE charged-particle yields $dn_{\text{ch}}^{\text{UE,Cone}}/dp_T^{\text{ch}}$ are evaluated over the 1–10 GeV range as a function of p_T^{ch} , p_T^{jet} , centrality, and r , and are subsequently averaged over all cones. Both of these sources of uncertainty are combined as uncorrelated uncertainties. The combined UE uncertainty in the $D(p_T, r)$ distributions is less than 10% for $r < 0.4$ and reaches a maximum of 40% at the largest angular distances from the jet axis. It is the dominant source of systematic uncertainty for low- p_T charged particles at large r and decreases sharply

with increasing charged-particle p_T . In particular, the component from the limited sample size dominates in the most-central collisions, while the component from the alternative estimation method dominates elsewhere.

The systematic uncertainty in the unfolding procedure is estimated by generating response matrices from the MC distributions without the reweighting that matched the shapes of the charged-particle and jet distributions in data. The 5–7% difference between the nominal $D(p_T, r)$ distribution and that unfolded with the un-reweighted response matrix is taken as the systematic uncertainty.

An additional uncertainty to account for possible residual limitations in the analysis procedure is assigned by evaluating the non-closure of the unfolded distributions in simulations. This is typically about 4%.

The correlations between the various systematic components are considered in evaluating the $R_{D(p_T, r)}$ and $\Delta D(p_T, r)$ distributions. The unfolding and non-closure uncertainties are taken to be uncorrelated between pp and Pb+Pb collisions, while all others are taken to be correlated. For these, the $R_{D(p_T, r)}$ and $\Delta D(p_T, r)$ distributions are re-evaluated by applying the variation to both collision systems; the resulting variations of the ratios from their central values are used as the correlated systematic uncertainty.

Examples of systematic uncertainties in the $D(p_T, r)$ distributions for jets in the 126–158 GeV p_T^{jet} range measured in pp and Pb+Pb collision systems are shown in Figure 2. The uncertainties in the $R_{D(p_T, r)}$ distributions are shown in Figure 3. It can be seen that the dominant systematic uncertainty in the Pb+Pb and the $R_{D(p_T, r)}$ distributions is from the UE subtraction. While it is less than 5% for $r < 0.3$, it is approximately 40% for charged particles with $p_T = 1$ GeV at $r = 0.8$. The uncertainties in the pp system are smaller, with the dominant systematic uncertainty at low p_T being due to the tracking. This is approximately 10% for $r < 0.1$ and decreases to less than 5% at larger distances.

7 Results

The $D(p_T, r)$ distributions are studied as a function of p_T^{jet} for pp data and Pb+Pb collisions with different centralities. The interplay between the hot and dense matter and the parton shower is explored by evaluating the ratios and differences between the $D(p_T, r)$ distributions in Pb+Pb and pp collisions. Some selected moments of these distributions are also investigated.

7.1 $D(p_T, r)$ distributions

The $D(p_T, r)$ distributions evaluated in pp and Pb+Pb collisions for $126 < p_T^{\text{jet}} < 158$ GeV are shown in Figure 4. These distributions decrease as a function of distance from the jet axis. The rate of fall-off increases sharply for higher- p_T particles, with most of these being concentrated near the jet axis. The distributions exhibit a difference in shape between Pb+Pb and pp collisions, with the Pb+Pb distributions being broader at low p_T ($p_T < 4$ GeV) and narrower at high p_T ($p_T > 4$ GeV) in 0–10% central collisions. This modification is centrality dependent and is smaller for peripheral Pb+Pb collisions.

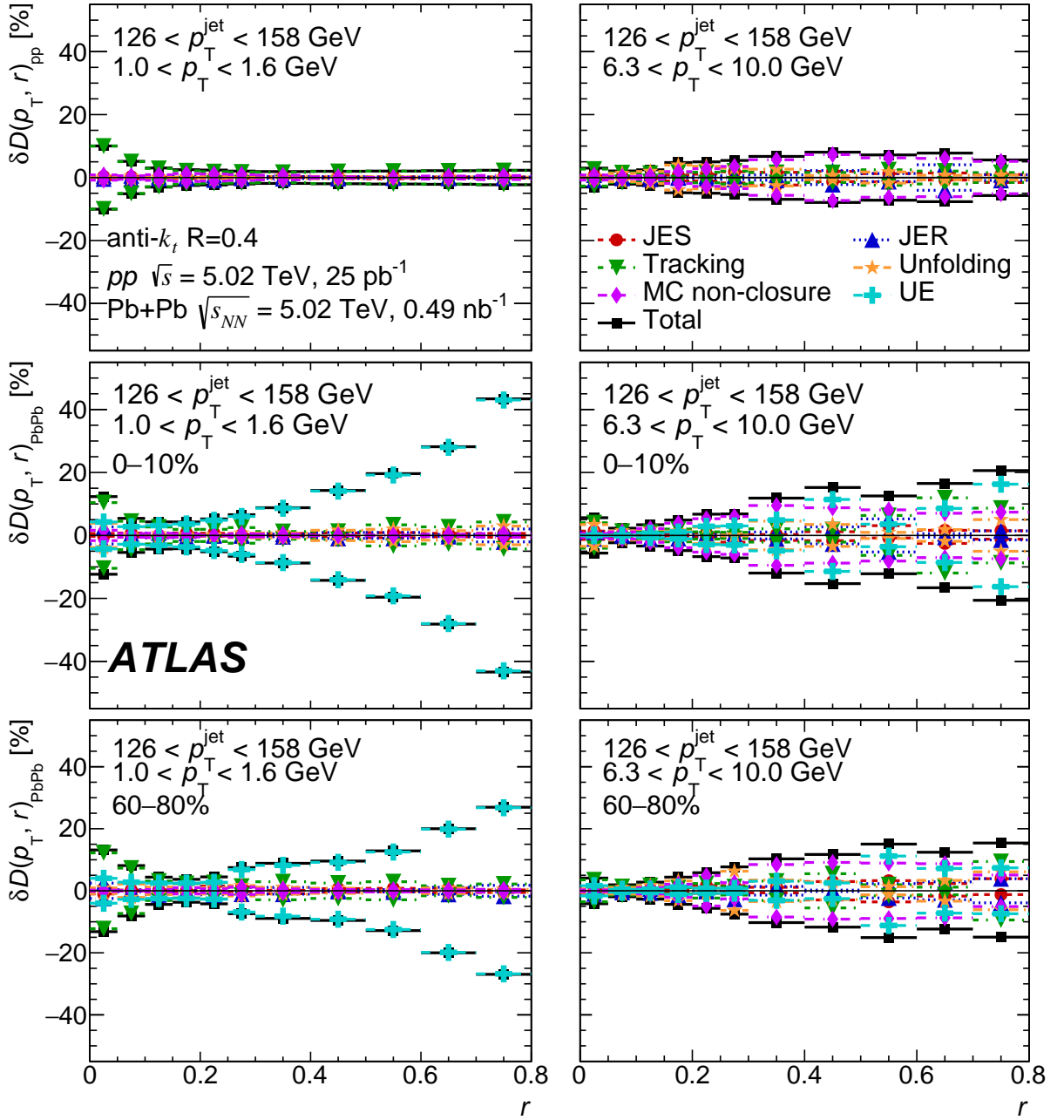


Figure 2: Relative size of the systematic uncertainties for $D(p_T, r)$ distributions in pp (top), central 0–10% $Pb+Pb$ (middle), and peripheral 60–80% $Pb+Pb$ (bottom) collisions for tracks with $1.0 < p_T < 1.6 \text{ GeV}$ (left) and $6.3 < p_T < 10 \text{ GeV}$ (right) in jets with $126 < p_T^{\text{jet}} < 158 \text{ GeV}$. The systematic uncertainties due to JES, JER, tracking, unfolding, MC non-closure, and UE contribution (for $Pb+Pb$) are shown along with the total systematic uncertainty from all sources.

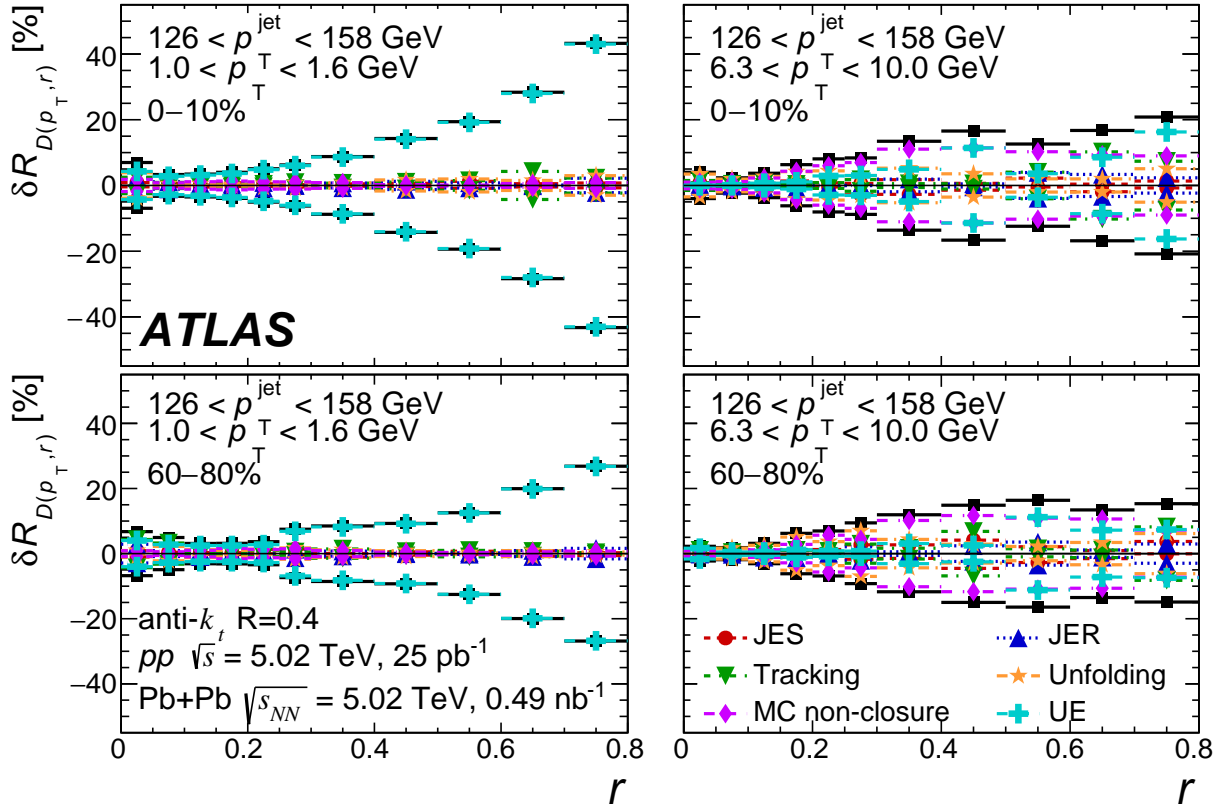


Figure 3: Relative size of the systematic uncertainties for $R_{D(p_T, r)}$ distributions for 0–10% (top) and 60–80% (bottom) Pb+Pb collisions, for tracks with $1.0 < p_T < 1.6 \text{ GeV}$ (left) and $6.3 < p_T < 10.0 \text{ GeV}$ (right), in jets with $126 < p_T^{\text{jet}} < 158 \text{ GeV}$. The systematic uncertainties due to JES, JER, tracking, unfolding, MC non-closure, and UE contribution are shown along with the total systematic uncertainty from all sources.

7.2 $R_{D(p_T, r)}$ distributions

In order to quantify the differences seen in Figure 4, ratios of the $D(p_T, r)$ distributions in Pb+Pb collisions to those measured in pp collisions for $126 < p_T^{\text{jet}} < 158 \text{ GeV}$ and $200 < p_T^{\text{jet}} < 251 \text{ GeV}$ jets are presented in Figure 5. They are shown as a function of r for different p_T and centrality selections. In 0–10% central collisions, $R_{D(p_T, r)}$ is greater than unity for $r < 0.8$ for charged particles with p_T less than 4.0 GeV for both p_T^{jet} selections. For these particles, the enhancement of yields in Pb+Pb collisions compared to those in pp collisions grows with increasing r up to approximately $r = 0.3$, with $R_{D(p_T, r)}$ reaching values up to two for $1.0 < p_T < 2.5 \text{ GeV}$. The value of $R_{D(p_T, r)}$ is approximately constant for r in the interval 0.3–0.6 and decreases for $r > 0.6$. For charged particles with $p_T > 4.0 \text{ GeV}$, $R_{D(p_T, r)}$ shows a depletion outside the jet core for $r > 0.05$. The magnitude of this depletion increases with increasing r up to $r = 0.3$ and is approximately constant thereafter. For 30–40% mid-central collisions, the enhancement in the yield of particles with $p_T < 4.0 \text{ GeV}$ has trends similar to those in the most central collisions, but the depletion of particles with $p_T > 4.0 \text{ GeV}$ is not as strong. For 60–80% peripheral collisions, $R_{D(p_T, r)}$ has no significant r dependence and the values of $R_{D(p_T, r)}$ are within approximately 50% of unity.

The observed behavior inside the jet cone, $r < 0.4$, agrees with the measurement of the inclusive jet fragmentation functions [10, 19, 20], where yields of fragments with $p_T < 4 \text{ GeV}$ are observed to be

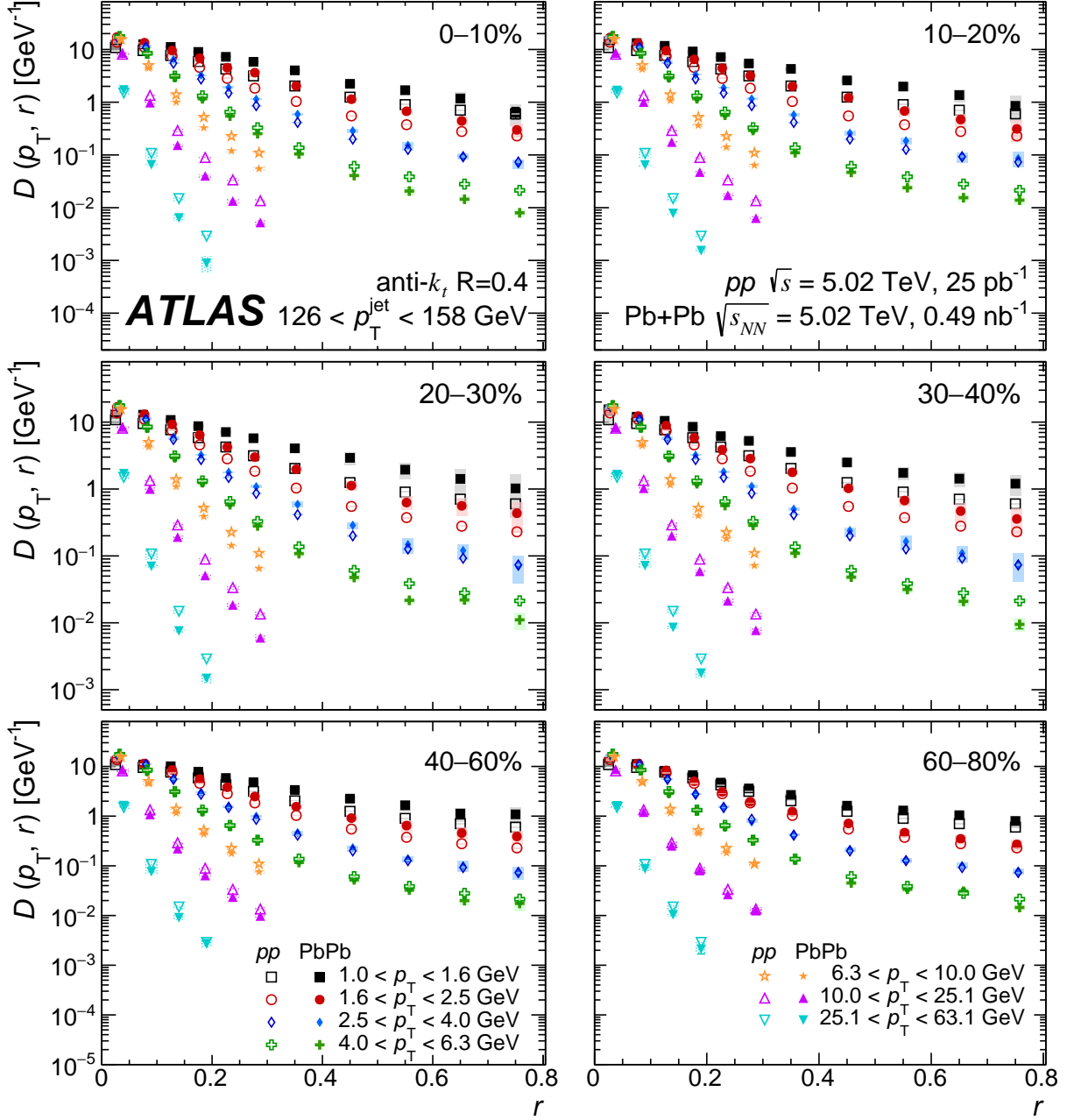


Figure 4: The $D(p_T, r)$ distributions in pp (open symbols) and $Pb+Pb$ (closed symbols) as a function of angular distance r for p_T^{jet} of 126 to 158 GeV. The symbols represent different track p_T ranges, and each panel is a different centrality selection. The vertical bars on the data points indicate statistical uncertainties, while the shaded boxes indicate systematic uncertainties. The widths of the boxes are not indicative of the bin size, and the points are shifted horizontally for better visibility. The distributions for $p_T > 6.3$ GeV are restricted to smaller r values as discussed in Section 5.

enhanced and yields of charged particles with intermediate p_T are suppressed in Pb+Pb collisions compared to those in pp collisions. The wake left in the medium from the passage of the jet compensates for some of the energy it loses [30, 31]. The plateau and slight decrease seen in Figure 5 for the $R_{D(p_T,r)}$ distributions in central Pb+Pb collisions beyond $r = 0.6$ from the jet axis suggests that this response of the medium is smaller than that predicted in Ref. [31].

The centrality dependence of $R_{D(p_T,r)}$ for two charged-particle p_T intervals (1.6–2.5 GeV and 6.3–10.0 GeV) and two different p_T^{jet} ranges (126–158 GeV and 200–251 GeV) is presented in Figure 6. For both p_T^{jet} selections, the magnitude of the excess for 1.6–2.5 GeV charged particles increases for more-central events and for $r < 0.3$. The magnitude of the excess is approximately a factor of two in the most-central collisions for $r > 0.3$. A continuous centrality-dependent suppression of yields of charged particles with $6.3 < p_T < 10.0$ GeV is observed. The magnitude of the modification decreases for more-peripheral collisions in both p_T intervals and p_T^{jet} selections.

Figure 7 shows the charged-particle p_T dependence of $R_{D(p_T,r)}$ for selections in r for 126–158 GeV and 200–251 GeV jets in the following centrality intervals: 0–10%, 30–40%, and 60–80%. Interestingly, there is no significant suppression of the yields in Pb+Pb collisions for $r < 0.05$ at all measured p_T . For larger r values the yields are enhanced for charged particles with $p_T < 4$ GeV and suppressed for higher- p_T charged particles in both the 0–10% and 30–40% centrality selections and both p_T^{jet} ranges presented here. The magnitude of the enhancement increases for decreasing p_T below 4 GeV while the suppression is enhanced with increasing p_T for 4–10 GeV, after which it is approximately constant. At fixed p_T the magnitude of the deviation from unity increases for larger distances from the jet axis. In the 60–80% peripheral collisions, the same trend is seen (but with smaller-magnitude modifications) for $126 < p_T^{\text{jet}} < 158$ GeV; for the higher- p_T^{jet} selection the larger uncertainties do not allow a clear conclusion to be drawn for peripheral collisions.

The enhancement of the charged-particle yield in the kinematic region of $p_T < 4$ GeV has two possible explanations. First, gluon radiation from the hard-scattered parton as it propagates through the QGP would lead to extra soft particles [63, 64]. Second, the interactions of a jet with the QGP and its hydrodynamic response could induce a wake that manifests itself as an enhancement in the number of low- p_T particles [31].

The observed modification at $p_T > 4$ GeV can be explained on the basis of the larger expected energy loss of gluon-initiated jets, resulting in a relative enhancement in the number of quark jets in Pb+Pb collisions compared to pp collisions at a given p_T^{jet} value [20, 65]. Since gluon jets have a broader distribution of particle momentum transverse to the jet direction compared to quark-initiated jets [66], the enhanced quark-jet contribution could describe the narrowing of the particle distribution around the jet direction for particles with $p_T > 4.0$ GeV observed here.

The $R_{D(p_T,r)}$ distributions for low- and high- p_T particles in the different p_T^{jet} selections are directly overlaid in Figure 8. These distributions are for the 0–10% most-central collisions, and show a hint of enhancement in $R_{D(p_T,r)}$ with increasing p_T^{jet} for $r < 0.25$ for low- p_T charged particles. No significant p_T^{jet} dependence is seen at larger r values, or for high- p_T charged particles at any r . This p_T^{jet} dependence is further explored by defining an integral over the low- p_T excess and is discussed in Section 7.4.

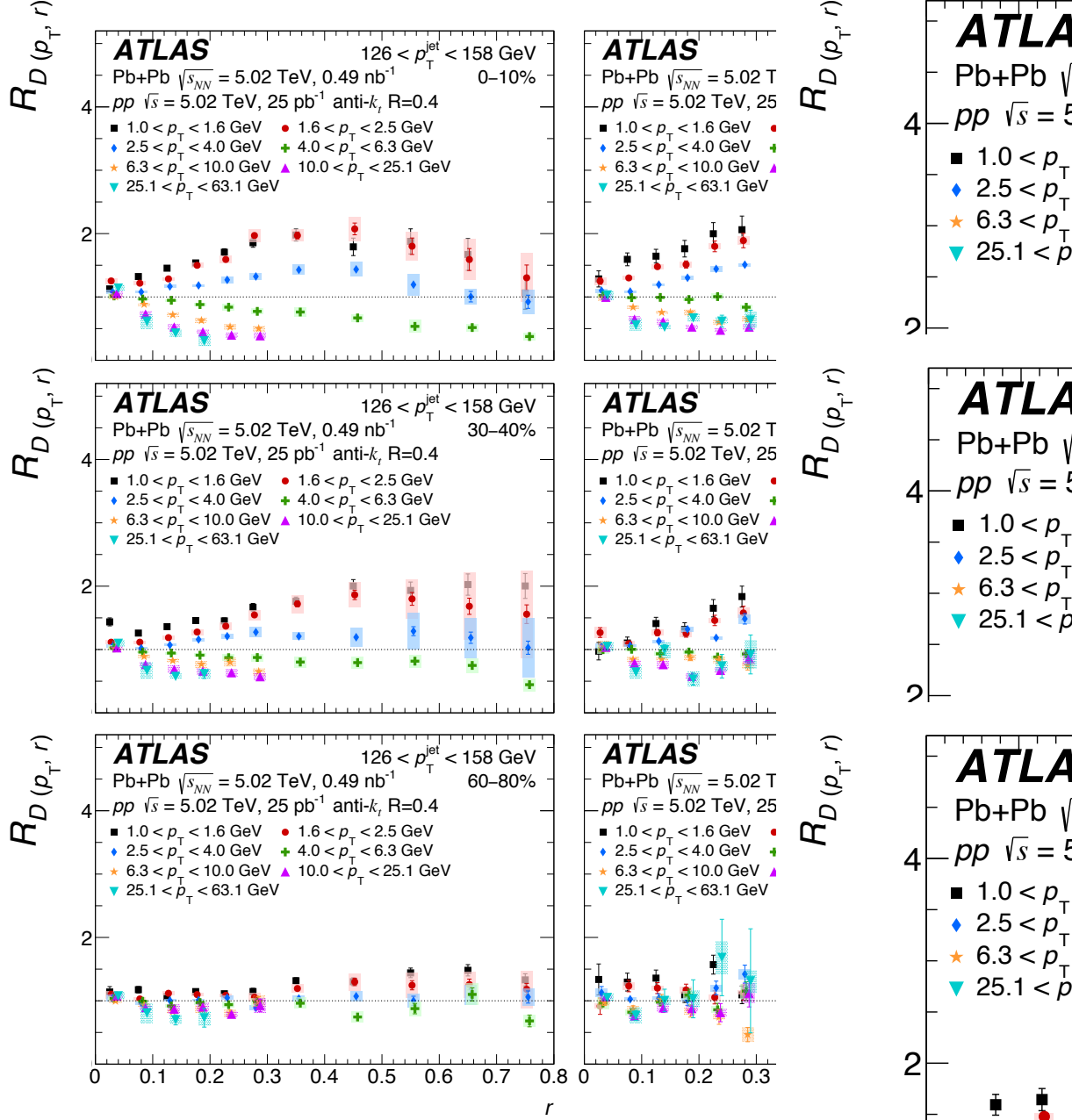


Figure 5: Ratios of $D(p_T, r)$ distributions in $\text{Pb}+\text{Pb}$ and pp collisions as a function of angular distance r for $126 < p_T^{\text{jet}} < 158 \text{ GeV}$ (left) and $200 < p_T^{\text{jet}} < 251 \text{ GeV}$ (right) for seven p_T selections. Different centrality selections are shown: 0–10% (top), 30–40% (middle), 60–80% (bottom). The vertical bars on the data points indicate statistical uncertainties, while the shaded boxes indicate systematic uncertainties. The widths of the boxes are not indicative of the bin size, and the points are shifted horizontally for better visibility.

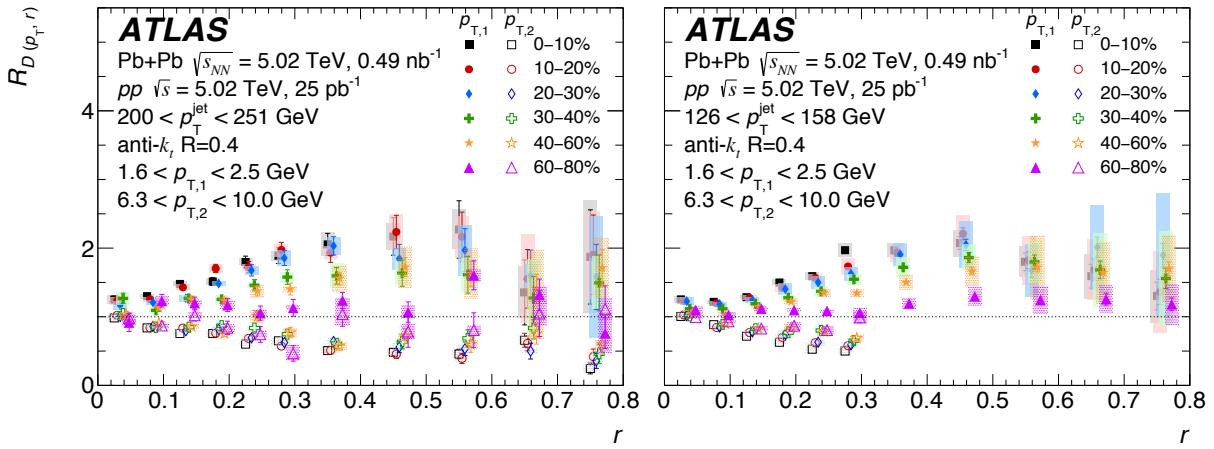


Figure 6: The $R_D(p_{\text{T}}, r)$ distributions for $p_{\text{T}}^{\text{jet}}$ of 126–158 GeV (left) and 200–251 GeV (right) as a function of angular distance r for two p_{T} selections, 1.6–2.5 GeV (closed symbols) and 6.3–10.0 GeV (open symbols), and six centrality intervals. The vertical bars on the data points indicate statistical uncertainties, while the shaded boxes indicate systematic uncertainties. The widths of the boxes are not indicative of the bin size, and the points are shifted horizontally for better visibility.

7.3 $\Delta D(p_{\text{T}}, r)$ distributions

In addition to the ratios of the $D(p_{\text{T}}, r)$ distributions, differences between the unfolded charged-particle yields are also evaluated as $\Delta D(p_{\text{T}}, r)$ to quantify the modification in terms of the particle density.

These differences are presented as a function of r for different p_{T} selections in 0–10% central collisions in Figure 9. These distributions show an excess in the charged-particle yield density for Pb+Pb collisions compared to pp collisions for charged particles with $p_{\text{T}} < 4.0$ GeV. This ranges from 0.5 to 4 particles per unit area per GeV for charged particles with $1 < p_{\text{T}} < 1.6$ GeV in jets with $126 < p_{\text{T}}^{\text{jet}} < 158$ GeV for 0–10% central Pb+Pb collisions and increases with increasing $p_{\text{T}}^{\text{jet}}$. The largest excess for charged particles with $p_{\text{T}} < 4.0$ GeV is within the jet cone. For large r values, the difference decreases but remains positive. A depletion for higher- p_{T} particles of up to approximately 0.5 particles per unit area per GeV is seen for 126–158 GeV jets in 0–10% central Pb+Pb collisions. The magnitude of this depletion increases for higher $p_{\text{T}}^{\text{jet}}$. A minimum in the $\Delta D(p_{\text{T}}, r)$ distributions for charged particles with $4.0 < p_{\text{T}} < 25.1$ GeV at $0.05 < r < 0.10$ is observed. The magnitudes of the excesses and deficits discussed here depend on the selected charged-particle p_{T} .

7.4 p_{T} integrated distributions

Motivated by similar studies of the enhancement of soft fragments in jet fragmentation functions in Pb+Pb compared to pp collisions from Ref. [20], the unfolded $D(p_{\text{T}}, r)$ distributions are integrated for charged particles with $p_{\text{T}} < 4$ GeV to construct the quantities $\Theta(r)$ and $P(r)$ defined as:

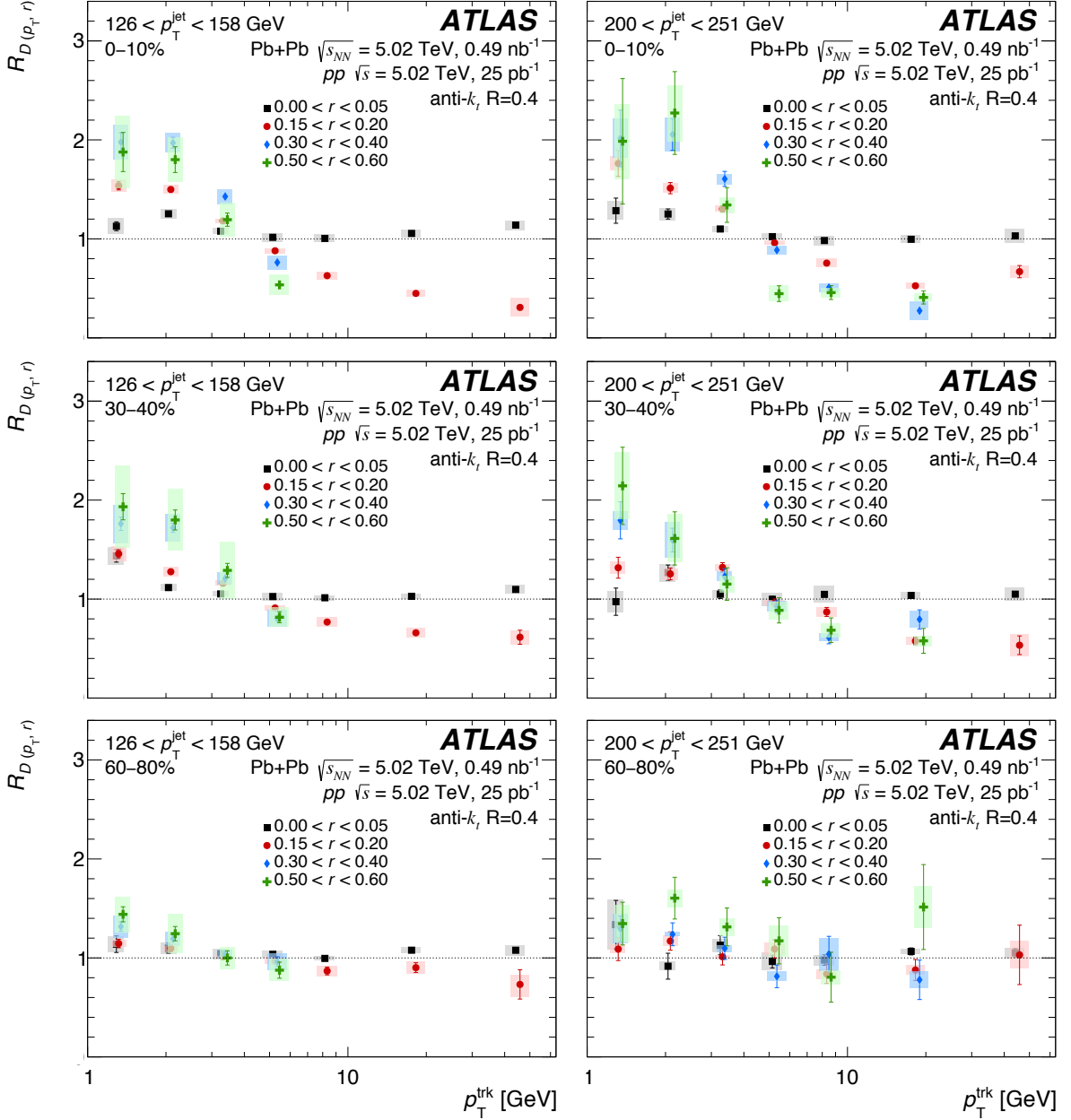


Figure 7: $R_{D(p_T,r)}$ as a function of p_T for 0–10% (top), 30–40% (middle), and 60–80% (bottom) Pb+Pb collisions in two different p_T^{jet} selections: 126–158 GeV (left) and 200–251 GeV (right). The different colors indicate different angular distances from the jet axis. The vertical bars on the data points indicate statistical uncertainties, while the shaded boxes indicate systematic uncertainties. The widths of the boxes are not indicative of the bin size, and the points are shifted horizontally for better visibility.

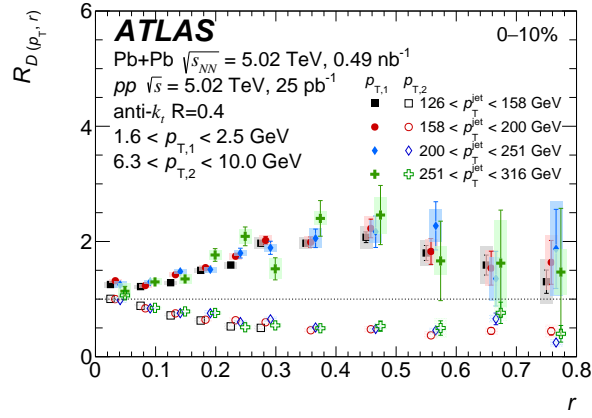


Figure 8: $R_{D(p_T, r)}$ as a function of r for 0–10% central collisions for charged particles with $1.6 < p_T < 2.5$ GeV (closed symbols) and $6.3 < p_T < 10.0$ GeV (open symbols) for different p_T^{jet} selections. The vertical bars on the data points indicate statistical uncertainties, while the shaded boxes indicate systematic uncertainties. The widths of the boxes are not indicative of the bin size, and the points are shifted horizontally for better visibility.

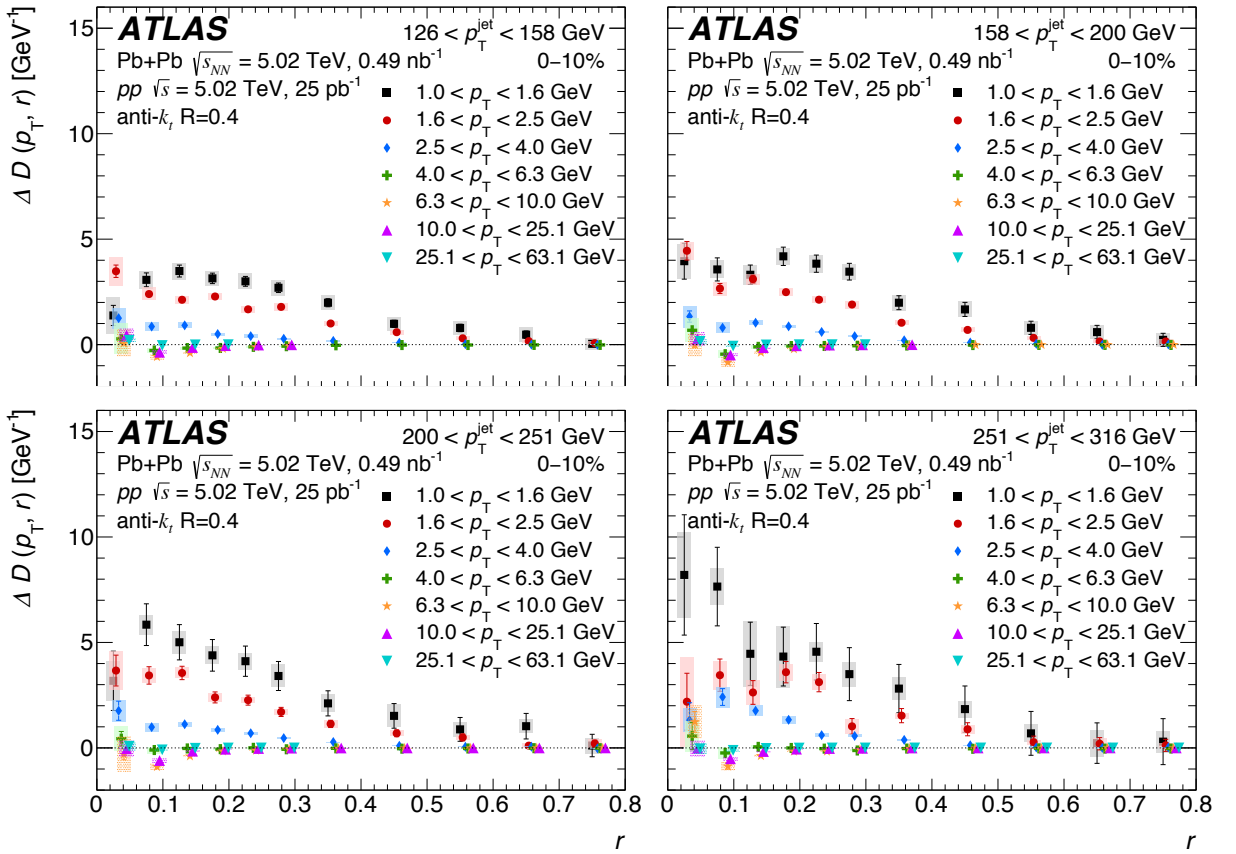


Figure 9: $\Delta D(p_T, r)$ as a function of r in central collisions for all p_T ranges in four p_T^{jet} selections: 126–158 GeV, 158–200 GeV, 200–251 GeV, and 251–316 GeV. The vertical bars on the data points indicate statistical uncertainties, while the shaded boxes indicate systematic uncertainties. The widths of the boxes are not indicative of the bin size, and the points are shifted horizontally for better visibility.

$$\Theta(r) = \int_{1 \text{ GeV}}^{4 \text{ GeV}} D(p_T, r) dp_T$$

$$P(r) = \int_0^r \int_{1 \text{ GeV}}^{4 \text{ GeV}} D(p_T, r') dp_T dr'.$$

The $\Theta(r)$ values are integrated over the charged-particle p_T interval of 1–4 GeV to provide a concise look at the p_T region of enhancement discussed above. The $P(r)$ values further add a running integral over r and provide information about the jet shape. Both of these quantities are compared between the pp and Pb+Pb systems to give the following distributions:

$$\Delta_{\Theta(r)} = \Theta(r)_{\text{Pb+Pb}} - \Theta(r)_{pp}$$

$$R_{\Theta(r)} = \frac{\Theta(r)_{\text{Pb+Pb}}}{\Theta(r)_{pp}}$$

$$R_{P(r)} = \frac{P(r)_{\text{Pb+Pb}}}{P(r)_{pp}}.$$

These integrated quantities are intended to provide aggregate information about the variation with angular distance from the jet axis, magnitude, and p_T^{jet} dependence of the low- p_T charged-particle excess discussed above. The ratio quantities are useful for comparisons with other Pb+Pb measurements; $\Delta_{\Theta(r)}$ is comparable to $\Delta D(p_T, r)$, but it is integrated over charged-particle p_T in the 1–4 GeV interval [20].

Figure 10 shows the $\Delta_{\Theta(r)}$ distributions as a function of r for the following centrality intervals: 0–10%, 30–40%, and 60–80%. In the most-central collisions, a significant p_T^{jet} dependence of $\Delta_{\Theta(r)}$ is observed; for $r < 0.4$ (particles within the jet cone) $\Delta_{\Theta(r)}$ increases with increasing p_T^{jet} . The value of $\Delta_{\Theta(r)}$ decreases in more-peripheral collisions, where its p_T^{jet} dependence is also no longer significant.

Figure 11 shows the $R_{\Theta(r)}$ and $R_{P(r)}$ distributions as a function of r for the 0–10%, 30–40%, and 60–80% centrality intervals. The $R_{\Theta(r)}$ distributions in the most-central collisions show a maximum for $r \sim 0.4$ and a flattening or a decrease for larger r . However, since $R_{\Theta(r)}$ remains at or above unity for the full range of r values presented, $R_{P(r)}$ shows no suppression with increasing r over the entire measured range. A significant p_T^{jet} dependence is seen in the $R_{P(r)}$ distributions for the most-central Pb+Pb collisions. A slow increase in $R_{P(r)}$ is clearly observed in 30–40% central collisions. In more-peripheral collisions the magnitude of the excess is reduced and the trends in $R_{\Theta(r)}$ are less clear, although $R_{P(r)}$ is still seen to be above unity. The flattening of the $R_{P(r)}$ distributions at large distances suggests that while wider jets have a softer fragmentation and contain more particles with less p_T in Pb+Pb collisions than in pp collisions [67, 68], this effect plateaus for jets with radius larger than 0.6.

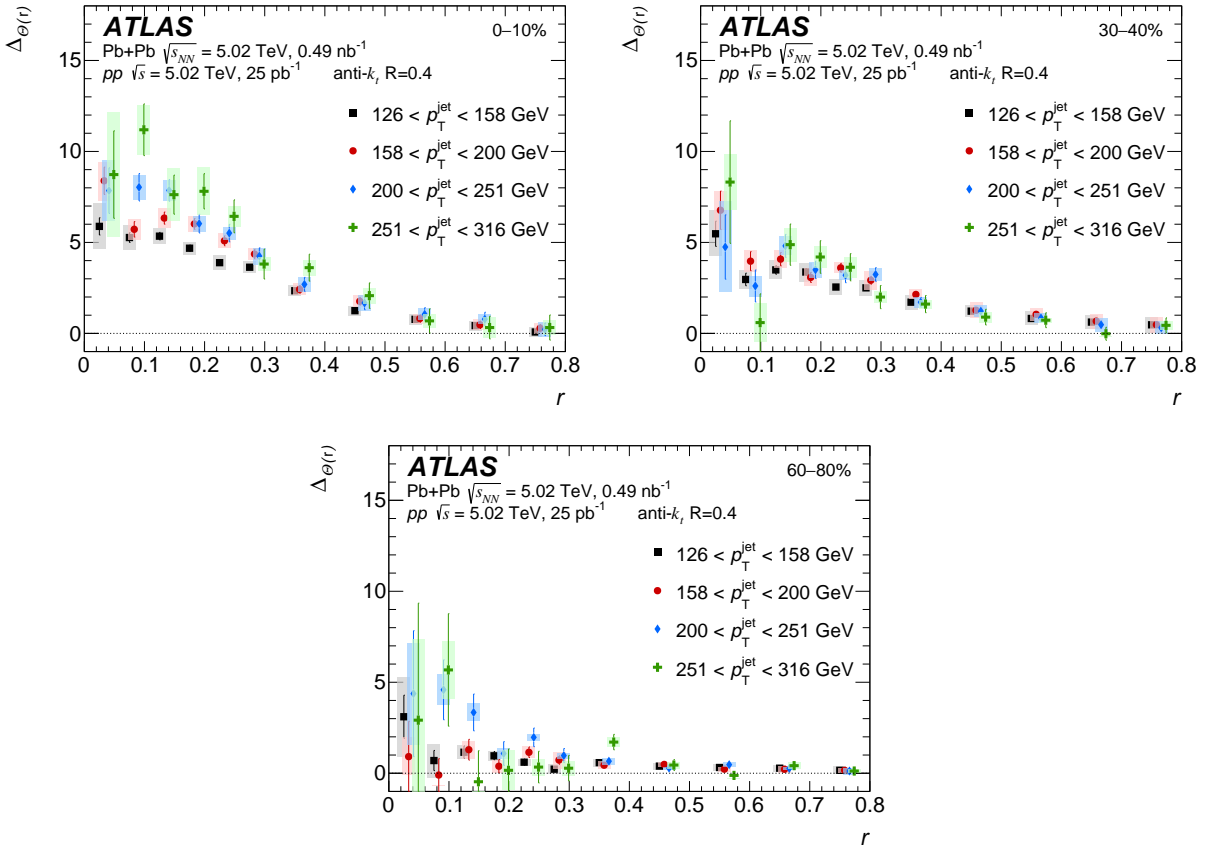


Figure 10: $\Delta_{\theta(r)}$ as a function of r for charged particles with $p_T < 4$ GeV in four p_T^{jet} selections: 126–158 GeV, 158–200 GeV, 200–251 GeV, and 251–316 GeV and three centrality selections: 0–10% (top left), 30–40% (top right) and 60–80% (bottom). The vertical bars on the data points indicate statistical uncertainties, while the shaded boxes indicate systematic uncertainties. The widths of the boxes are not indicative of the bin size, and the points are shifted horizontally for better visibility.

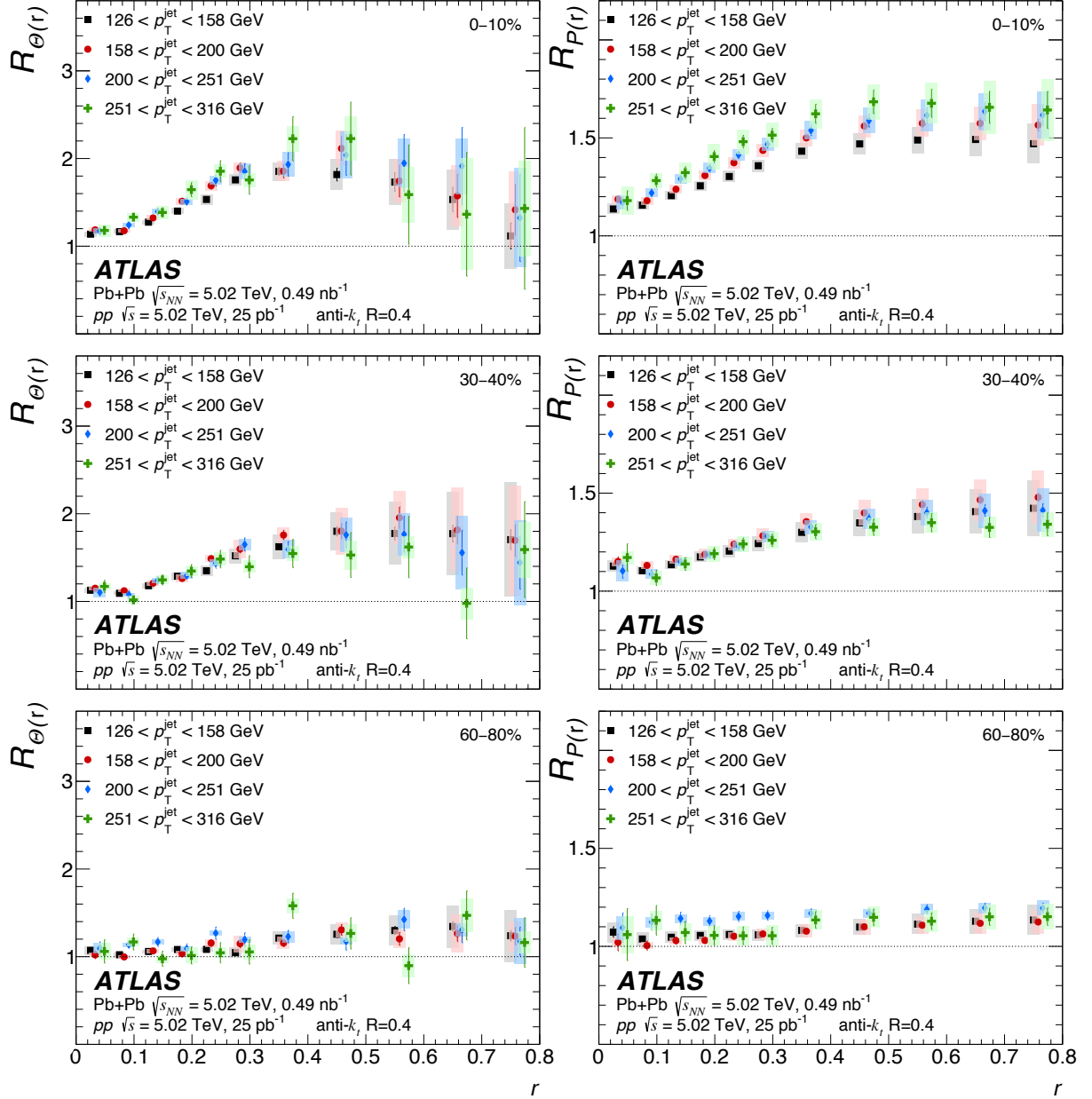


Figure 11: $R_{\Theta(r)}$ (left) and $R_{P(r)}$ (right) as a function of r for charged particles with $p_T < 4$ GeV in four p_T^{jet} selections: 126–158 GeV, 158–200 GeV, 200–251 GeV, and 251–316 GeV and three centrality selections: 0–10% (top), 30–40% (middle) and 60–80% (bottom). The vertical bars on the data points indicate statistical uncertainties, while the shaded boxes indicate systematic uncertainties. The widths of the boxes are not indicative of the bin size, and the points are shifted horizontally for better visibility.

8 Summary

This paper presents a measurement of the yields of charged particles, $D(p_T, r)$, inside and around $R = 0.4$ anti- k_t jets with $|y^{\text{jet}}| < 1.7$ up to an angular distance of $r = 0.8$ from the jet axis, using the ATLAS detector at the LHC. The yields are measured in intervals of p_T^{jet} from 126 to 316 GeV in Pb+Pb and pp collisions at $\sqrt{s_{\text{NN}}} = 5.02$ TeV as a function of charged-particle p_T and the angular distance r between the jet axis and charged particle. The integrated luminosities of the Pb+Pb and pp data sets are 0.49 nb^{-1} and 25 pb^{-1} , respectively.

The measurements show a broadening of the $D(p_T, r)$ distribution for low- p_T particles inside the jet in central Pb+Pb collisions compared to those in pp collisions, while for higher- p_T particles the angular distributions are narrower in Pb+Pb collisions than in pp collisions. These modifications are centrality dependent and decrease for more-peripheral collisions. The Pb+Pb-to- pp ratio of the $D(p_T, r)$ distributions, $R_{D(p_T,r)}$, is also examined. The $R_{D(p_T,r)}$ distributions for charged particles with $p_T < 4$ GeV are above unity and grow with increasing angular separation up to $r \sim 0.3$, showing weak to no dependence on r in the interval $0.3 < r < 0.6$ followed with a small decrease in the enhancement for $0.6 < r < 0.8$. For charged particles with $p_T > 4$ GeV, a suppression in $R_{D(p_T,r)}$ is observed and the size of the modification increases with increasing r for $0.05 < r < 0.3$ with no r dependence for $r > 0.3$. For all charged-particle p_T values, the $R_{D(p_T,r)}$ values are greater than or equal to unity for $r < 0.05$. Between $0.1 < r < 0.25$, a statistically significant trend of increasing $R_{D(p_T,r)}$ with increasing p_T^{jet} is observed for low- p_T particles. No significant p_T^{jet} dependence is seen for particles with $p_T > 4$ GeV.

This measurement provides information about the modification of the jet at large distances from the jet axis that can be used to constrain models of how the jet is modified by the presence of the quark–gluon plasma and how the quark–gluon plasma responds to the jet.

Acknowledgments

We thank CERN for the very successful operation of the LHC, as well as the support staff from our institutions without whom ATLAS could not be operated efficiently.

We acknowledge the support of ANPCyT, Argentina; YerPhI, Armenia; ARC, Australia; BMWFW and FWF, Austria; ANAS, Azerbaijan; SSTC, Belarus; CNPq and FAPESP, Brazil; NSERC, NRC and CFI, Canada; CERN; CONICYT, Chile; CAS, MOST and NSFC, China; COLCIENCIAS, Colombia; MSMT CR, MPO CR and VSC CR, Czech Republic; DNRF and DNSRC, Denmark; IN2P3-CNRS and CEA-DRF/IRFU, France; SRNSFG, Georgia; BMBF, HGF and MPG, Germany; GSRT, Greece; RGC and Hong Kong SAR, China; ISF and Benoziyo Center, Israel; INFN, Italy; MEXT and JSPS, Japan; CNRST, Morocco; NWO, Netherlands; RCN, Norway; MNiSW and NCN, Poland; FCT, Portugal; MNE/IFA, Romania; MES of Russia and NRC KI, Russia Federation; JINR; MESTD, Serbia; MSSR, Slovakia; ARRS and MIZŠ, Slovenia; DST/NRF, South Africa; MICINN, Spain; SRC and Wallenberg Foundation, Sweden; SERI, SNSF and Cantons of Bern and Geneva, Switzerland; MOST, Taiwan; TAEK, Turkey; STFC, United Kingdom; DOE and NSF, United States of America. In addition, individual groups and members have received support from BCKDF, CANARIE, Compute Canada and CRC, Canada; ERC, ERDF, Horizon 2020, Marie Skłodowska-Curie Actions and COST, European Union; Investissements d’Avenir Labex, Investissements d’Avenir Idex and ANR, France; DFG and AvH Foundation, Germany; Herakleitos, Thales and Aristeia programmes co-financed by EU-ESF and the Greek NSRF, Greece; BSF-NSF and GIF, Israel;

La Caixa Banking Foundation, CERCA Programme Generalitat de Catalunya and PROMETEO and GenT Programmes Generalitat Valenciana, Spain; Göran Gustafssons Stiftelse, Sweden; The Royal Society and Leverhulme Trust, United Kingdom.

The crucial computing support from all WLCG partners is acknowledged gratefully, in particular from CERN, the ATLAS Tier-1 facilities at TRIUMF (Canada), NDGF (Denmark, Norway, Sweden), CC-IN2P3 (France), KIT/GridKA (Germany), INFN-CNAF (Italy), NL-T1 (Netherlands), PIC (Spain), ASGC (Taiwan), RAL (UK) and BNL (USA), the Tier-2 facilities worldwide and large non-WLCG resource providers. Major contributors of computing resources are listed in Ref. [comp_Tier2s].

References

- [1] G. Roland, K. Šafařík, and P. Steinberg, *Heavy-ion collisions at the LHC*, *Prog. Part. Nucl. Phys.* **77** (2014) 70.
- [2] W. Busza, K. Rajagopal, and W. van der Schee, *Heavy Ion Collisions: The Big Picture, and the Big Questions*, *Ann. Rev. Nucl. Part. Sci.* **68** (2018) 339, arXiv: [1802.04801 \[hep-ph\]](#).
- [3] ALICE Collaboration, *Measurement of charged jet suppression in Pb-Pb collisions at $\sqrt{s_{NN}} = 2.76 \text{ TeV}$* , *JHEP* **03** (2014) 013, arXiv: [1311.0633 \[nucl-ex\]](#).
- [4] ATLAS Collaboration, *Measurements of the Nuclear Modification Factor for Jets in Pb+Pb Collisions at $\sqrt{s_{NN}} = 2.76 \text{ TeV}$ with the ATLAS Detector*, *Phys. Rev. Lett.* **114** (2015) 072302, arXiv: [1411.2357 \[hep-ex\]](#).
- [5] ALICE Collaboration, *Measurement of jet suppression in central Pb-Pb collisions at $\sqrt{s_{NN}} = 2.76 \text{ TeV}$* , *Phys. Lett. B* **746** (2015) 1, arXiv: [1502.01689 \[nucl-ex\]](#).
- [6] CMS Collaboration, *Measurement of inclusive jet cross sections in pp and PbPb collisions at $\sqrt{s_{NN}} = 2.76 \text{ TeV}$* , *Phys. Rev. C* **96** (2017) 015202, arXiv: [1609.05383 \[nucl-ex\]](#).
- [7] ATLAS Collaboration, *Measurement of the nuclear modification factor for inclusive jets in Pb+Pb collisions at $\sqrt{s_{NN}} = 5.02 \text{ TeV}$ with the ATLAS detector*, *Phys. Lett. B* **790** (2019) 108, arXiv: [1805.05635 \[nucl-ex\]](#).
- [8] ATLAS Collaboration, *Observation of a Centrality-Dependent Dijet Asymmetry in Lead-Lead Collisions at $\sqrt{s_{NN}} = 2.76 \text{ TeV}$ with the ATLAS Detector at the LHC*, *Phys. Rev. Lett.* **105** (2010) 252303, arXiv: [1011.6182 \[hep-ex\]](#).
- [9] CMS Collaboration, *Observation and studies of jet quenching in PbPb collisions at $\sqrt{s_{NN}} = 2.76 \text{ TeV}$* , *Phys. Rev. C* **84** (2011) 024906, arXiv: [1102.1957 \[nucl-ex\]](#).
- [10] ATLAS Collaboration, *Measurement of jet p_T correlations in Pb+Pb and pp collisions at $\sqrt{s_{NN}} = 2.76 \text{ TeV}$ with the ATLAS detector*, *Phys. Lett. B* **774** (2017) 379, arXiv: [1706.09363 \[hep-ex\]](#).
- [11] CMS Collaboration, *Studies of jet quenching using isolated-photon+jet correlations in PbPb and pp collisions at $\sqrt{s_{NN}} = 2.76 \text{ TeV}$* , *Phys. Lett. B* **718** (2013) 773, arXiv: [1205.0206 \[nucl-ex\]](#).
- [12] ATLAS Collaboration, *Measurement of photon–jet transverse momentum correlations in 5.02 TeV Pb+Pb and pp collisions with ATLAS*, *Phys. Lett. B* **789** (2019) 167, arXiv: [1809.07280 \[nucl-ex\]](#).

- [13] ATLAS Collaboration, *Measurement of the jet fragmentation function and transverse profile in proton-proton collisions at a center-of-mass energy of 7 TeV with the ATLAS detector*, *Eur. Phys. J. C* **71** (2011) 1795, arXiv: [1109.5816 \[hep-ex\]](#).
- [14] ALICE Collaboration, *Medium modification of the shape of small-radius jets in central Pb-Pb collisions at $\sqrt{s_{NN}} = 2.76$ TeV*, *JHEP* **10** (2018) 139, arXiv: [1807.06854 \[nucl-ex\]](#).
- [15] CMS Collaboration, *Shape, transverse size, and charged-hadron multiplicity of jets in pp collisions at $\sqrt{s} = 7$ TeV*, *JHEP* **06** (2012) 160, arXiv: [1204.3170 \[hep-ex\]](#).
- [16] CMS Collaboration, *Modification of jet shapes in PbPb collisions at $\sqrt{s_{NN}} = 2.76$ TeV*, *Phys. Lett. B* **730** (2014) 243, arXiv: [1310.0878 \[nucl-ex\]](#).
- [17] ATLAS Collaboration, *Measurement of inclusive jet charged-particle fragmentation functions in Pb+Pb collisions at $\sqrt{s_{NN}} = 2.76$ TeV with the ATLAS detector*, *Phys. Lett. B* **739** (2014) 320, arXiv: [1406.2979 \[hep-ex\]](#).
- [18] CMS Collaboration, *Measurement of jet fragmentation in PbPb and pp collisions at $\sqrt{s_{NN}} = 2.76$ TeV*, *Phys. Rev. C* **90** (2014) 024908, arXiv: [1406.0932 \[nucl-ex\]](#).
- [19] ATLAS Collaboration, *Measurement of jet fragmentation in Pb+Pb and pp collisions at $\sqrt{s_{NN}} = 2.76$ TeV with the ATLAS detector at the LHC*, *Eur. Phys. J. C* **77** (2017) 379, arXiv: [1702.00674 \[hep-ex\]](#).
- [20] ATLAS Collaboration, *Measurement of jet fragmentation in Pb+Pb and pp collisions at $\sqrt{s_{NN}} = 5.02$ TeV with the ATLAS detector*, *Phys. Rev. C* **98** (2018) 024908, arXiv: [1805.05424 \[nucl-ex\]](#).
- [21] CMS Collaboration, *Measurement of transverse momentum relative to dijet systems in PbPb and pp collisions at $\sqrt{s_{NN}} = 2.76$ TeV*, *JHEP* **01** (2016) 006, arXiv: [1509.09029 \[nucl-ex\]](#).
- [22] CMS Collaboration, *Decomposing transverse momentum balance contributions for quenched jets in PbPb collisions at $\sqrt{s_{NN}} = 2.76$ TeV*, *JHEP* **11** (2016) 055, arXiv: [1609.02466 \[nucl-ex\]](#).
- [23] CMS Collaboration, *Jet properties in PbPb and pp collisions at $\sqrt{s_{NN}} = 5.02$ TeV*, *JHEP* **05** (2018) 006, arXiv: [1803.00042 \[nucl-ex\]](#).
- [24] ALICE Collaboration, *Measurement of jet radial profiles in Pb-Pb collisions at $\sqrt{s_{NN}} = 2.76$ TeV*, *Phys. Lett. B* **796** (2019) 204, arXiv: [1904.13118 \[nucl-ex\]](#).
- [25] I. Vitev, S. Wicks, and B.-W. Zhang, *A theory of jet shapes and cross sections: from hadrons to nuclei*, *JHEP* **11** (2008) 093, arXiv: [0810.2807 \[hep-ph\]](#).
- [26] G. Ovanesyan and I. Vitev, *An effective theory for jet propagation in dense QCD matter: jet broadening and medium-induced bremsstrahlung*, *JHEP* **06** (2011) 080, arXiv: [1103.1074 \[hep-ph\]](#).
- [27] J.-P. Blaizot, Y. Mehtar-Tani, and M. A. C. Torres, *Angular Structure of the In-Medium QCD Cascade*, *Phys. Rev. Lett.* **114** (2015) 222002, arXiv: [1407.0326 \[hep-ph\]](#).
- [28] G.-Y. Qin and X.-N. Wang, *Jet quenching in high-energy heavy-ion collisions*, *Int. J. Mod. Phys. E* **24** (2015) 1530014, arXiv: [1511.00790 \[hep-ph\]](#).
- [29] M. A. Escobedo and E. Iancu, *Event-by-event fluctuations in the medium-induced jet evolution*, *JHEP* **05** (2016) 008, arXiv: [1601.03629 \[hep-ph\]](#).
- [30] J. Casalderrey-Solana, D. Gulhan, G. Milhano, D. Pablos, and K. Rajagopal, *Angular structure of jet quenching within a hybrid strong/weak coupling model*, *JHEP* **03** (2017) 135, arXiv: [1609.05842 \[hep-ph\]](#).

- [31] Y. Tachibana, N.-B. Chang, and G.-Y. Qin, *Full jet in quark-gluon plasma with hydrodynamic medium response*, *Phys. Rev. C* **95** (2017) 044909, arXiv: [1701.07951 \[nucl-th\]](#).
- [32] ATLAS Collaboration, *The ATLAS Experiment at the CERN Large Hadron Collider*, *JINST* **3** (2008) S08003.
- [33] ATLAS Collaboration, *ATLAS Insertable B-Layer Technical Design Report*, ATLAS-TDR-19, 2010, URL: <https://cds.cern.ch/record/1291633>, Addendum: ATLAS-TDR-19-ADD-1, 2012, URL: <https://cds.cern.ch/record/1451888>.
- [34] B. Abbott et al., *Production and integration of the ATLAS Insertable B-Layer*, *JINST* **13** (2018) T05008, arXiv: [1803.00844 \[physics.ins-det\]](#).
- [35] ATLAS Collaboration, *Performance of the ATLAS trigger system in 2015*, *Eur. Phys. J. C* **77** (2017) 317, arXiv: [1611.09661 \[hep-ex\]](#).
- [36] ATLAS Collaboration, *Measurement of longitudinal flow decorrelations in Pb+Pb collisions at $\sqrt{s_{NN}} = 2.76$ and 5.02 TeV with the ATLAS detector*, *Eur. Phys. J. C* **78** (2018) 142, arXiv: [1709.02301 \[nucl-ex\]](#).
- [37] P. Nason, *A new method for combining NLO QCD with shower Monte Carlo algorithms*, *JHEP* **11** (2004) 040, arXiv: [hep-ph/0409146](#).
- [38] S. Frixione, P. Nason, and C. Oleari, *Matching NLO QCD computations with Parton Shower simulations: the POWHEG method*, *JHEP* **11** (2007) 070, arXiv: [0709.2092 \[hep-ph\]](#).
- [39] S. Alioli, P. Nason, C. Oleari, and E. Re, *A general framework for implementing NLO calculations in shower Monte Carlo programs: the POWHEG BOX*, *JHEP* **06** (2010) 043, arXiv: [1002.2581 \[hep-ph\]](#).
- [40] S. Alioli, K. Hamilton, P. Nason, C. Oleari, and E. Re, *Jet pair production in POWHEG*, *JHEP* **04** (2011) 081, arXiv: [1012.3380 \[hep-ph\]](#).
- [41] T. Sjöstrand et al., *An introduction to PYTHIA 8.2*, *Comput. Phys. Commun.* **191** (2015) 159, arXiv: [1410.3012 \[hep-ph\]](#).
- [42] ATLAS Collaboration, *ATLAS Pythia 8 tunes to 7 TeV data*, ATL-PHYS-PUB-2014-021, 2014, URL: <https://cds.cern.ch/record/1966419>.
- [43] R. D. Ball et al., *Parton distributions with LHC data*, *Nucl. Phys. B* **867** (2013) 244, arXiv: [1207.1303 \[hep-ph\]](#).
- [44] X.-N. Wang and M. Gyulassy, *HJING: A Monte Carlo model for multiple jet production in pp, pA, and AA collisions*, *Phys. Rev. D* **44** (1991) 3501.
- [45] S. Agostinelli et al., *GEANT4—a simulation toolkit*, *Nucl. Instrum. Meth. A* **506** (2003) 250.
- [46] ATLAS Collaboration, *The ATLAS Simulation Infrastructure*, *Eur. Phys. J. C* **70** (2010) 823, arXiv: [1005.4568 \[physics.ins-det\]](#).
- [47] M. Cacciari, G. P. Salam, and G. Soyez, *The Anti- k_t jet clustering algorithm*, *JHEP* **04** (2008) 063, arXiv: [0802.1189 \[hep-ph\]](#).
- [48] M. Cacciari, G. P. Salam, and G. Soyez, *FastJet User Manual*, *Eur. Phys. J. C* **72** (2012) 1896, arXiv: [1111.6097 \[hep-ph\]](#).
- [49] ATLAS Collaboration, *Measurement of the azimuthal anisotropy for charged particle production in $\sqrt{s_{NN}} = 2.76$ TeV lead-lead collisions with the ATLAS detector*, *Phys. Rev. C* **86** (2012) 014907, arXiv: [1203.3087 \[hep-ex\]](#).

- [50] ATLAS Collaboration, *Jet energy scale measurements and their systematic uncertainties in proton-proton collisions at $\sqrt{s} = 13$ TeV with the ATLAS detector*, *Phys. Rev. D* **96** (2017) 072002, arXiv: [1703.09665 \[hep-ex\]](#).
- [51] ATLAS Collaboration, *Measurement of photon-jet transverse momentum correlations in 5.02 TeV Pb+Pb and pp collisions with ATLAS*, *Phys. Lett. B* **789** (2019) 167, arXiv: [1809.07280 \[nucl-ex\]](#).
- [52] ATLAS Collaboration, *Performance of the ATLAS track reconstruction algorithms in dense environments in LHC Run 2*, *Eur. Phys. J. C* **77** (2017) 673, arXiv: [1704.07983 \[hep-ex\]](#).
- [53] ATLAS Collaboration, *Performance of primary vertex reconstruction in proton–proton collisions at $\sqrt{s} = 7$ TeV in the ATLAS experiment*, ATLAS-CONF-2010-069, 2010, URL: <https://cds.cern.ch/record/1281344>.
- [54] ATLAS Collaboration, *Measurement of jet fragmentation in 5.02 TeV proton-lead and proton-proton collisions with the ATLAS detector*, *Nucl. Phys. A* **978** (2018) 65, arXiv: [1706.02859 \[hep-ex\]](#).
- [55] G. D’Agostini, *A multidimensional unfolding method based on Bayes’ theorem*, *Nucl. Instrum. Meth. A* **362** (1995) 487.
- [56] T. Adye, *Unfolding algorithms and tests using RooUnfold*, 2011, arXiv: [1105.1160 \[physics.data-an\]](#).
- [57] ATLAS Collaboration, *Jet energy measurement with the ATLAS detector in proton-proton collisions at $\sqrt{s} = 7$ TeV*, *Eur. Phys. J. C* **73** (2013) 2304, arXiv: [1112.6426 \[hep-ex\]](#).
- [58] ATLAS Collaboration, *Jet energy scale and its uncertainty for jets reconstructed using the ATLAS heavy ion jet algorithm*, ATLAS-CONF-2015-016, 2015, URL: <https://cds.cern.ch/record/2008677>.
- [59] ATLAS Collaboration, *Jet energy resolution in proton-proton collisions at $\sqrt{s} = 7$ TeV recorded in 2010 with the ATLAS detector*, *Eur. Phys. J. C* **73** (2013) 2306, arXiv: [1210.6210 \[hep-ex\]](#).
- [60] ATLAS Collaboration, *Data-driven determination of the energy scale and resolution of jets reconstructed in the ATLAS calorimeters using dijet and multijet events at $\sqrt{s} = 8$ TeV*, ATLAS-CONF-2015-017, 2015, URL: <https://cds.cern.ch/record/2008678>.
- [61] ATLAS Collaboration, *Early Inner Detector Tracking Performance in the 2015 Data at $\sqrt{s} = 13$ TeV*, ATL-PHYS-PUB-2015-051, 2015, URL: <https://cds.cern.ch/record/2110140>.
- [62] ATLAS Collaboration, *Measurement of track reconstruction inefficiencies in the core of jets via pixel dE/dx with the ATLAS experiment using $\sqrt{s} = 13$ TeV pp collision data*, ATL-PHYS-PUB-2016-007, 2016, URL: <https://cds.cern.ch/record/2140460>.
- [63] Y.-T. Chien, A. Emeran, Z.-B. Kang, G. Ovanesyan, and I. Vitev, *Jet quenching from QCD evolution*, *Phys. Rev. D* **93** (2016) 074030, arXiv: [1509.02936 \[hep-ph\]](#).
- [64] Z.-B. Kang, F. Ringer, and I. Vitev, *Inclusive production of small radius jets in heavy-ion collisions*, *Phys. Lett. B* **769** (2017) 242, arXiv: [1701.05839 \[hep-ph\]](#).
- [65] M. Spousta and B. Cole, *Interpreting single jet measurements in Pb+Pb collisions at the LHC*, *Eur. Phys. J. C* **76** (2016) 50, arXiv: [1504.05169 \[hep-ph\]](#).
- [66] OPAL Collaboration, *A model independent measurement of quark and gluon jet properties and differences*, *Z. Phys. C* **68** (1995) 179.
- [67] P. M. Chesler and K. Rajagopal, *On the evolution of jet energy and opening angle in strongly coupled plasma*, *JHEP* **05** (2016) 098, arXiv: [1511.07567 \[hep-th\]](#).

- [68] Z. Hulcher, D. Pablos, and K. Rajagopal, *Resolution effects in the hybrid strong/weak coupling model*, JHEP **03** (2018) 010, arXiv: [1707.05245 \[hep-ph\]](#).

The ATLAS Collaboration

G. Aad¹⁰², B. Abbott¹²⁹, D.C. Abbott¹⁰³, A. Abed Abud^{71a,71b}, K. Abeling⁵³, D.K. Abhayasinghe⁹⁴, S.H. Abidi¹⁶⁷, O.S. AbouZeid⁴⁰, N.L. Abraham¹⁵⁶, H. Abramowicz¹⁶¹, H. Abreu¹⁶⁰, Y. Abulaiti⁶, B.S. Acharya^{67a,67b,o}, B. Achkar⁵³, S. Adachi¹⁶³, L. Adam¹⁰⁰, C. Adam Bourdarios⁵, L. Adamczyk^{84a}, L. Adamek¹⁶⁷, J. Adelman¹²¹, M. Adersberger¹¹⁴, A. Adiguzel^{12c}, S. Adorni⁵⁴, T. Adye¹⁴⁴, A.A. Affolder¹⁴⁶, Y. Afik¹⁶⁰, C. Agapopoulou⁶⁵, M.N. Agaras³⁸, A. Aggarwal¹¹⁹, C. Agheorghiesei^{27c}, J.A. Aguilar-Saavedra^{140f,140a,aj}, F. Ahmadov⁸⁰, W.S. Ahmed¹⁰⁴, X. Ai¹⁸, G. Aielli^{74a,74b}, S. Akatsuka⁸⁶, T.P.A. Åkesson⁹⁷, E. Akilli⁵⁴, A.V. Akimov¹¹¹, K. Al Khoury⁶⁵, G.L. Alberghini^{23b,23a}, J. Albert¹⁷⁶, M.J. Alconada Verzini¹⁶¹, S. Alderweireldt³⁶, M. Aleksandrov⁸⁰, C. Alexa^{27b}, D. Alexandre¹⁹, T. Alexopoulos¹⁰, A. Alfonsi¹²⁰, F. Alfonsi^{23b,23a}, M. Alhroob¹²⁹, B. Ali¹⁴², G. Alimonti^{69a}, J. Alison³⁷, S.P. Alkire¹⁴⁸, C. Allaire⁶⁵, B.M.M. Allbrooke¹⁵⁶, B.W. Allen¹³², P.P. Allport²¹, A. Aloisio^{70a,70b}, A. Alonso⁴⁰, F. Alonso⁸⁹, C. Alpigiani¹⁴⁸, A.A. Alshehri⁵⁷, M. Alvarez Estevez⁹⁹, D. Álvarez Piqueras¹⁷⁴, M.G. Alviggi^{70a,70b}, Y. Amaral Coutinho^{81b}, A. Ambler¹⁰⁴, L. Ambroz¹³⁵, C. Amelung²⁶, D. Amidei¹⁰⁶, S.P. Amor Dos Santos^{140a}, S. Amoroso⁴⁶, C.S. Amrouche⁵⁴, F. An⁷⁹, C. Anastopoulos¹⁴⁹, N. Andari¹⁴⁵, T. Andeen¹¹, C.F. Anders^{61b}, J.K. Anders²⁰, A. Andreazza^{69a,69b}, V. Andrei^{61a}, C.R. Anelli¹⁷⁶, S. Angelidakis³⁸, A. Angerami³⁹, A.V. Anisenkov^{122b,122a}, A. Annovi^{72a}, C. Antel^{61a}, M.T. Anthony¹⁴⁹, M. Antonelli⁵¹, D.J.A. Antrim¹⁷¹, F. Anulli^{73a}, M. Aoki⁸², J.A. Aparisi Pozo¹⁷⁴, L. Aperio Bella^{15a}, G. Arabidze¹⁰⁷, J.P. Araque^{140a}, V. Araujo Ferraz^{81b}, R. Araujo Pereira^{81b}, C. Arcangeletti⁵¹, A.T.H. Arce⁴⁹, F.A. Arduh⁸⁹, J-F. Arguin¹¹⁰, S. Argyropoulos⁷⁸, J.-H. Arling⁴⁶, A.J. Armbruster³⁶, A. Armstrong¹⁷¹, O. Arnaez¹⁶⁷, H. Arnold¹²⁰, Z.P. Arrubarrena Tame¹¹⁴, A. Artamonov^{124,*}, G. Artoni¹³⁵, S. Artz¹⁰⁰, S. Asai¹⁶³, N. Asbah⁵⁹, E.M. Asimakopoulou¹⁷², L. Asquith¹⁵⁶, J. Assahsah^{35d}, K. Assamagan²⁹, R. Astalos^{28a}, R.J. Atkin^{33a}, M. Atkinson¹⁷³, N.B. Atlay¹⁹, H. Atmani⁶⁵, K. Augsten¹⁴², G. Avolio³⁶, R. Avramidou^{60a}, M.K. Ayoub^{15a}, A.M. Azoulay^{168b}, G. Azuelos^{110,aw}, H. Bachacou¹⁴⁵, K. Bachas^{68a,68b}, M. Backes¹³⁵, F. Backman^{45a,45b}, P. Bagnaia^{73a,73b}, M. Bahmani⁸⁵, H. Bahrasemani¹⁵², A.J. Bailey¹⁷⁴, V.R. Bailey¹⁷³, J.T. Baines¹⁴⁴, M. Bajic⁴⁰, C. Bakalis¹⁰, O.K. Baker¹⁸³, P.J. Bakker¹²⁰, D. Bakshi Gupta⁸, S. Balaji¹⁵⁷, E.M. Baldin^{122b,122a}, P. Balek¹⁸⁰, F. Balli¹⁴⁵, W.K. Balunas¹³⁵, J. Balz¹⁰⁰, E. Banas⁸⁵, A. Bandyopadhyay²⁴, Sw. Banerjee^{181,j}, A.A.E. Bannoura¹⁸², L. Barak¹⁶¹, W.M. Barbe³⁸, E.L. Barberio¹⁰⁵, D. Barberis^{55b,55a}, M. Barbero¹⁰², G. Barbour⁹⁵, T. Barillari¹¹⁵, M-S. Barisits³⁶, J. Barkeloo¹³², T. Barklow¹⁵³, R. Barnea¹⁶⁰, S.L. Barnes^{60c}, B.M. Barnett¹⁴⁴, R.M. Barnett¹⁸, Z. Barnovska-Blenessy^{60a}, A. Baroncelli^{60a}, G. Barone²⁹, A.J. Barr¹³⁵, L. Barranco Navarro^{45a,45b}, F. Barreiro⁹⁹, J. Barreiro Guimarães da Costa^{15a}, S. Barsov¹³⁸, R. Bartoldus¹⁵³, G. Bartolini¹⁰², A.E. Barton⁹⁰, P. Bartos^{28a}, A. Basalaev⁴⁶, A. Bassalat^{65,aq}, M.J. Basso¹⁶⁷, R.L. Bates⁵⁷, S. Batlamous^{35e}, J.R. Batley³², B. Batool¹⁵¹, M. Battaglia¹⁴⁶, M. Bauce^{73a,73b}, F. Bauer¹⁴⁵, K.T. Bauer¹⁷¹, H.S. Bawa^{31,m}, J.B. Beacham⁴⁹, T. Beau¹³⁶, P.H. Beauchemin¹⁷⁰, F. Becherer⁵², P. Bechtle²⁴, H.C. Beck⁵³, H.P. Beck^{20,s}, K. Becker⁵², M. Becker¹⁰⁰, C. Becot⁴⁶, A. Beddall^{12d}, A.J. Beddall^{12a}, V.A. Bednyakov⁸⁰, M. Bedognetti¹²⁰, C.P. Bee¹⁵⁵, T.A. Beermann⁷⁷, M. Begalli^{81b}, M. Begel²⁹, A. Behera¹⁵⁵, J.K. Behr⁴⁶, F. Beisiegel²⁴, A.S. Bell⁹⁵, G. Bella¹⁶¹, L. Bellagamba^{23b}, A. Bellerive³⁴, P. Bellos⁹, K. Beloborodov^{122b,122a}, K. Belotskiy¹¹², N.L. Belyaev¹¹², D. Benchekroun^{35a}, N. Benekos¹⁰, Y. Benhammou¹⁶¹, D.P. Benjamin⁶, M. Benoit⁵⁴, J.R. Bensinger²⁶, S. Bentvelsen¹²⁰, L. Beresford¹³⁵, M. Beretta⁵¹, D. Berge⁴⁶, E. Bergeaas Kuutmann¹⁷², N. Berger⁵, B. Bergmann¹⁴², L.J. Bergsten²⁶, J. Beringer¹⁸, S. Berlendis⁷, N.R. Bernard¹⁰³, G. Bernardi¹³⁶, C. Bernius¹⁵³, F.U. Bernlochner²⁴, T. Berry⁹⁴, P. Berta¹⁰⁰, C. Bertella^{15a}, I.A. Bertram⁹⁰, O. Bessidskaia Bylund¹⁸², N. Besson¹⁴⁵, A. Bethani¹⁰¹, S. Bethke¹¹⁵, A. Betti²⁴, A.J. Bevan⁹³, J. Beyer¹¹⁵, D.S. Bhattacharya¹⁷⁷, P. Bhattacharai²⁶, R. Bi¹³⁹, R.M. Bianchi¹³⁹, O. Biebel¹¹⁴, D. Biedermann¹⁹, R. Bielski³⁶, K. Bierwagen¹⁰⁰, N.V. Biesuz^{72a,72b}, M. Biglietti^{75a}, T.R.V. Billoud¹¹⁰,

M. Bindi⁵³, A. Bingul^{12d}, C. Bini^{73a,73b}, S. Biondi^{23b,23a}, M. Birman¹⁸⁰, T. Bisanz⁵³, J.P. Biswal¹⁶¹, D. Biswas^{181,j}, A. Bitadze¹⁰¹, C. Bitrich⁴⁸, K. Bjørke¹³⁴, K.M. Black²⁵, T. Blazek^{28a}, I. Bloch⁴⁶, C. Blocker²⁶, A. Blue⁵⁷, U. Blumenschein⁹³, G.J. Bobbink¹²⁰, V.S. Bobrovnikov^{122b,122a}, S.S. Bocchetta⁹⁷, A. Bocci⁴⁹, D. Boerner⁴⁶, D. Bogavac¹⁴, A.G. Bogdanchikov^{122b,122a}, C. Bohm^{45a}, V. Boisvert⁹⁴, P. Bokan^{53,172,53}, T. Bold^{84a}, A.S. Boldyrev¹¹³, A.E. Bolz^{61b}, M. Bomben¹³⁶, M. Bona⁹³, J.S. Bonilla¹³², M. Boonekamp¹⁴⁵, C.D. Booth⁹⁴, H.M. Borecka-Bielska⁹¹, A. Borisov¹²³, G. Borissov⁹⁰, J. Bortfeldt³⁶, D. Bortoletto¹³⁵, D. Boscherini^{23b}, M. Bosman¹⁴, J.D. Bossio Sola¹⁰⁴, K. Bouaouda^{35a}, J. Boudreau¹³⁹, E.V. Bouhova-Thacker⁹⁰, D. Boumediene³⁸, S.K. Boutle⁵⁷, A. Boveia¹²⁷, J. Boyd³⁶, D. Boye^{33c,ar}, I.R. Boyko⁸⁰, A.J. Bozson⁹⁴, J. Bracinik²¹, N. Brahimi¹⁰², G. Brandt¹⁸², O. Brandt³², F. Braren⁴⁶, B. Brau¹⁰³, J.E. Brau¹³², W.D. Breaden Madden⁵⁷, K. Brendlinger⁴⁶, L. Brenner⁴⁶, R. Brenner¹⁷², S. Bressler¹⁸⁰, B. Brickwedde¹⁰⁰, D.L. Briglin²¹, D. Britton⁵⁷, D. Britzger¹¹⁵, I. Brock²⁴, R. Brock¹⁰⁷, G. Brooijmans³⁹, W.K. Brooks^{147d}, E. Brost¹²¹, J.H. Broughton²¹, P.A. Bruckman de Renstrom⁸⁵, D. Bruncko^{28b}, A. Bruni^{23b}, G. Bruni^{23b}, L.S. Bruni¹²⁰, S. Bruno^{74a,74b}, B.H. Brunt³², M. Bruschi^{23b}, N. Bruscino¹³⁹, P. Bryant³⁷, L. Bryngemark⁹⁷, T. Buanes¹⁷, Q. Buat³⁶, P. Buchholz¹⁵¹, A.G. Buckley⁵⁷, I.A. Budagov⁸⁰, M.K. Bugge¹³⁴, F. Bührer⁵², O. Bulekov¹¹², T.J. Burch¹²¹, S. Burdin⁹¹, C.D. Burgard¹²⁰, A.M. Burger¹³⁰, B. Burghgrave⁸, J.T.P. Burr⁴⁶, C.D. Burton¹¹, J.C. Burzynski¹⁰³, V. Büscher¹⁰⁰, E. Buschmann⁵³, P.J. Bussey⁵⁷, J.M. Butler²⁵, C.M. Buttar⁵⁷, J.M. Butterworth⁹⁵, P. Butt³⁶, W. Buttinger³⁶, C.J. Buxo Vazquez¹⁰⁷, A. Buzatu¹⁵⁸, A.R. Buzykaev^{122b,122a}, G. Cabras^{23b,23a}, S. Cabrera Urbán¹⁷⁴, D. Caforio⁵⁶, H. Cai¹⁷³, V.M.M. Cairo¹⁵³, O. Cakir^{4a}, N. Calace³⁶, P. Calafiura¹⁸, A. Calandri¹⁰², G. Calderini¹³⁶, P. Calfayan⁶⁶, G. Callea⁵⁷, L.P. Caloba^{81b}, S. Calvente Lopez⁹⁹, D. Calvet³⁸, S. Calvet³⁸, T.P. Calvet¹⁵⁵, M. Calvetti^{72a,72b}, R. Camacho Toro¹³⁶, S. Camarda³⁶, D. Camarero Munoz⁹⁹, P. Camarri^{74a,74b}, D. Cameron¹³⁴, R. Caminal Armadans¹⁰³, C. Camincher³⁶, S. Campana³⁶, M. Campanelli⁹⁵, A. Camplani⁴⁰, A. Campoverde¹⁵¹, V. Canale^{70a,70b}, A. Canesse¹⁰⁴, M. Cano Bret^{60c}, J. Cantero¹³⁰, T. Cao¹⁶¹, Y. Cao¹⁷³, M.D.M. Capeans Garrido³⁶, M. Capua^{41b,41a}, R. Cardarelli^{74a}, F. Cardillo¹⁴⁹, G. Carducci^{41b,41a}, I. Carli¹⁴³, T. Carli³⁶, G. Carlino^{70a}, B.T. Carlson¹³⁹, L. Carminati^{69a,69b}, R.M.D. Carney^{45a,45b}, S. Caron¹¹⁹, E. Carquin^{147d}, S. Carrá⁴⁶, J.W.S. Carter¹⁶⁷, M.P. Casado^{14,e}, A.F. Casha¹⁶⁷, D.W. Casper¹⁷¹, R. Castelijn¹²⁰, F.L. Castillo¹⁷⁴, V. Castillo Gimenez¹⁷⁴, N.F. Castro^{140a,140e}, A. Catinaccio³⁶, J.R. Catmore¹³⁴, A. Cattai³⁶, J. Caudron²⁴, V. Cavaliere²⁹, E. Cavallaro¹⁴, M. Cavalli-Sforza¹⁴, V. Cavasinni^{72a,72b}, E. Celebi^{12b}, F. Ceradini^{75a,75b}, L. Cerdá Alberich¹⁷⁴, K. Cerny¹³¹, A.S. Cerqueira^{81a}, A. Cerri¹⁵⁶, L. Cerrito^{74a,74b}, F. Cerutti¹⁸, A. Cervelli^{23b,23a}, S.A. Cetin^{12b}, Z. Chadi^{35a}, D. Chakraborty¹²¹, S.K. Chan⁵⁹, W.S. Chan¹²⁰, W.Y. Chan⁹¹, J.D. Chapman³², B. Chargeishvili^{159b}, D.G. Charlton²¹, T.P. Charman⁹³, C.C. Chau³⁴, S. Che¹²⁷, S. Chekanov⁶, S.V. Chekulaev^{168a}, G.A. Chelkov^{80,ao}, M.A. Chelstowska³⁶, B. Chen⁷⁹, C. Chen^{60a}, C.H. Chen⁷⁹, H. Chen²⁹, J. Chen^{60a}, J. Chen³⁹, S. Chen¹³⁷, S.J. Chen^{15c}, X. Chen^{15b,av}, Y. Chen⁸³, Y-H. Chen⁴⁶, H.C. Cheng^{63a}, H.J. Cheng^{15a}, A. Cheplakov⁸⁰, E. Cheremushkina¹²³, R. Cherkaoui El Moursli^{35e}, E. Cheu⁷, K. Cheung⁶⁴, T.J.A. Chevaléries¹⁴⁵, L. Chevalier¹⁴⁵, V. Chiarella⁵¹, G. Chiarelli^{72a}, G. Chiodini^{68a}, A.S. Chisholm²¹, A. Chitan^{27b}, I. Chiu¹⁶³, Y.H. Chiu¹⁷⁶, M.V. Chizhov⁸⁰, K. Choi⁶⁶, A.R. Chomont^{73a,73b}, S. Chouridou¹⁶², Y.S. Chow¹²⁰, M.C. Chu^{63a}, X. Chu^{15a,15d}, J. Chudoba¹⁴¹, A.J. Chuinard¹⁰⁴, J.J. Chwastowski⁸⁵, L. Chytka¹³¹, D. Cieri¹¹⁵, K.M. Ciesla⁸⁵, D. Cinca⁴⁷, V. Cindro⁹², I.A. Cioara^{27b}, A. Ciocio¹⁸, F. Cirotto^{70a,70b}, Z.H. Citron^{180,k}, M. Citterio^{69a}, D.A. Ciubotaru^{27b}, B.M. Ciungu¹⁶⁷, A. Clark⁵⁴, M.R. Clark³⁹, P.J. Clark⁵⁰, C. Clement^{45a,45b}, Y. Coadou¹⁰², M. Cobal^{67a,67c}, A. Coccaro^{55b}, J. Cochran⁷⁹, H. Cohen¹⁶¹, A.E.C. Coimbra³⁶, L. Colasurdo¹¹⁹, B. Cole³⁹, A.P. Colijn¹²⁰, J. Collot⁵⁸, P. Conde Muñoz^{140a,f}, E. Coniavitis⁵², S.H. Connell^{33c}, I.A. Connelly⁵⁷, S. Constantinescu^{27b}, F. Conventi^{70a,ax}, A.M. Cooper-Sarkar¹³⁵, F. Cormier¹⁷⁵, K.J.R. Cormier¹⁶⁷, L.D. Corpe⁹⁵, M. Corradi^{73a,73b}, E.E. Corrigan⁹⁷, F. Corriveau^{104,af}, M.J. Costa¹⁷⁴, F. Costanza⁵, D. Costanzo¹⁴⁹, G. Cowan⁹⁴, J.W. Cowley³², J. Crane¹⁰¹, K. Cranmer¹²⁵, S.J. Crawley⁵⁷, R.A. Creager¹³⁷, S. Crépé-Renaudin⁵⁸, F. Crescioli¹³⁶, M. Cristinziani²⁴, V. Croft¹²⁰,

G. Crosetti^{41b,41a}, A. Cueto⁵, T. Cuhadar Donszelmann¹⁴⁹, A.R. Cukierman¹⁵³, W.R. Cunningham⁵⁷,
 S. Czekierda⁸⁵, P. Czodrowski³⁶, M.J. Da Cunha Sargedas De Sousa^{60b}, J.V. Da Fonseca Pinto^{81b},
 C. Da Via¹⁰¹, W. Dabrowski^{84a}, T. Dado^{28a}, S. Dahbi^{35e}, T. Dai¹⁰⁶, C. Dallapiccola¹⁰³, M. Dam⁴⁰,
 G. D'amen²⁹, V. D'Amico^{75a,75b}, J. Damp¹⁰⁰, J.R. Dandoy¹³⁷, M.F. Daneri³⁰, N.P. Dang^{181,j}, N.S. Dann¹⁰¹,
 M. Dannerger¹⁷⁵, V. Dao³⁶, G. Darbo^{55b}, O. Dartsi⁵, A. Dattagupta¹³², T. Daubney⁴⁶, S. D'Auria^{69a,69b},
 W. Davey²⁴, C. David⁴⁶, T. Davidek¹⁴³, D.R. Davis⁴⁹, I. Dawson¹⁴⁹, K. De⁸, R. De Asmundis^{70a},
 M. De Beurs¹²⁰, S. De Castro^{23b,23a}, S. De Cecco^{73a,73b}, N. De Groot¹¹⁹, P. de Jong¹²⁰, H. De la Torre¹⁰⁷,
 A. De Maria^{15c}, D. De Pedis^{73a}, A. De Salvo^{73a}, U. De Sanctis^{74a,74b}, M. De Santis^{74a,74b}, A. De Santo¹⁵⁶,
 K. De Vasconcelos Corga¹⁰², J.B. De Vivie De Regie⁶⁵, C. Debenedetti¹⁴⁶, D.V. Dedovich⁸⁰,
 A.M. Deiana⁴², M. Del Gaudio^{41b,41a}, J. Del Peso⁹⁹, Y. Delabat Diaz⁴⁶, D. Delgove⁶⁵, F. Deliot^{145,r},
 C.M. Delitzsch⁷, M. Della Pietra^{70a,70b}, D. Della Volpe⁵⁴, A. Dell'Acqua³⁶, L. Dell'Asta^{74a,74b},
 M. Delmastro⁵, C. Delporte⁶⁵, P.A. Delsart⁵⁸, D.A. DeMarco¹⁶⁷, S. Demers¹⁸³, M. Demichev⁸⁰,
 G. Demontigny¹¹⁰, S.P. Denisov¹²³, D. Denysiuk¹²⁰, L. D'Eramo¹³⁶, D. Derendarz⁸⁵, J.E. Derkaoui^{35d},
 F. Derue¹³⁶, P. Dervan⁹¹, K. Desch²⁴, C. Deterre⁴⁶, K. Dette¹⁶⁷, C. Deutsch²⁴, M.R. Devesa³⁰,
 P.O. Deviveiros³⁶, A. Dewhurst¹⁴⁴, F.A. Di Bello⁵⁴, A. Di Ciaccio^{74a,74b}, L. Di Ciaccio⁵,
 W.K. Di Clemente¹³⁷, C. Di Donato^{70a,70b}, A. Di Girolamo³⁶, G. Di Gregorio^{72a,72b}, B. Di Micco^{75a,75b},
 R. Di Nardo¹⁰³, K.F. Di Petrillo⁵⁹, R. Di Sipio¹⁶⁷, D. Di Valentino³⁴, C. Diaconu¹⁰², F.A. Dias⁴⁰,
 T. Dias Do Vale^{140a}, M.A. Diaz^{147a}, J. Dickinson¹⁸, E.B. Diehl¹⁰⁶, J. Dietrich¹⁹, S. Díez Cornell⁴⁶,
 A. Dimitrievska¹⁸, W. Ding^{15b}, J. Dingfelder²⁴, F. Dittus³⁶, F. Djama¹⁰², T. Djobava^{159b}, J.I. Djuvsland¹⁷,
 M.A.B. Do Vale^{81c}, M. Dobre^{27b}, D. Dodsworth²⁶, C. Doglioni⁹⁷, J. Dolejsi¹⁴³, Z. Dolezal¹⁴³,
 M. Donadelli^{81d}, B. Dong^{60c}, J. Donini³⁸, A. D'onofrio⁹³, M. D'Onofrio⁹¹, J. Dopke¹⁴⁴, A. Doria^{70a},
 M.T. Dova⁸⁹, A.T. Doyle⁵⁷, E. Drechsler¹⁵², E. Dreyer¹⁵², T. Dreyer⁵³, A.S. Drobac¹⁷⁰, D. Du^{60b},
 Y. Duan^{60b}, F. Dubinin¹¹¹, M. Dubovsky^{28a}, A. Dubreuil⁵⁴, E. Duchovni¹⁸⁰, G. Duckeck¹¹⁴,
 A. Ducourthial¹³⁶, O.A. Ducu¹¹⁰, D. Duda¹¹⁵, A. Dudarev³⁶, A.C. Dudder¹⁰⁰, E.M. Duffield¹⁸,
 L. Duflot⁶⁵, M. Dührssen³⁶, C. Dülsen¹⁸², M. Dumancic¹⁸⁰, A.E. Dumitriu^{27b}, A.K. Duncan⁵⁷,
 M. Dunford^{61a}, A. Duperrin¹⁰², H. Duran Yildiz^{4a}, M. Düren⁵⁶, A. Durglishvili^{159b}, D. Duschinger⁴⁸,
 B. Dutta⁴⁶, D. Duvnjak¹, G.I. Dyckes¹³⁷, M. Dyndal³⁶, S. Dysch¹⁰¹, B.S. Dziedzic⁸⁵, K.M. Ecker¹¹⁵,
 R.C. Edgar¹⁰⁶, M.G. Eggleston⁴⁹, T. Eifert³⁶, G. Eigen¹⁷, K. Einsweiler¹⁸, T. Ekelof¹⁷², H. El Jarrai^{35e},
 M. El Kacimi^{35c}, R. El Kosseifi¹⁰², V. Ellajosyula¹⁷², M. Ellert¹⁷², F. Ellinghaus¹⁸², A.A. Elliot⁹³,
 N. Ellis³⁶, J. Elmsheuser²⁹, M. Elsing³⁶, D. Emeliyanov¹⁴⁴, A. Emerman³⁹, Y. Enari¹⁶³, M.B. Epland⁴⁹,
 J. Erdmann⁴⁷, A. Ereditato²⁰, M. Errenst³⁶, M. Escalier⁶⁵, C. Escobar¹⁷⁴, O. Estrada Pastor¹⁷⁴,
 E. Etzion¹⁶¹, H. Evans⁶⁶, A. Ezhilov¹³⁸, F. Fabbri⁵⁷, L. Fabbri^{23b,23a}, V. Fabiani¹¹⁹, G. Facini⁹⁵,
 R.M. Faisca Rodrigues Pereira^{140a}, R.M. Fakhrutdinov¹²³, S. Falciano^{73a}, P.J. Falke⁵, S. Falke⁵,
 J. Faltova¹⁴³, Y. Fang^{15a}, Y. Fang^{15a}, G. Fanourakis⁴⁴, M. Fanti^{69a,69b}, M. Faraj^{67a,67c,u}, A. Farbin⁸,
 A. Farilla^{75a}, E.M. Farina^{71a,71b}, T. Farooque¹⁰⁷, S. Farrell¹⁸, S.M. Farrington⁵⁰, P. Farthouat³⁶, F. Fassi^{35e},
 P. Fassnacht³⁶, D. Fassouliotis⁹, M. Faucci Giannelli⁵⁰, W.J. Fawcett³², L. Fayard⁶⁵, O.L. Fedin^{138,p},
 W. Fedorko¹⁷⁵, M. Feickert⁴², L. Feligioni¹⁰², A. Fell¹⁴⁹, C. Feng^{60b}, E.J. Feng³⁶, M. Feng⁴⁹,
 M.J. Fenton⁵⁷, A.B. Fenyuk¹²³, J. Ferrando⁴⁶, A. Ferrante¹⁷³, A. Ferrari¹⁷², P. Ferrari¹²⁰, R. Ferrari^{71a},
 D.E. Ferreira de Lima^{61b}, A. Ferrer¹⁷⁴, D. Ferrere⁵⁴, C. Ferretti¹⁰⁶, F. Fiedler¹⁰⁰, A. Filipčič⁹²,
 F. Filthaut¹¹⁹, K.D. Finelli²⁵, M.C.N. Fiolhais^{140a,140c,a}, L. Fiorini¹⁷⁴, F. Fischer¹¹⁴, W.C. Fisher¹⁰⁷,
 I. Fleck¹⁵¹, P. Fleischmann¹⁰⁶, R.R.M. Fletcher¹³⁷, T. Flick¹⁸², B.M. Flierl¹¹⁴, L. Flores¹³⁷,
 L.R. Flores Castillo^{63a}, F.M. Follega^{76a,76b}, N. Fomin¹⁷, J.H. Foo¹⁶⁷, G.T. Forcolin^{76a,76b}, A. Formica¹⁴⁵,
 F.A. Förster¹⁴, A.C. Forti¹⁰¹, A.G. Foster²¹, M.G. Foti¹³⁵, D. Fournier⁶⁵, H. Fox⁹⁰, P. Francavilla^{72a,72b},
 S. Francescato^{73a,73b}, M. Franchini^{23b,23a}, S. Franchino^{61a}, D. Francis³⁶, L. Franconi²⁰, M. Franklin⁵⁹,
 A.N. Fray⁹³, P.M. Freeman²¹, B. Freund¹¹⁰, W.S. Freund^{81b}, E.M. Freundlich⁴⁷, D.C. Frizzell¹²⁹,
 D. Froidevaux³⁶, J.A. Frost¹³⁵, C. Fukunaga¹⁶⁴, E. Fullana Torregrosa¹⁷⁴, E. Fumagalli^{55b,55a},
 T. Fusayasu¹¹⁶, J. Fuster¹⁷⁴, A. Gabrielli^{23b,23a}, A. Gabrielli¹⁸, G.P. Gach^{84a}, S. Gadatsch⁵⁴, P. Gadow¹¹⁵,

G. Gagliardi^{55b,55a}, L.G. Gagnon¹¹⁰, C. Galea^{27b}, B. Galhardo^{140a}, G.E. Gallardo¹³⁵, E.J. Gallas¹³⁵,
 B.J. Gallop¹⁴⁴, G. Galster⁴⁰, R. Gamboa Goni⁹³, K.K. Gan¹²⁷, S. Ganguly¹⁸⁰, J. Gao^{60a}, Y. Gao⁵⁰,
 Y.S. Gao^{31,m}, C. García¹⁷⁴, J.E. García Navarro¹⁷⁴, J.A. García Pascual^{15a}, C. Garcia-Argos⁵²,
 M. Garcia-Sciveres¹⁸, R.W. Gardner³⁷, N. Garelli¹⁵³, S. Gargiulo⁵², V. Garonne¹³⁴, A. Gaudiello^{55b,55a},
 G. Gaudio^{71a}, I.L. Gavrilenco¹¹¹, A. Gavrilyuk¹²⁴, C. Gay¹⁷⁵, G. Gaycken⁴⁶, E.N. Gazis¹⁰,
 A.A. Geanta^{27b}, C.M. Gee¹⁴⁶, C.N.P. Gee¹⁴⁴, J. Geisen⁵³, M. Geisen¹⁰⁰, M.P. Geisler^{61a}, C. Gemme^{55b},
 M.H. Genest⁵⁸, C. Geng¹⁰⁶, S. Gentile^{73a,73b}, S. George⁹⁴, T. Geralis⁴⁴, L.O. Gerlach⁵³,
 P. Gessinger-Befurt¹⁰⁰, G. Gessner⁴⁷, S. Ghasemi¹⁵¹, M. Ghasemi Bostanabad¹⁷⁶, A. Ghosh⁶⁵,
 A. Ghosh⁷⁸, B. Giacobbe^{23b}, S. Giagu^{73a,73b}, N. Giangiocomi^{23b,23a}, P. Giannetti^{72a}, A. Giannini^{70a,70b},
 G. Giannini¹⁴, S.M. Gibson⁹⁴, M. Gignac¹⁴⁶, D. Gillberg³⁴, G. Gilles¹⁸², D.M. Gingrich^{3,aw},
 M.P. Giordani^{67a,67c}, F.M. Giorgi^{23b}, P.F. Giraud¹⁴⁵, G. Giugliarelli^{67a,67c}, D. Giugni^{69a}, F. Giuli^{74a,74b},
 S. Gkaitatzis¹⁶², I. Gkialas^{9,h}, E.L. Gkougkousis¹⁴, P. Gkountoumis¹⁰, L.K. Gladilin¹¹³, C. Glasman⁹⁹,
 J. Glatzer¹⁴, P.C.F. Glaysher⁴⁶, A. Glazov⁴⁶, G.R. Gledhill¹³², M. Goblirsch-Kolb²⁶, D. Godin¹¹⁰,
 S. Goldfarb¹⁰⁵, T. Golling⁵⁴, D. Golubkov¹²³, A. Gomes^{140a,140b}, R. Goncalves Gama⁵³, R. Gonçalo^{140a},
 G. Gonella⁵², L. Gonella²¹, A. Gongadze⁸⁰, F. Gonnella²¹, J.L. Gonski⁵⁹, S. González de la Hoz¹⁷⁴,
 S. Gonzalez-Sevilla⁵⁴, G.R. Gonzalvo Rodriguez¹⁷⁴, L. Goossens³⁶, P.A. Gorbounov¹²⁴, H.A. Gordon²⁹,
 B. Gorini³⁶, E. Gorini^{68a,68b}, A. Gorišek⁹², A.T. Goshaw⁴⁹, M.I. Gostkin⁸⁰, C.A. Gottardo¹¹⁹,
 M. Gouighri^{35b}, D. Goujdami^{35c}, A.G. Goussiou¹⁴⁸, N. Govender^{33c}, C. Goy⁵, E. Gozani¹⁶⁰,
 I. Grabowska-Bold^{84a}, E.C. Graham⁹¹, J. Gramling¹⁷¹, E. Gramstad¹³⁴, S. Grancagnolo¹⁹, M. Grandi¹⁵⁶,
 V. Gratchev¹³⁸, P.M. Gravila^{27f}, F.G. Gravili^{68a,68b}, C. Gray⁵⁷, H.M. Gray¹⁸, C. Grefe²⁴, K. Gregersen⁹⁷,
 I.M. Gregor⁴⁶, P. Grenier¹⁵³, K. Grevtsov⁴⁶, C. Grieco¹⁴, N.A. Grieser¹²⁹, J. Griffiths⁸, A.A. Grillo¹⁴⁶,
 K. Grimm^{31,l}, S. Grinstein^{14,aa}, J.-F. Grivaz⁶⁵, S. Groh¹⁰⁰, E. Gross¹⁸⁰, J. Grosse-Knetter⁵³, Z.J. Grout⁹⁵,
 C. Grud¹⁰⁶, A. Grummer¹¹⁸, L. Guan¹⁰⁶, W. Guan¹⁸¹, J. Guenther³⁶, A. Guerguichon⁶⁵,
 J.G.R. Guerrero Rojas¹⁷⁴, F. Guescini¹¹⁵, D. Guest¹⁷¹, R. Gugel⁵², T. Guillemin⁵, S. Guindon³⁶, U. Gul⁵⁷,
 J. Guo^{60c}, W. Guo¹⁰⁶, Y. Guo^{60a,t}, Z. Guo¹⁰², R. Gupta⁴⁶, S. Gurbuz^{12c}, G. Gustavino¹²⁹, M. Guth⁵²,
 P. Gutierrez¹²⁹, C. Gutschow⁹⁵, C. Guyot¹⁴⁵, C. Gwenlan¹³⁵, C.B. Gwilliam⁹¹, A. Haas¹²⁵, C. Haber¹⁸,
 H.K. Hadavand⁸, N. Haddad^{35e}, A. Hadef^{60a}, S. Hageböck³⁶, M. Haleem¹⁷⁷, J. Haley¹³⁰, G. Halladjian¹⁰⁷,
 G.D. Hallewell¹⁰², K. Hamacher¹⁸², P. Hamal¹³¹, K. Hamano¹⁷⁶, H. Hamdaoui^{35e}, G.N. Hamity¹⁴⁹,
 K. Han^{60a,z}, L. Han^{60a}, S. Han^{15a}, Y.F. Han¹⁶⁷, K. Hanagaki^{82,x}, M. Hance¹⁴⁶, D.M. Handl¹¹⁴,
 B. Haney¹³⁷, R. Hankache¹³⁶, E. Hansen⁹⁷, J.B. Hansen⁴⁰, J.D. Hansen⁴⁰, M.C. Hansen²⁴, P.H. Hansen⁴⁰,
 E.C. Hanson¹⁰¹, K. Hara¹⁶⁹, T. Harenberg¹⁸², S. Harkusha¹⁰⁸, P.F. Harrison¹⁷⁸, N.M. Hartmann¹¹⁴,
 Y. Hasegawa¹⁵⁰, A. Hasib⁵⁰, S. Hassani¹⁴⁵, S. Haug²⁰, R. Hauser¹⁰⁷, L.B. Havener³⁹, M. Havranek¹⁴²,
 C.M. Hawkes²¹, R.J. Hawkings³⁶, D. Hayden¹⁰⁷, C. Hayes¹⁵⁵, R.L. Hayes¹⁷⁵, C.P. Hays¹³⁵, J.M. Hays⁹³,
 H.S. Hayward⁹¹, S.J. Haywood¹⁴⁴, F. He^{60a}, M.P. Heath⁵⁰, V. Hedberg⁹⁷, L. Heelan⁸, S. Heer²⁴,
 K.K. Heidegger⁵², W.D. Heidorn⁷⁹, J. Heilman³⁴, S. Heim⁴⁶, T. Heim¹⁸, B. Heinemann^{46,as},
 J.J. Heinrich¹³², L. Heinrich³⁶, C. Heinz⁵⁶, J. Hejbal¹⁴¹, L. Helary^{61b}, A. Held¹⁷⁵, S. Hellesund¹³⁴,
 C.M. Helling¹⁴⁶, S. Hellman^{45a,45b}, C. Helsens³⁶, R.C.W. Henderson⁹⁰, Y. Heng¹⁸¹, S. Henkelmann¹⁷⁵,
 A.M. Henriques Correia³⁶, G.H. Herbert¹⁹, H. Herde²⁶, V. Herget¹⁷⁷, Y. Hernández Jiménez^{33e},
 H. Herr¹⁰⁰, M.G. Herrmann¹¹⁴, T. Herrmann⁴⁸, G. Herten⁵², R. Hertenberger¹¹⁴, L. Hervas³⁶,
 T.C. Herwig¹³⁷, G.G. Hesketh⁹⁵, N.P. Hessey^{168a}, A. Higashida¹⁶³, S. Higashino⁸²,
 E. Higón-Rodríguez¹⁷⁴, K. Hildebrand³⁷, E. Hill¹⁷⁶, J.C. Hill³², K.K. Hill²⁹, K.H. Hiller⁴⁶, S.J. Hillier²¹,
 M. Hils⁴⁸, I. Hinchliffe¹⁸, F. Hinterkeuser²⁴, M. Hirose¹³³, S. Hirose⁵², D. Hirschbuehl¹⁸², B. Hiti⁹²,
 O. Hladík¹⁴¹, D.R. Hlaluku^{33e}, X. Hoad⁵⁰, J. Hobbs¹⁵⁵, N. Hod¹⁸⁰, M.C. Hodgkinson¹⁴⁹, A. Hoecker³⁶,
 F. Hoenig¹¹⁴, D. Hohn⁵², D. Hohov⁶⁵, T.R. Holmes³⁷, M. Holzbock¹¹⁴, L.B.A.H. Hommels³²,
 S. Honda¹⁶⁹, T.M. Hong¹³⁹, J.C. Honig⁵², A. Hönl¹¹⁵, B.H. Hooberman¹⁷³, W.H. Hopkins⁶, Y. Horii¹¹⁷,
 P. Horn⁴⁸, L.A. Horyn³⁷, S. Hou¹⁵⁸, A. Hoummada^{35a}, J. Howarth¹⁰¹, J. Hoya⁸⁹, M. Hrabovsky¹³¹,
 J. Hrdinka⁷⁷, I. Hristova¹⁹, J. Hrvnac⁶⁵, A. Hrynevich¹⁰⁹, T. Hrynn'ova⁵, P.J. Hsu⁶⁴, S.-C. Hsu¹⁴⁸, Q. Hu²⁹,

S. Hu^{60c}, Y.F. Hu^{15a,15d}, D.P. Huang⁹⁵, Y. Huang^{60a}, Y. Huang^{15a}, Z. Hubacek¹⁴², F. Hubaut¹⁰²,
 M. Huebner²⁴, F. Huegging²⁴, T.B. Huffman¹³⁵, M. Huhtinen³⁶, R.F.H. Hunter³⁴, P. Huo¹⁵⁵, A.M. Hupe³⁴,
 N. Huseynov^{80,ah}, J. Huston¹⁰⁷, J. Huth⁵⁹, R. Hynehan¹⁰⁶, S. Hyrych^{28a}, G. Iacobucci⁵⁴, G. Iakovidis²⁹,
 I. Ibragimov¹⁵¹, L. Iconomou-Fayard⁶⁵, Z. Idrissi^{35e}, P. Iengo³⁶, R. Ignazzi⁴⁰, O. Igonkina^{120,ac,*},
 R. Iguchi¹⁶³, T. Iizawa⁵⁴, Y. Ikegami⁸², M. Ikeno⁸², D. Iliadis¹⁶², N. Ilic^{119,167,af}, F. Iltzsche⁴⁸,
 G. Introzzi^{71a,71b}, M. Iodice^{75a}, K. Iordanidou^{168a}, V. Ippolito^{73a,73b}, M.F. Isacson¹⁷², M. Ishino¹⁶³,
 W. Islam¹³⁰, C. Issever¹³⁵, S. Istin¹⁶⁰, F. Ito¹⁶⁹, J.M. Iturbe Ponce^{63a}, R. Iuppa^{76a,76b}, A. Ivina¹⁸⁰,
 H. Iwasaki⁸², J.M. Izen⁴³, V. Izzo^{70a}, P. Jacka¹⁴¹, P. Jackson¹, R.M. Jacobs²⁴, B.P. Jaeger¹⁵², V. Jain²,
 G. Jäkel¹⁸², K.B. Jakobi¹⁰⁰, K. Jakobs⁵², S. Jakobsen⁷⁷, T. Jakoubek¹⁴¹, J. Jamieson⁵⁷, K.W. Janas^{84a},
 R. Jansky⁵⁴, J. Janssen²⁴, M. Janus⁵³, P.A. Janus^{84a}, G. Jarlskog⁹⁷, N. Javadov^{80,ah}, T. Javůrek³⁶,
 M. Javurkova⁵², F. Jeanneau¹⁴⁵, L. Jeanty¹³², J. Jejelava^{159a,ai}, A. Jelinskas¹⁷⁸, P. Jenni^{52,b}, J. Jeong⁴⁶,
 N. Jeong⁴⁶, S. Jézéquel⁵, H. Ji¹⁸¹, J. Jia¹⁵⁵, H. Jiang⁷⁹, Y. Jiang^{60a}, Z. Jiang^{153,q}, S. Jiggins⁵²,
 F.A. Jimenez Morales³⁸, J. Jimenez Pena¹¹⁵, S. Jin^{15c}, A. Jinaru^{27b}, O. Jinnouchi¹⁶⁵, H. Jivan^{33e},
 P. Johansson¹⁴⁹, K.A. Johns⁷, C.A. Johnson⁶⁶, K. Jon-And^{45a,45b}, R.W.L. Jones⁹⁰, S.D. Jones¹⁵⁶, S. Jones⁷,
 T.J. Jones⁹¹, J. Jongmanns^{61a}, P.M. Jorge^{140a}, J. Jovicevic³⁶, X. Ju¹⁸, J.J. Junggeburth¹¹⁵,
 A. Juste Rozas^{14,aa}, A. Kaczmarśka⁸⁵, M. Kado^{73a,73b}, H. Kagan¹²⁷, M. Kagan¹⁵³, C. Kahra¹⁰⁰, T. Kaji¹⁷⁹,
 E. Kajomovitz¹⁶⁰, C.W. Kalderon⁹⁷, A. Kaluza¹⁰⁰, A. Kamenshchikov¹²³, M. Kaneda¹⁶³, L. Kanjur⁹²,
 Y. Kano¹⁶³, V.A. Kantserov¹¹², J. Kanzaki⁸², L.S. Kaplan¹⁸¹, D. Kar^{33e}, K. Karava¹³⁵, M.J. Kareem^{168b},
 S.N. Karpov⁸⁰, Z.M. Karpova⁸⁰, V. Kartvelishvili⁹⁰, A.N. Karyukhin¹²³, L. Kashif¹⁸¹, R.D. Kass¹²⁷,
 A. Kastanas^{45a,45b}, C. Kato^{60d,60c}, J. Katzy⁴⁶, K. Kawade¹⁵⁰, K. Kawagoe⁸⁸, T. Kawaguchi¹¹⁷,
 T. Kawamoto¹⁶³, G. Kawamura⁵³, E.F. Kay¹⁷⁶, V.F. Kazanin^{122b,122a}, R. Keeler¹⁷⁶, R. Kehoe⁴²,
 J.S. Keller³⁴, E. Kellermann⁹⁷, D. Kelsey¹⁵⁶, J.J. Kempster²¹, J. Kendrick²¹, O. Kepka¹⁴¹, S. Kersten¹⁸²,
 B.P. Kerševan⁹², S. Ketabchi Haghigat¹⁶⁷, M. Khader¹⁷³, F. Khalil-Zada¹³, M. Khandoga¹⁴⁵,
 A. Khanov¹³⁰, A.G. Kharlamov^{122b,122a}, T. Kharlamova^{122b,122a}, E.E. Khoda¹⁷⁵, A. Khodinov¹⁶⁶,
 T.J. Khoo⁵⁴, E. Khramov⁸⁰, J. Khubua^{159b}, S. Kido⁸³, M. Kiehn⁵⁴, C.R. Kilby⁹⁴, Y.K. Kim³⁷, N. Kimura⁹⁵,
 O.M. Kind¹⁹, B.T. King^{91,*}, D. Kirchmeier⁴⁸, J. Kirk¹⁴⁴, A.E. Kiryunin¹¹⁵, T. Kishimoto¹⁶³,
 D.P. Kisliuk¹⁶⁷, V. Kitali⁴⁶, O. Kivernyk⁵, T. Klapdor-Kleingrothaus⁵², M. Klassen^{61a}, M.H. Klein¹⁰⁶,
 M. Klein⁹¹, U. Klein⁹¹, K. Kleinknecht¹⁰⁰, P. Klimek¹²¹, A. Klimentov²⁹, T. Klingl²⁴, T. Klioutchnikova³⁶,
 F.F. Klitzner¹¹⁴, P. Kluit¹²⁰, S. Kluth¹¹⁵, E. Kneringer⁷⁷, E.B.F.G. Knoops¹⁰², A. Knue⁵², D. Kobayashi⁸⁸,
 T. Kobayashi¹⁶³, M. Kobel⁴⁸, M. Kocian¹⁵³, P. Kodys¹⁴³, P.T. Koenig²⁴, T. Koffas³⁴, N.M. Köhler³⁶,
 T. Koi¹⁵³, M. Kolb^{61b}, I. Koletsou⁵, T. Komarek¹³¹, T. Kondo⁸², N. Kondrashova^{60c}, K. Köneke⁵²,
 A.C. König¹¹⁹, T. Kono¹²⁶, R. Konoplich^{125,an}, V. Konstantinides⁹⁵, N. Konstantinidis⁹⁵, B. Konya⁹⁷,
 R. Kopeliansky⁶⁶, S. Koperny^{84a}, K. Korcyl⁸⁵, K. Kordas¹⁶², G. Koren¹⁶¹, A. Korn⁹⁵, I. Korolkov¹⁴,
 E.V. Korolkova¹⁴⁹, N. Korotkova¹¹³, O. Kortner¹¹⁵, S. Kortner¹¹⁵, T. Kosek¹⁴³, V.V. Kostyukhin¹⁶⁶,
 A. Kotsokechagia⁶⁵, A. Kotwal¹⁴⁹, A. Koulouris¹⁰, A. Kourkoumeli-Charalampidi^{71a,71b}, C. Kourkoumelis⁹,
 E. Kourlitis¹⁴⁹, V. Kouskoura²⁹, A.B. Kowalewska⁸⁵, R. Kowalewski¹⁷⁶, C. Kozakai¹⁶³, W. Kozanecki¹⁴⁵,
 A.S. Kozhin¹²³, V.A. Kramarenko¹¹³, G. Kramberger⁹², D. Krasnopevtsev^{60a}, M.W. Krasny¹³⁶,
 A. Krasznahorkay³⁶, D. Krauss¹¹⁵, J.A. Kremer^{84a}, J. Kretschmar⁹¹, P. Krieger¹⁶⁷, F. Krieter¹¹⁴,
 A. Krishnan^{61b}, K. Krizka¹⁸, K. Kroeninger⁴⁷, H. Kroha¹¹⁵, J. Kroll¹⁴¹, J. Kroll¹³⁷, K.S. Krowpman¹⁰⁷,
 J. Krstic¹⁶, U. Kruchonak⁸⁰, H. Krüger²⁴, N. Krumnack⁷⁹, M.C. Kruse⁴⁹, J.A. Krzysiak⁸⁵, T. Kubota¹⁰⁵,
 O. Kuchinskaya¹⁶⁶, S. Kuday^{4b}, J.T. Kuechler⁴⁶, S. Kuehn³⁶, A. Kugel^{61a}, T. Kuhl⁴⁶, V. Kukhtin⁸⁰,
 R. Kukla¹⁰², Y. Kulchitsky^{108,ak}, S. Kuleshov^{147d}, Y.P. Kulinich¹⁷³, M. Kuna⁵⁸, T. Kunigo⁸⁶, A. Kupco¹⁴¹,
 T. Kupfer⁴⁷, O. Kuprash⁵², H. Kurashige⁸³, L.L. Kurchaninov^{168a}, Y.A. Kurochkin¹⁰⁸, A. Kurova¹¹²,
 M.G. Kurth^{15a,15d}, E.S. Kuwertz³⁶, M. Kuze¹⁶⁵, A.K. Kvam¹⁴⁸, J. Kvita¹³¹, T. Kwan¹⁰⁴, A. La Rosa¹¹⁵,
 L. La Rotonda^{41b,41a}, F. La Ruffa^{41b,41a}, C. Lacasta¹⁷⁴, F. Lacava^{73a,73b}, D.P.J. Lack¹⁰¹, H. Lacker¹⁹,
 D. Lacour¹³⁶, E. Ladygin⁸⁰, R. Lafaye⁵, B. Laforge¹³⁶, T. Lagouri^{33e}, S. Lai⁵³, S. Lammers⁶⁶, W. Lampl⁷,
 C. Lampoudis¹⁶², E. Lançon²⁹, U. Landgraf⁵², M.P.J. Landon⁹³, M.C. Lanfermann⁵⁴, V.S. Lang⁴⁶,

J.C. Lange⁵³, R.J. Langenberg³⁶, A.J. Lankford¹⁷¹, F. Lanni²⁹, K. Lantzsch²⁴, A. Lanza^{71a},
 A. Lapertosa^{55b,55a}, S. Laplace¹³⁶, J.F. Laporte¹⁴⁵, T. Lari^{69a}, F. Lasagni Manghi^{23b,23a}, M. Lassnig³⁶,
 T.S. Lau^{63a}, A. Laudrain⁶⁵, A. Laurier³⁴, M. Lavorgna^{70a,70b}, S.D. Lawlor⁹⁴, M. Lazzaroni^{69a,69b}, B. Le¹⁰⁵,
 E. Le Guirriec¹⁰², M. LeBlanc⁷, T. LeCompte⁶, F. Ledroit-Guillon⁵⁸, A.C.A. Lee⁹⁵, C.A. Lee²⁹,
 G.R. Lee¹⁷, L. Lee⁵⁹, S.C. Lee¹⁵⁸, S.J. Lee³⁴, S. Lee⁷⁹, B. Lefebvre^{168a}, H.P. Lefebvre⁹⁴, M. Lefebvre¹⁷⁶,
 F. Legger¹¹⁴, C. Leggett¹⁸, K. Lehmann¹⁵², N. Lehmann¹⁸², G. Lehmann Miotto³⁶, W.A. Leight⁴⁶,
 A. Leisos^{162,y}, M.A.L. Leite^{81d}, C.E. Leitgeb¹¹⁴, R. Leitner¹⁴³, D. Lelouch^{180,*}, K.J.C. Leney⁴²,
 T. Lenz²⁴, B. Lenzi³⁶, R. Leone⁷, S. Leone^{72a}, C. Leonidopoulos⁵⁰, A. Leopold¹³⁶, G. Lerner¹⁵⁶,
 C. Leroy¹¹⁰, R. Les¹⁶⁷, C.G. Lester³², M. Levchenko¹³⁸, J. Levêque⁵, D. Levin¹⁰⁶, L.J. Levinson¹⁸⁰,
 D.J. Lewis²¹, B. Li^{15b}, B. Li¹⁰⁶, C-Q. Li^{60a}, F. Li^{60c}, H. Li^{60a}, H. Li^{60b}, J. Li^{60c}, K. Li¹⁵³, L. Li^{60c},
 M. Li^{15a,15d}, Q. Li^{15a,15d}, Q.Y. Li^{60a}, S. Li^{60d,60c}, X. Li⁴⁶, Y. Li⁴⁶, Z. Li^{60b}, Z. Liang^{15a}, B. Liberti^{74a},
 A. Liblong¹⁶⁷, K. Lie^{63c}, C.Y. Lin³², K. Lin¹⁰⁷, T.H. Lin¹⁰⁰, R.A. Linck⁶⁶, J.H. Lindon²¹, A.L. Lionti⁵⁴,
 E. Lipeles¹³⁷, A. Lipniacka¹⁷, M. Lisovyi^{61b}, T.M. Liss^{173,au}, A. Lister¹⁷⁵, A.M. Litke¹⁴⁶, J.D. Little⁸,
 B. Liu⁷⁹, B.L. Liu⁶, H.B. Liu²⁹, H. Liu¹⁰⁶, J.B. Liu^{60a}, J.K.K. Liu¹³⁵, K. Liu¹³⁶, M. Liu^{60a}, P. Liu¹⁸,
 Y. Liu^{15a,15d}, Y.L. Liu¹⁰⁶, Y.W. Liu^{60a}, M. Livan^{71a,71b}, A. Lleres⁵⁸, J. Llorente Merino¹⁵², S.L. Lloyd⁹³,
 C.Y. Lo^{63b}, F. Lo Sterzo⁴², E.M. Lobodzinska⁴⁶, P. Loch⁷, S. Loffredo^{74a,74b}, T. Lohse¹⁹, K. Lohwasser¹⁴⁹,
 M. Lokajicek¹⁴¹, J.D. Long¹⁷³, R.E. Long⁹⁰, L. Longo³⁶, K.A.Looper¹²⁷, J.A. Lopez^{147d}, I. Lopez Paz¹⁰¹,
 A. Lopez Solis¹⁴⁹, J. Lorenz¹¹⁴, N. Lorenzo Martinez⁵, M. Losada^{22a}, P.J. Lösel¹¹⁴, A. Lösle⁵², X. Lou⁴⁶,
 X. Lou^{15a}, A. Lounis⁶⁵, J. Love⁶, P.A. Love⁹⁰, J.J. Lozano Bahilo¹⁷⁴, M. Lu^{60a}, Y.J. Lu⁶⁴, H.J. Lubatti¹⁴⁸,
 C. Luci^{73a,73b}, A. Lucotte⁵⁸, C. Luedtke⁵², F. Luehring⁶⁶, I. Luise¹³⁶, L. Luminari^{73a}, B. Lund-Jensen¹⁵⁴,
 M.S. Lutz¹⁰³, D. Lynn²⁹, R. Lysak¹⁴¹, E. Lytken⁹⁷, F. Lyu^{15a}, V. Lyubushkin⁸⁰, T. Lyubushkina⁸⁰, H. Ma²⁹,
 L.L. Ma^{60b}, Y. Ma^{60b}, G. Maccarrone⁵¹, A. Macchiolo¹¹⁵, C.M. Macdonald¹⁴⁹, J. Machado Miguens¹³⁷,
 D. Madaffari¹⁷⁴, R. Madar³⁸, W.F. Mader⁴⁸, N. Madysa⁴⁸, J. Maeda⁸³, S. Maeland¹⁷, T. Maeno²⁹,
 M. Maerker⁴⁸, A.S. Maevskiy¹¹³, V. Magerl⁵², N. Magini⁷⁹, D.J. Mahon³⁹, C. Maidantchik^{81b}, T. Maier¹¹⁴,
 A. Maio^{140a,140b,140d}, K. Maj^{84a}, O. Majersky^{28a}, S. Majewski¹³², Y. Makida⁸², N. Makovec⁶⁵,
 B. Malaescu¹³⁶, Pa. Malecki⁸⁵, V.P. Maleev¹³⁸, F. Malek⁵⁸, U. Mallik⁷⁸, D. Malon⁶, C. Malone³²,
 S. Maltezos¹⁰, S. Malyukov⁸⁰, J. Mamuzic¹⁷⁴, G. Mancini⁵¹, I. Mandić⁹², L. Manhaes de Andrade Filho^{81a},
 I.M. Maniatis¹⁶², J. Manjarres Ramos⁴⁸, K.H. Mankinen⁹⁷, A. Mann¹¹⁴, A. Manousos⁷⁷, B. Mansoulie¹⁴⁵,
 I. Manthos¹⁶², S. Manzoni¹²⁰, A. Marantis¹⁶², G. Marceca³⁰, L. Marchese¹³⁵, G. Marchiori¹³⁶,
 M. Marcisovsky¹⁴¹, L. Marcoccia^{74a,74b}, C. Marcon⁹⁷, C.A. Marin Tobon³⁶, M. Marjanovic¹²⁹,
 Z. Marshall¹⁸, M.U.F. Martensson¹⁷², S. Marti-Garcia¹⁷⁴, C.B. Martin¹²⁷, T.A. Martin¹⁷⁸, V.J. Martin⁵⁰,
 B. Martin dit Latour¹⁷, L. Martinelli^{75a,75b}, M. Martinez^{14,aa}, V.I. Martinez Outshoorn¹⁰³,
 S. Martin-Haugh¹⁴⁴, V.S. Martoiu^{27b}, A.C. Martyniuk⁹⁵, A. Marzin³⁶, S.R. Maschek¹¹⁵, L. Masetti¹⁰⁰,
 T. Mashimo¹⁶³, R. Mashinistov¹¹¹, J. Masik¹⁰¹, A.L. Maslennikov^{122b,122a}, L. Massa^{74a,74b},
 P. Massarotti^{70a,70b}, P. Mastrandrea^{72a,72b}, A. Mastroberardino^{41b,41a}, T. Masubuchi¹⁶³, D. Matakias¹⁰,
 A. Matic¹¹⁴, P. Mättig²⁴, J. Maurer^{27b}, B. Maček⁹², D.A. Maximov^{122b,122a}, R. Mazini¹⁵⁸, I. Maznas¹⁶²,
 S.M. Mazza¹⁴⁶, S.P. Mc Kee¹⁰⁶, T.G. McCarthy¹¹⁵, W.P. McCormack¹⁸, E.F. McDonald¹⁰⁵,
 J.A. McFayden³⁶, G. Mchedlidze^{159b}, M.A. McKay⁴², K.D. McLean¹⁷⁶, S.J. McMahon¹⁴⁴,
 P.C. McNamara¹⁰⁵, C.J. McNicol¹⁷⁸, R.A. McPherson^{176,af}, J.E. Mdhluli^{33e}, Z.A. Meadows¹⁰³,
 S. Meehan³⁶, T. Megy⁵², S. Mehlhase¹¹⁴, A. Mehta⁹¹, T. Meideck⁵⁸, B. Meirose⁴³, D. Melini¹⁷⁴,
 B.R. Mellado Garcia^{33e}, J.D. Mellenthin⁵³, M. Melo^{28a}, F. Meloni⁴⁶, A. Melzer²⁴, S.B. Menary¹⁰¹,
 E.D. Mendes Gouveia^{140a,140e}, L. Meng³⁶, X.T. Meng¹⁰⁶, S. Menke¹¹⁵, E. Meoni^{41b,41a}, S. Mergelmeyer¹⁹,
 S.A.M. Merkt¹³⁹, C. Merlassino²⁰, P. Mermod⁵⁴, L. Merola^{70a,70b}, C. Meroni^{69a}, O. Meshkov^{113,111},
 J.K.R. Meshreki¹⁵¹, A. Messina^{73a,73b}, J. Metcalfe⁶, A.S. Mete¹⁷¹, C. Meyer⁶⁶, J. Meyer¹⁶⁰, J.-P. Meyer¹⁴⁵,
 H. Meyer Zu Theenhausen^{61a}, F. Miano¹⁵⁶, M. Michetti¹⁹, R.P. Middleton¹⁴⁴, L. Mijović⁵⁰,
 G. Mikenberg¹⁸⁰, M. Mikestikova¹⁴¹, M. Mikuž⁹², H. Mildner¹⁴⁹, M. Milesi¹⁰⁵, A. Milic¹⁶⁷, D.A. Millar⁹³,
 D.W. Miller³⁷, A. Milov¹⁸⁰, D.A. Milstead^{45a,45b}, R.A. Mina^{153,q}, A.A. Minaenko¹²³, M. Miñano Moya¹⁷⁴,

I.A. Minashvili^{159b}, A.I. Mincer¹²⁵, B. Mindur^{84a}, M. Mineev⁸⁰, Y. Minegishi¹⁶³, L.M. Mir¹⁴,
 A. Mirta^{68a,68b}, K.P. Mistry¹³⁷, T. Mitani¹⁷⁹, J. Mitrevski¹¹⁴, V.A. Mitsou¹⁷⁴, M. Mittal^{60c}, O. Miu¹⁶⁷,
 A. Miucci²⁰, P.S. Miyagawa¹⁴⁹, A. Mizukami⁸², J.U. Mjörnmark⁹⁷, T. Mkrtchyan¹⁸⁴, M. Mlynarikova¹⁴³,
 T. Moa^{45a,45b}, K. Mochizuki¹¹⁰, P. Mogg⁵², S. Mohapatra³⁹, R. Moles-Valls²⁴, M.C. Mondragon¹⁰⁷,
 K. Mönig⁴⁶, J. Monk⁴⁰, E. Monnier¹⁰², A. Montalbano¹⁵², J. Montejo Berlingen³⁶, M. Montella⁹⁵,
 F. Monticelli⁸⁹, S. Monzani^{69a}, N. Morange⁶⁵, D. Moreno^{22a}, M. Moreno Llácer³⁶, C. Moreno Martinez¹⁴,
 P. Morettini^{55b}, M. Morgenstern¹²⁰, S. Morgenstern⁴⁸, D. Mori¹⁵², M. Morii⁵⁹, M. Morinaga¹⁷⁹,
 V. Morisbak¹³⁴, A.K. Morley³⁶, G. Mornacchi³⁶, A.P. Morris⁹⁵, L. Morvaj¹⁵⁵, P. Moschovakos³⁶,
 B. Moser¹²⁰, M. Mosidze^{159b}, T. Moskalets¹⁴⁵, H.J. Moss¹⁴⁹, J. Moss^{31,n}, E.J.W. Moyse¹⁰³, S. Muanza¹⁰²,
 J. Mueller¹³⁹, R.S.P. Mueller¹¹⁴, D. Muenstermann⁹⁰, G.A. Mullier⁹⁷, J.L. Munoz Martinez¹⁴,
 F.J. Munoz Sanchez¹⁰¹, P. Murin^{28b}, W.J. Murray^{178,144}, A. Murrone^{69a,69b}, M. Muškinja¹⁸, C. Mwewa^{33a},
 A.G. Myagkov^{123,ao}, J. Myers¹³², M. Myska¹⁴², B.P. Nachman¹⁸, O. Nackenhorst⁴⁷, A.Nag Nag⁴⁸,
 K. Nagai¹³⁵, K. Nagano⁸², Y. Nagasaka⁶², M. Nagel⁵², J.L. Nagle²⁹, E. Nagy¹⁰², A.M. Nairz³⁶,
 Y. Nakahama¹¹⁷, K. Nakamura⁸², T. Nakamura¹⁶³, I. Nakano¹²⁸, H. Nanjo¹³³, F. Napolitano^{61a},
 R.F. Naranjo Garcia⁴⁶, R. Narayan⁴², I. Naryshkin¹³⁸, T. Naumann⁴⁶, G. Navarro^{22a}, P.Y. Nechaeva¹¹¹,
 F. Nechansky⁴⁶, T.J. Neep²¹, A. Negri^{71a,71b}, M. Negrini^{23b}, C. Nellist⁵³, M.E. Nelson¹³⁵, S. Nemecek¹⁴¹,
 P. Nemethy¹²⁵, M. Nessi^{36,d}, M.S. Neubauer¹⁷³, M. Neumann¹⁸², P.R. Newman²¹, Y.S. Ng¹⁹,
 Y.W.Y. Ng¹⁷¹, B. Ngair^{35e}, H.D.N. Nguyen¹⁰², T. Nguyen Manh¹¹⁰, E. Nibigira³⁸, R.B. Nickerson¹³⁵,
 R. Nicolaïdou¹⁴⁵, D.S. Nielsen⁴⁰, J. Nielsen¹⁴⁶, N. Nikiforou¹¹, V. Nikolaenko^{123,ao}, I. Nikolic-Audit¹³⁶,
 K. Nikolopoulos²¹, P. Nilsson²⁹, H.R. Nindhito⁵⁴, Y. Ninomiya⁸², A. Nisati^{73a}, N. Nishu^{60c}, R. Nisius¹¹⁵,
 I. Nitsche⁴⁷, T. Nitta¹⁷⁹, T. Nobe¹⁶³, Y. Noguchi⁸⁶, I. Nomidis¹³⁶, M.A. Nomura²⁹, M. Nordberg³⁶,
 N. Norjoharuddeen¹³⁵, T. Novak⁹², O. Novgorodova⁴⁸, R. Novotny¹⁴², L. Nozka¹³¹, K. Ntekas¹⁷¹,
 E. Nurse⁹⁵, F.G. Oakham^{34,aw}, H. Oberlack¹¹⁵, J. Ocariz¹³⁶, A. Ochi⁸³, I. Ochoa³⁹, J.P. Ochoa-Ricoux^{147a},
 K. O'Connor²⁶, S. Oda⁸⁸, S. Odaka⁸², S. Oerdekk⁵³, A. Ogródniak^{84a}, A. Oh¹⁰¹, S.H. Oh⁴⁹, C.C. Ohm¹⁵⁴,
 H. Oide¹⁶⁵, M.L. Ojeda¹⁶⁷, H. Okawa¹⁶⁹, Y. Okazaki⁸⁶, Y. Okumura¹⁶³, T. Okuyama⁸², A. Olariu^{27b},
 L.F. Oleiro Seabra^{140a}, S.A. Olivares Pino^{147a}, D. Oliveira Damazio²⁹, J.L. Oliver¹, M.J.R. Olsson¹⁷¹,
 A. Olszewski⁸⁵, J. Olszowska⁸⁵, D.C. O'Neil¹⁵², A.P. O'neill¹³⁵, A. Onofre^{140a,140e}, P.U.E. Onyisi¹¹,
 H. Oppen¹³⁴, M.J. Oreglia³⁷, G.E. Orellana⁸⁹, D. Orestano^{75a,75b}, N. Orlando¹⁴, R.S. Orr¹⁶⁷, V. O'Shea⁵⁷,
 R. Ospanov^{60a}, G. Otero y Garzon³⁰, H. Otono⁸⁸, P.S. Ott^{61a}, M. Ouchrif^{35d}, J. Ouellette²⁹,
 F. Ould-Saada¹³⁴, A. Ouraou¹⁴⁵, Q. Ouyang^{15a}, M. Owen⁵⁷, R.E. Owen²¹, V.E. Ozcan^{12c}, N. Ozturk⁸,
 J. Pacalt¹³¹, H.A. Pacey³², K. Pachal⁴⁹, A. Pacheco Pages¹⁴, C. Padilla Aranda¹⁴, S. Pagan Griso¹⁸,
 M. Paganini¹⁸³, G. Palacino⁶⁶, S. Palazzo⁵⁰, S. Palestini³⁶, M. Palka^{84b}, D. Pallin³⁸, I. Panagoulias¹⁰,
 C.E. Pandini³⁶, J.G. Panduro Vazquez⁹⁴, P. Pani⁴⁶, G. Panizzo^{67a,67c}, L. Paolozzi⁵⁴, C. Papadatos¹¹⁰,
 K. Papageorgiou^{9,h}, S. Parajuli⁴³, A. Paramonov⁶, D. Paredes Hernandez^{63b}, S.R. Paredes Saenz¹³⁵,
 B. Parida¹⁶⁶, T.H. Park¹⁶⁷, A.J. Parker³¹, M.A. Parker³², F. Parodi^{55b,55a}, E.W. Parrish¹²¹, J.A. Parsons³⁹,
 U. Parzefall⁵², L. Pascual Dominguez¹³⁶, V.R. Pascuzzi¹⁶⁷, J.M.P. Pasner¹⁴⁶, F. Pasquali¹²⁰,
 E. Pasqualucci^{73a}, S. Passaggio^{55b}, F. Pastore⁹⁴, P. Pasuwan^{45a,45b}, S. Pataraia¹⁰⁰, J.R. Pater¹⁰¹,
 A. Pathak^{181,j}, T. Pauly³⁶, B. Pearson¹¹⁵, M. Pedersen¹³⁴, L. Pedraza Diaz¹¹⁹, R. Pedro^{140a}, T. Peiffer⁵³,
 S.V. Peleganchuk^{122b,122a}, O. Penc¹⁴¹, H. Peng^{60a}, B.S. Peralva^{81a}, M.M. Perego⁶⁵,
 A.P. Pereira Peixoto^{140a}, D.V. Perepelitsa²⁹, F. Peri¹⁹, L. Perini^{69a,69b}, H. Pernegger³⁶, S. Perrella^{70a,70b},
 K. Peters⁴⁶, R.F.Y. Peters¹⁰¹, B.A. Petersen³⁶, T.C. Petersen⁴⁰, E. Petit¹⁰², A. Petridis¹, C. Petridou¹⁶²,
 P. Petroff⁶⁵, M. Petrov¹³⁵, F. Petrucci^{75a,75b}, M. Pettee¹⁸³, N.E. Pettersson¹⁰³, K. Petukhova¹⁴³,
 A. Peyaud¹⁴⁵, R. Pezoa^{147d}, L. Pezzotti^{71a,71b}, T. Pham¹⁰⁵, F.H. Phillips¹⁰⁷, P.W. Phillips¹⁴⁴,
 M.W. Phipps¹⁷³, G. Piacquadio¹⁵⁵, E. Pianori¹⁸, A. Picazio¹⁰³, R.H. Pickles¹⁰¹, R. Piegala³⁰,
 D. Pietreanu^{27b}, J.E. Pilcher³⁷, A.D. Pilkington¹⁰¹, M. Pinamonti^{74a,74b}, J.L. Pinfold³, M. Pitt¹⁶¹,
 L. Pizzimento^{74a,74b}, M.-A. Pleier²⁹, V. Pleskot¹⁴³, E. Plotnikova⁸⁰, P. Podberezko^{122b,122a}, R. Poettgen⁹⁷,
 R. Poggi⁵⁴, L. Poggioli⁶⁵, I. Pogrebnyak¹⁰⁷, D. Pohl²⁴, I. Pokharel⁵³, G. Polesello^{71a}, A. Poley¹⁸,

A. Policicchio^{73a,73b}, R. Polifka¹⁴³, A. Polini^{23b}, C.S. Pollard⁴⁶, V. Polychronakos²⁹, D. Ponomarenko¹¹², L. Pontecorvo³⁶, S. Popa^{27a}, G.A. Popeneciu^{27d}, L. Portales⁵, D.M. Portillo Quintero⁵⁸, S. Pospisil¹⁴², K. Potamianos⁴⁶, I.N. Potrap⁸⁰, C.J. Potter³², H. Potti¹¹, T. Poulsen⁹⁷, J. Poveda³⁶, T.D. Powell¹⁴⁹, G. Pownall⁴⁶, M.E. Pozo Astigarraga³⁶, P. Pralavorio¹⁰², S. Prell⁷⁹, D. Price¹⁰¹, M. Primavera^{68a}, S. Prince¹⁰⁴, M.L. Proffitt¹⁴⁸, N. Proklova¹¹², K. Prokofiev^{63c}, F. Prokoshin⁸⁰, S. Protopopescu²⁹, J. Proudfoot⁶, M. Przybycien^{84a}, D. Pudzha¹³⁸, A. Puri¹⁷³, P. Puzo⁶⁵, J. Qian¹⁰⁶, Y. Qin¹⁰¹, A. Quadt⁵³, M. Queitsch-Maitland⁴⁶, A. Qureshi¹, M. Racko^{28a}, P. Rados¹⁰⁵, F. Ragusa^{69a,69b}, G. Rahal⁹⁸, J.A. Raine⁵⁴, S. Rajagopalan²⁹, A. Ramirez Morales⁹³, K. Ran^{15a,15d}, T. Rashid⁶⁵, S. Raspopov⁵, D.M. Rauch⁴⁶, F. Rauscher¹¹⁴, S. Rave¹⁰⁰, B. Ravina¹⁴⁹, I. Ravinovich¹⁸⁰, J.H. Rawling¹⁰¹, M. Raymond³⁶, A.L. Read¹³⁴, N.P. Readloff⁵⁸, M. Reale^{68a,68b}, D.M. Rebuzzi^{71a,71b}, A. Redelbach¹⁷⁷, G. Redlinger²⁹, K. Reeves⁴³, L. Rehnisch¹⁹, J. Reichert¹³⁷, D. Reikher¹⁶¹, A. Reiss¹⁰⁰, A. Rej¹⁵¹, C. Rembser³⁶, M. Renda^{27b}, M. Rescigno^{73a}, S. Resconi^{69a}, E.D. Ressegueie¹³⁷, S. Rettie¹⁷⁵, E. Reynolds²¹, O.L. Rezanova^{122b,122a}, P. Reznicek¹⁴³, E. Ricci^{76a,76b}, R. Richter¹¹⁵, S. Richter⁴⁶, E. Richter-Was^{84b}, O. Ricken²⁴, M. Ridel¹³⁶, P. Rieck¹¹⁵, C.J. Riegel¹⁸², O. Rifki⁴⁶, M. Rijssenbeek¹⁵⁵, A. Rimoldi^{71a,71b}, M. Rimoldi⁴⁶, L. Rinaldi^{23b}, G. Ripellino¹⁵⁴, I. Riu¹⁴, J.C. Rivera Vergara¹⁷⁶, F. Rizatdinova¹³⁰, E. Rizvi⁹³, C. Rizzi³⁶, R.T. Roberts¹⁰¹, S.H. Robertson^{104,af}, M. Robin⁴⁶, D. Robinson³², J.E.M. Robinson⁴⁶, C.M. Robles Gajardo^{147d}, A. Robson⁵⁷, A. Rocchi^{74a,74b}, E. Rocco¹⁰⁰, C. Roda^{72a,72b}, S. Rodriguez Bosca¹⁷⁴, A. Rodriguez Perez¹⁴, D. Rodriguez Rodriguez¹⁷⁴, A.M. Rodríguez Vera^{168b}, S. Roe³⁶, O. Røhne¹³⁴, R. Röhrlig¹¹⁵, R.A. Rojas^{147d}, C.P.A. Roland⁶⁶, J. Roloff⁵⁹, A. Romaniouk¹¹², M. Romano^{23b,23a}, N. Rompotis⁹¹, M. Ronzani¹²⁵, L. Roos¹³⁶, S. Rosati^{73a}, K. Rosbach⁵², G. Rosin¹⁰³, B.J. Rosser¹³⁷, E. Rossi⁴⁶, E. Rossi^{75a,75b}, E. Rossi^{70a,70b}, L.P. Rossi^{55b}, L. Rossini^{69a,69b}, R. Rosten¹⁴, M. Rotaru^{27b}, J. Rothberg¹⁴⁸, D. Rousseau⁶⁵, G. Rovelli^{71a,71b}, A. Roy¹¹, D. Roy^{33e}, A. Rozanov¹⁰², Y. Rozen¹⁶⁰, X. Ruan^{33e}, F. Rubbo¹⁵³, F. Rühr⁵², A. Ruiz-Martinez¹⁷⁴, A. Rummler³⁶, Z. Rurikova⁵², N.A. Rusakovich⁸⁰, H.L. Russell¹⁰⁴, L. Rustige^{38,47}, J.P. Rutherford⁷, E.M. Rüttinger¹⁴⁹, M. Rybar³⁹, G. Rybkin⁶⁵, E.B. Rye¹³⁴, A. Ryzhov¹²³, P. Sabatini⁵³, G. Sabato¹²⁰, S. Sacerdoti⁶⁵, H.F-W. Sadrozinski¹⁴⁶, R. Sadykov⁸⁰, F. Safai Tehrani^{73a}, B. Safarzadeh Samani¹⁵⁶, P. Saha¹²¹, S. Saha¹⁰⁴, M. Sahinsoy^{61a}, A. Sahu¹⁸², M. Saimpert⁴⁶, M. Saito¹⁶³, T. Saito¹⁶³, H. Sakamoto¹⁶³, A. Sakharov^{125,an}, D. Salamani⁵⁴, G. Salamanna^{75a,75b}, J.E. Salazar Loyola^{147d}, P.H. Sales De Bruin¹⁷², A. Salnikov¹⁵³, J. Salt¹⁷⁴, D. Salvatore^{41b,41a}, F. Salvatore¹⁵⁶, A. Salvucci^{63a,63b,63c}, A. Salzburger³⁶, J. Samarati³⁶, D. Sammel⁵², D. Sampsonidis¹⁶², D. Sampsonidou¹⁶², J. Sánchez¹⁷⁴, A. Sanchez Pineda^{67a,67c}, H. Sandaker¹³⁴, C.O. Sander⁴⁶, I.G. Sanderswood⁹⁰, M. Sandhoff¹⁸², C. Sandoval^{22a}, D.P.C. Sankey¹⁴⁴, M. Sannino^{55b,55a}, Y. Sano¹¹⁷, A. Sansoni⁵¹, C. Santoni³⁸, H. Santos^{140a,140b}, S.N. Santpur¹⁸, A. Santra¹⁷⁴, A. Sapronov⁸⁰, J.G. Saraiva^{140a,140d}, O. Sasaki⁸², K. Sato¹⁶⁹, F. Sauerburger⁵², E. Sauvan⁵, P. Savard^{167,aw}, N. Savic¹¹⁵, R. Sawada¹⁶³, C. Sawyer¹⁴⁴, L. Sawyer^{96,al}, C. Sbarra^{23b}, A. Sbrizzi^{23a}, T. Scanlon⁹⁵, J. Schaarschmidt¹⁴⁸, P. Schacht¹¹⁵, B.M. Schachtner¹¹⁴, D. Schaefer³⁷, L. Schaefer¹³⁷, J. Schaeffer¹⁰⁰, S. Schaepe³⁶, U. Schäfer¹⁰⁰, A.C. Schaffer⁶⁵, D. Schaile¹¹⁴, R.D. Schamberger¹⁵⁵, N. Scharmberg¹⁰¹, V.A. Schegelsky¹³⁸, D. Scheirich¹⁴³, F. Schenck¹⁹, M. Schernau¹⁷¹, C. Schiavi^{55b,55a}, S. Schier¹⁴⁶, L.K. Schildgen²⁴, Z.M. Schillaci²⁶, E.J. Schioppa³⁶, M. Schioppa^{41b,41a}, K.E. Schleicher⁵², S. Schlenker³⁶, K.R. Schmidt-Sommerfeld¹¹⁵, K. Schmieden³⁶, C. Schmitt¹⁰⁰, S. Schmitt⁴⁶, S. Schmitz¹⁰⁰, J.C. Schmoeckel⁴⁶, U. Schnoor⁵², L. Schoeffel¹⁴⁵, A. Schoening^{61b}, P.G. Scholer⁵², E. Schopf¹³⁵, M. Schott¹⁰⁰, J.F.P. Schouwenberg¹¹⁹, J. Schovancova³⁶, S. Schramm⁵⁴, F. Schroeder¹⁸², A. Schulte¹⁰⁰, H-C. Schultz-Coulon^{61a}, M. Schumacher⁵², B.A. Schumm¹⁴⁶, Ph. Schune¹⁴⁵, A. Schwartzman¹⁵³, T.A. Schwarz¹⁰⁶, Ph. Schwemling¹⁴⁵, R. Schwienhorst¹⁰⁷, A. Sciandra¹⁴⁶, G. Sciolla²⁶, M. Scodeggio⁴⁶, M. Scornajenghi^{41b,41a}, F. Scuri^{72a}, F. Scutti¹⁰⁵, L.M. Scyboz¹¹⁵, C.D. Sebastiani^{73a,73b}, P. Seema¹⁹, S.C. Seidel¹¹⁸, A. Seiden¹⁴⁶, B.D. Seidlitz²⁹, T. Seiss³⁷, J.M. Seixas^{81b}, G. Sekhniaidze^{70a}, K. Sekhon¹⁰⁶, S.J. Sekula⁴², N. Semprini-Cesari^{23b,23a}, S. Sen⁴⁹, S. Senkin³⁸, C. Serfon⁷⁷, L. Serin⁶⁵, L. Serkin^{67a,67b}, M. Sessa^{60a}, H. Severini¹²⁹, T. Šfiligoj⁹², F. Sforza^{55b,55a}, A. Sfyrla⁵⁴, E. Shabalina⁵³, J.D. Shahinian¹⁴⁶,

N.W. Shaikh^{45a,45b}, D. Shaked Renous¹⁸⁰, L.Y. Shan^{15a}, R. Shang¹⁷³, J.T. Shank²⁵, M. Shapiro¹⁸,
 A. Sharma¹³⁵, A.S. Sharma¹, P.B. Shatalov¹²⁴, K. Shaw¹⁵⁶, S.M. Shaw¹⁰¹, A. Shcherbakova¹³⁸,
 M. Shehade¹⁸⁰, Y. Shen¹²⁹, N. Sherafati³⁴, A.D. Sherman²⁵, P. Sherwood⁹⁵, L. Shi^{158,at}, S. Shimizu⁸²,
 C.O. Shimmin¹⁸³, Y. Shimogama¹⁷⁹, M. Shimojima¹¹⁶, I.P.J. Shipsey¹³⁵, S. Shirabe⁸⁸, M. Shiyakova^{80,ad},
 J. Shlomi¹⁸⁰, A. Shmeleva¹¹¹, M.J. Shochet³⁷, J. Shojaii¹⁰⁵, D.R. Shope¹²⁹, S. Shrestha¹²⁷, E.M. Shrif^{33e},
 E. Shulga¹⁸⁰, P. Sicho¹⁴¹, A.M. Sickles¹⁷³, P.E. Sidebo¹⁵⁴, E. Sideras Haddad^{33e}, O. Sidiropoulou³⁶,
 A. Sidoti^{23b,23a}, F. Siegert⁴⁸, Dj. Sijacki¹⁶, M.Jr. Silva¹⁸¹, M.V. Silva Oliveira^{81a}, S.B. Silverstein^{45a},
 S. Simion⁶⁵, E. Simioni¹⁰⁰, R. Simoniello¹⁰⁰, S. Simsek^{12b}, P. Sinervo¹⁶⁷, V. Sinetckii^{113,111},
 N.B. Sinev¹³², M. Sioli^{23b,23a}, I. Siral¹⁰⁶, S.Yu. Sivoklokov¹¹³, J. Sjölin^{45a,45b}, E. Skorda⁹⁷, P. Skubic¹²⁹,
 M. Slawinska⁸⁵, K. Sliwa¹⁷⁰, R. Slovak¹⁴³, V. Smakhtin¹⁸⁰, B.H. Smart¹⁴⁴, J. Smiesko^{28a}, N. Smirnov¹¹²,
 S.Yu. Smirnov¹¹², Y. Smirnov¹¹², L.N. Smirnova^{113,v}, O. Smirnova⁹⁷, J.W. Smith⁵³, M. Smizanska⁹⁰,
 K. Smolek¹⁴², A. Smykiewicz⁸⁵, A.A. Snesarev¹¹¹, H.L. Snoek¹²⁰, I.M. Snyder¹³², S. Snyder²⁹,
 R. Sobie^{176,af}, A. Soffer¹⁶¹, A. Søgaard⁵⁰, F. Sohns⁵³, C.A. Solans Sanchez³⁶, E.Yu. Soldatov¹¹²,
 U. Soldevila¹⁷⁴, A.A. Solodkov¹²³, A. Soloshenko⁸⁰, O.V. Solovyanov¹²³, V. Solovyev¹³⁸, P. Sommer¹⁴⁹,
 H. Son¹⁷⁰, W. Song¹⁴⁴, W.Y. Song^{168b}, A. Sopczak¹⁴², F. Sopkova^{28b}, C.L. Sotropoulou^{72a,72b},
 S. Sottocornola^{71a,71b}, R. Soualah^{67a,67c,g}, A.M. Soukharev^{122b,122a}, D. South⁴⁶, S. Spagnolo^{68a,68b},
 M. Spalla¹¹⁵, M. Spangenberg¹⁷⁸, F. Spanò⁹⁴, D. Sperlich⁵², T.M. Spieker^{61a}, R. Spighi^{23b}, G. Spigo³⁶,
 M. Spina¹⁵⁶, D.P. Spiteri⁵⁷, M. Spousta¹⁴³, A. Stabile^{69a,69b}, B.L. Stamas¹²¹, R. Stamen^{61a},
 M. Stamenkovic¹²⁰, E. Stanecka⁸⁵, B. Stanislaus¹³⁵, M.M. Stanitzki⁴⁶, M. Stankaityte¹³⁵, B. Stapf¹²⁰,
 E.A. Starchenko¹²³, G.H. Stark¹⁴⁶, J. Stark⁵⁸, S.H. Stark⁴⁰, P. Staroba¹⁴¹, P. Starovoitov^{61a}, S. Stärz¹⁰⁴,
 R. Staszewski⁸⁵, G. Stavropoulos⁴⁴, M. Stegler⁴⁶, P. Steinberg²⁹, A.L. Steinhebel¹³², B. Stelzer¹⁵²,
 H.J. Stelzer¹³⁹, O. Stelzer-Chilton^{168a}, H. Stenzel⁵⁶, T.J. Stevenson¹⁵⁶, G.A. Stewart³⁶, M.C. Stockton³⁶,
 G. Stoica^{27b}, M. Stolarski^{140a}, S. Stonjek¹¹⁵, A. Straessner⁴⁸, J. Strandberg¹⁵⁴, S. Strandberg^{45a,45b},
 M. Strauss¹²⁹, P. Strizenec^{28b}, R. Ströhmer¹⁷⁷, D.M. Strom¹³², R. Stroynowski⁴², A. Strubig⁵⁰,
 S.A. Stucci²⁹, B. Stugu¹⁷, J. Stupak¹²⁹, N.A. Styles⁴⁶, D. Su¹⁵³, S. Suchek^{61a}, V.V. Sulin¹¹¹,
 M.J. Sullivan⁹¹, D.M.S. Sultan⁵⁴, S. Sultansoy^{4c}, T. Sumida⁸⁶, S. Sun¹⁰⁶, X. Sun³, K. Suruliz¹⁵⁶,
 C.J.E. Suster¹⁵⁷, M.R. Sutton¹⁵⁶, S. Suzuki⁸², M. Svatos¹⁴¹, M. Swiatlowski³⁷, S.P. Swift², T. Swirski¹⁷⁷,
 A. Sydorenko¹⁰⁰, I. Sykora^{28a}, M. Sykora¹⁴³, T. Sykora¹⁴³, D. Ta¹⁰⁰, K. Tackmann^{46,ab}, J. Taenzer¹⁶¹,
 A. Taffard¹⁷¹, R. Tafirout^{168a}, H. Takai²⁹, R. Takashima⁸⁷, K. Takeda⁸³, T. Takeshita¹⁵⁰, E.P. Takeva⁵⁰,
 Y. Takubo⁸², M. Talby¹⁰², A.A. Talyshев^{122b,122a}, N.M. Tamir¹⁶¹, J. Tanaka¹⁶³, M. Tanaka¹⁶⁵, R. Tanaka⁶⁵,
 S. Tapia Araya¹⁷³, S. Tapprogge¹⁰⁰, A. Tarek Abouelfadl Mohamed¹³⁶, S. Tarem¹⁶⁰, K. Tariq^{60b},
 G. Tarna^{27b,c}, G.F. Tartarelli^{69a}, P. Tas¹⁴³, M. Tasevsky¹⁴¹, T. Tashiro⁸⁶, E. Tassi^{41b,41a},
 A. Tavares Delgado^{140a,140b}, Y. Tayalati^{35e}, A.J. Taylor⁵⁰, G.N. Taylor¹⁰⁵, W. Taylor^{168b}, A.S. Tee⁹⁰,
 R. Teixeira De Lima¹⁵³, P. Teixeira-Dias⁹⁴, H. Ten Kate³⁶, J.J. Teoh¹²⁰, S. Terada⁸², K. Terashi¹⁶³,
 J. Terron⁹⁹, S. Terzo¹⁴, M. Testa⁵¹, R.J. Teuscher^{167,af}, S.J. Thais¹⁸³, T. Theveneaux-Pelzer⁴⁶, F. Thiele⁴⁰,
 D.W. Thomas⁹⁴, J.O. Thomas⁴², J.P. Thomas²¹, A.S. Thompson⁵⁷, P.D. Thompson²¹, L.A. Thomsen¹⁸³,
 E. Thomson¹³⁷, E.J. Thorpe⁹³, R.E. Ticse Torres⁵³, V.O. Tikhomirov^{111,ap}, Yu.A. Tikhonov^{122b,122a},
 S. Timoshenko¹¹², P. Tipton¹⁸³, S. Tisserant¹⁰², K. Todome^{23b,23a}, S. Todorova-Nova⁵, S. Todt⁴⁸, J. Tojo⁸⁸,
 S. Tokár^{28a}, K. Tokushuku⁸², E. Tolley¹²⁷, K.G. Tomiwa^{33e}, M. Tomoto¹¹⁷, L. Tompkins^{153,q}, B. Tong⁵⁹,
 P. Tornambe¹⁰³, E. Torrence¹³², H. Torres⁴⁸, E. Torró Pastor¹⁴⁸, C. Tosciri¹³⁵, J. Toth^{102,ae}, D.R. Tovey¹⁴⁹,
 A. Traeet¹⁷, C.J. Treado¹²⁵, T. Trefzger¹⁷⁷, F. Tresoldi¹⁵⁶, A. Tricoli²⁹, I.M. Trigger^{168a},
 S. Trincaz-Duvold¹³⁶, W. Trischuk¹⁶⁷, B. Trocmé⁵⁸, A. Trofymov¹⁴⁵, C. Troncon^{69a}, M. Trovatelli¹⁷⁶,
 F. Trovato¹⁵⁶, L. Truong^{33c}, M. Trzebinski⁸⁵, A. Trzupek⁸⁵, F. Tsai⁴⁶, J.C.-L. Tseng¹³⁵,
 P.V. Tsiareshka^{108,ak}, A. Tsirigotis¹⁶², V. Tsiskaridze¹⁵⁵, E.G. Tskhadadze^{159a}, M. Tsopoulou¹⁶²,
 I.I. Tsukerman¹²⁴, V. Tsulaia¹⁸, S. Tsuno⁸², D. Tsybychev¹⁵⁵, Y. Tu^{63b}, A. Tudorache^{27b}, V. Tudorache^{27b},
 T.T. Tulbure^{27a}, A.N. Tuna⁵⁹, S. Turchikhin⁸⁰, D. Turgeman¹⁸⁰, I. Turk Cakir^{4b,w}, R.J. Turner²¹,
 R. Turra^{69a}, P.M. Tuts³⁹, S. Tzamarias¹⁶², E. Tzovara¹⁰⁰, G. Ucchielli⁴⁷, K. Uchida¹⁶³, I. Ueda⁸²,

M. Ughetto^{45a,45b}, F. Ukegawa¹⁶⁹, G. Unal³⁶, A. Undrus²⁹, G. Unel¹⁷¹, F.C. Ungaro¹⁰⁵, Y. Unno⁸²,
 K. Uno¹⁶³, J. Urban^{28b}, P. Urquijo¹⁰⁵, G. Usai⁸, Z. Uysal^{12d}, L. Vacavant¹⁰², V. Vacek¹⁴², B. Vachon¹⁰⁴,
 K.O.H. Vadla¹³⁴, A. Vaidya⁹⁵, C. Valderanis¹¹⁴, E. Valdes Santurio^{45a,45b}, M. Valente⁵⁴,
 S. Valentinetto^{23b,23a}, A. Valero¹⁷⁴, L. Valéry⁴⁶, R.A. Vallance²¹, A. Vallier³⁶, J.A. Valls Ferrer¹⁷⁴,
 T.R. Van Daalen¹⁴, P. Van Gemmeren⁶, I. Van Vulpen¹²⁰, M. Vanadia^{74a,74b}, W. Vandelli³⁶,
 E.R. Vandewall¹³⁰, A. Vaniachine¹⁶⁶, D. Vannicola^{73a,73b}, R. Vari^{73a}, E.W. Varnes⁷, C. Varni^{55b,55a},
 T. Varol¹⁵⁸, D. Varouchas⁶⁵, K.E. Varvell¹⁵⁷, M.E. Vasile^{27b}, G.A. Vasquez¹⁷⁶, J.G. Vasquez¹⁸³,
 F. Vazeille³⁸, D. Vazquez Furelos¹⁴, T. Vazquez Schroeder³⁶, J. Veatch⁵³, V. Vecchio^{75a,75b}, M.J. Veen¹²⁰,
 L.M. Veloce¹⁶⁷, F. Veloso^{140a,140c}, S. Veneziano^{73a}, A. Ventura^{68a,68b}, N. Venturi³⁶, A. Verbytskyi¹¹⁵,
 V. Vercesi^{71a}, M. Verducci^{72a,72b}, C.M. Vergel Infante⁷⁹, C. Vergis²⁴, W. Verkerke¹²⁰, A.T. Vermeulen¹²⁰,
 J.C. Vermeulen¹²⁰, M.C. Vetterli^{152,aw}, N. Viaux Maira^{147d}, M. Vicente Barreto Pinto⁵⁴, T. Vickey¹⁴⁹,
 O.E. Vickey Boeriu¹⁴⁹, G.H.A. Viehhauser¹³⁵, L. Vigani^{61b}, M. Villa^{23b,23a}, M. Villaplana Perez^{69a,69b},
 E. Vilucchi⁵¹, M.G. Vincter³⁴, G.S. Virdee²¹, A. Vishwakarma⁴⁶, C. Vittori^{23b,23a}, I. Vivarelli¹⁵⁶,
 M. Vogel¹⁸², P. Vokac¹⁴², S.E. von Buddenbrock^{33e}, E. Von Toerne²⁴, V. Vorobel¹⁴³, K. Vorobev¹¹²,
 M. Vos¹⁷⁴, J.H. Vossebeld⁹¹, M. Vozak¹⁰¹, N. Vranjes¹⁶, M. Vranjes Milosavljevic¹⁶, V. Vrba¹⁴²,
 M. Vreeswijk¹²⁰, R. Vuillermet³⁶, I. Vukotic³⁷, P. Wagner²⁴, W. Wagner¹⁸², J. Wagner-Kuhr¹¹⁴,
 S. Wahdan¹⁸², H. Wahlberg⁸⁹, V.M. Walbrecht¹¹⁵, J. Walder⁹⁰, R. Walker¹¹⁴, S.D. Walker⁹⁴,
 W. Walkowiak¹⁵¹, V. Wallangen^{45a,45b}, A.M. Wang⁵⁹, C. Wang^{60c}, C. Wang^{60b}, F. Wang¹⁸¹, H. Wang¹⁸,
 H. Wang³, J. Wang^{63a}, J. Wang¹⁵⁷, J. Wang^{61b}, P. Wang⁴², Q. Wang¹²⁹, R.-J. Wang¹⁰⁰, R. Wang^{60a},
 R. Wang⁶, S.M. Wang¹⁵⁸, W.T. Wang^{60a}, W. Wang^{15c,ag}, W.X. Wang^{60a,ag}, Y. Wang^{60a,am}, Z. Wang^{60c},
 C. Wanotayaroj⁴⁶, A. Warburton¹⁰⁴, C.P. Ward³², D.R. Wardrope⁹⁵, N. Warrack⁵⁷, A. Washbrook⁵⁰,
 A.T. Watson²¹, M.F. Watson²¹, G. Watts¹⁴⁸, B.M. Waugh⁹⁵, A.F. Webb¹¹, S. Webb¹⁰⁰, C. Weber¹⁸³,
 M.S. Weber²⁰, S.A. Weber³⁴, S.M. Weber^{61a}, A.R. Weidberg¹³⁵, J. Weingarten⁴⁷, M. Weirich¹⁰⁰,
 C. Weiser⁵², P.S. Wells³⁶, T. Wenaus²⁹, T. Wengler³⁶, S. Wenig³⁶, N. Wermes²⁴, M.D. Werner⁷⁹,
 M. Wessels^{61a}, T.D. Weston²⁰, K. Whalen¹³², N.L. Whallon¹⁴⁸, A.M. Wharton⁹⁰, A.S. White¹⁰⁶,
 A. White⁸, M.J. White¹, D. Whiteson¹⁷¹, B.W. Whitmore⁹⁰, W. Wiedenmann¹⁸¹, M. Wielers¹⁴⁴,
 N. Wieseotte¹⁰⁰, C. Wiglesworth⁴⁰, L.A.M. Wiik-Fuchs⁵², F. Wilk¹⁰¹, H.G. Wilkens³⁶, L.J. Wilkins⁹⁴,
 H.H. Williams¹³⁷, S. Williams³², C. Willis¹⁰⁷, S. Willocq¹⁰³, J.A. Wilson²¹, I. Wingerter-Seez⁵,
 E. Winkels¹⁵⁶, F. Winklmeier¹³², O.J. Winston¹⁵⁶, B.T. Winter⁵², M. Wittgen¹⁵³, M. Wobisch⁹⁶,
 A. Wolf¹⁰⁰, T.M.H. Wolf¹²⁰, R. Wolff¹⁰², R. Wölker¹³⁵, J. Wollrath⁵², M.W. Wolter⁸⁵, H. Wolters^{140a,140c},
 V.W.S. Wong¹⁷⁵, N.L. Woods¹⁴⁶, S.D. Worm²¹, B.K. Wosiek⁸⁵, K.W. Woźniak⁸⁵, K. Wraight⁵⁷,
 S.L. Wu¹⁸¹, X. Wu⁵⁴, Y. Wu^{60a}, T.R. Wyatt¹⁰¹, B.M. Wynne⁵⁰, S. Xella⁴⁰, Z. Xi¹⁰⁶, L. Xia¹⁷⁸, X. Xiao¹⁰⁶,
 I. Xiotidis¹⁵⁶, D. Xu^{15a}, H. Xu^{60a,c}, L. Xu²⁹, T. Xu¹⁴⁵, W. Xu¹⁰⁶, Z. Xu^{60b}, Z. Xu¹⁵³, B. Yabsley¹⁵⁷,
 S. Yacoob^{33a}, K. Yajima¹³³, D.P. Yallup⁹⁵, D. Yamaguchi¹⁶⁵, Y. Yamaguchi¹⁶⁵, A. Yamamoto⁸²,
 M. Yamatani¹⁶³, T. Yamazaki¹⁶³, Y. Yamazaki⁸³, Z. Yan²⁵, H.J. Yang^{60c,60d}, H.T. Yang¹⁸, S. Yang⁷⁸,
 X. Yang^{60b,58}, Y. Yang¹⁶³, W.-M. Yao¹⁸, Y.C. Yap⁴⁶, Y. Yasu⁸², E. Yatsenko^{60c,60d}, J. Ye⁴², S. Ye²⁹,
 I. Yeletskikh⁸⁰, M.R. Yexley⁹⁰, E. Yigitbasi²⁵, K. Yorita¹⁷⁹, K. Yoshihara¹³⁷, C.J.S. Young³⁶, C. Young¹⁵³,
 J. Yu⁷⁹, R. Yuan^{60b,i}, X. Yue^{61a}, S.P.Y. Yuen²⁴, M. Zaazoua^{35e}, B. Zabinski⁸⁵, G. Zacharis¹⁰,
 E. Zaffaroni⁵⁴, J. Zahreddine¹³⁶, A.M. Zaitsev^{123,ao}, T. Zakareishvili^{159b}, N. Zakharchuk³⁴, S. Zambito⁵⁹,
 D. Zanzi³⁶, D.R. Zaripovas⁵⁷, S.V. Zeißner⁴⁷, C. Zeitnitz¹⁸², G. Zemaityte¹³⁵, J.C. Zeng¹⁷³, O. Zenin¹²³,
 T. Ženiš^{28a}, D. Zerwas⁶⁵, M. Zgubic¹³⁵, B. Zhang^{15c}, D.F. Zhang^{15b}, G. Zhang^{15b}, H. Zhang^{15c}, J. Zhang⁶,
 L. Zhang^{15c}, L. Zhang^{60a}, M. Zhang¹⁷³, R. Zhang²⁴, X. Zhang^{60b}, Y. Zhang^{15a,15d}, Z. Zhang^{63a},
 Z. Zhang⁶⁵, P. Zhao⁴⁹, Y. Zhao^{60b}, Z. Zhao^{60a}, A. Zhemchugov⁸⁰, Z. Zheng¹⁰⁶, D. Zhong¹⁷³, B. Zhou¹⁰⁶,
 C. Zhou¹⁸¹, M.S. Zhou^{15a,15d}, M. Zhou¹⁵⁵, N. Zhou^{60c}, Y. Zhou⁷, C.G. Zhu^{60b}, C. Zhu^{15a,15d}, H.L. Zhu^{60a},
 H. Zhu^{15a}, J. Zhu¹⁰⁶, Y. Zhu^{60a}, X. Zhuang^{15a}, K. Zhukov¹¹¹, V. Zhulanov^{122b,122a}, D. Ziemińska⁶⁶,
 N.I. Zimine⁸⁰, S. Zimmermann⁵², Z. Zinonos¹¹⁵, M. Ziolkowski¹⁵¹, L. Živković¹⁶, G. Zobernig¹⁸¹,
 A. Zoccoli^{23b,23a}, K. Zoch⁵³, T.G. Zorbas¹⁴⁹, R. Zou³⁷, L. Zwalski³⁶.

- ¹Department of Physics, University of Adelaide, Adelaide; Australia.
- ²Physics Department, SUNY Albany, Albany NY; United States of America.
- ³Department of Physics, University of Alberta, Edmonton AB; Canada.
- ^{4(a)}Department of Physics, Ankara University, Ankara;^(b)Istanbul Aydin University, Application and Research Center for Advanced Studies, Istanbul;^(c)Division of Physics, TOBB University of Economics and Technology, Ankara; Turkey.
- ⁵LAPP, Université Grenoble Alpes, Université Savoie Mont Blanc, CNRS/IN2P3, Annecy; France.
- ⁶High Energy Physics Division, Argonne National Laboratory, Argonne IL; United States of America.
- ⁷Department of Physics, University of Arizona, Tucson AZ; United States of America.
- ⁸Department of Physics, University of Texas at Arlington, Arlington TX; United States of America.
- ⁹Physics Department, National and Kapodistrian University of Athens, Athens; Greece.
- ¹⁰Physics Department, National Technical University of Athens, Zografou; Greece.
- ¹¹Department of Physics, University of Texas at Austin, Austin TX; United States of America.
- ^{12(a)}Bahcesehir University, Faculty of Engineering and Natural Sciences, Istanbul;^(b)Istanbul Bilgi University, Faculty of Engineering and Natural Sciences, Istanbul;^(c)Department of Physics, Bogazici University, Istanbul;^(d)Department of Physics Engineering, Gaziantep University, Gaziantep; Turkey.
- ¹³Institute of Physics, Azerbaijan Academy of Sciences, Baku; Azerbaijan.
- ¹⁴Institut de Física d'Altes Energies (IFAE), Barcelona Institute of Science and Technology, Barcelona; Spain.
- ^{15(a)}Institute of High Energy Physics, Chinese Academy of Sciences, Beijing;^(b)Physics Department, Tsinghua University, Beijing;^(c)Department of Physics, Nanjing University, Nanjing;^(d)University of Chinese Academy of Science (UCAS), Beijing; China.
- ¹⁶Institute of Physics, University of Belgrade, Belgrade; Serbia.
- ¹⁷Department for Physics and Technology, University of Bergen, Bergen; Norway.
- ¹⁸Physics Division, Lawrence Berkeley National Laboratory and University of California, Berkeley CA; United States of America.
- ¹⁹Institut für Physik, Humboldt Universität zu Berlin, Berlin; Germany.
- ²⁰Albert Einstein Center for Fundamental Physics and Laboratory for High Energy Physics, University of Bern, Bern; Switzerland.
- ²¹School of Physics and Astronomy, University of Birmingham, Birmingham; United Kingdom.
- ^{22(a)}Facultad de Ciencias y Centro de Investigaciones, Universidad Antonio Nariño, Bogotá;^(b)Departamento de Física, Universidad Nacional de Colombia, Bogotá, Colombia; Colombia.
- ^{23(a)}INFN Bologna and Universita' di Bologna, Dipartimento di Fisica;^(b)INFN Sezione di Bologna; Italy.
- ²⁴Physikalisch Institut, Universität Bonn, Bonn; Germany.
- ²⁵Department of Physics, Boston University, Boston MA; United States of America.
- ²⁶Department of Physics, Brandeis University, Waltham MA; United States of America.
- ^{27(a)}Transilvania University of Brasov, Brasov;^(b)Horia Hulubei National Institute of Physics and Nuclear Engineering, Bucharest;^(c)Department of Physics, Alexandru Ioan Cuza University of Iasi, Iasi;^(d)National Institute for Research and Development of Isotopic and Molecular Technologies, Physics Department, Cluj-Napoca;^(e)University Politehnica Bucharest, Bucharest;^(f)West University in Timisoara, Timisoara; Romania.
- ^{28(a)}Faculty of Mathematics, Physics and Informatics, Comenius University, Bratislava;^(b)Department of Subnuclear Physics, Institute of Experimental Physics of the Slovak Academy of Sciences, Kosice; Slovak Republic.
- ²⁹Physics Department, Brookhaven National Laboratory, Upton NY; United States of America.
- ³⁰Departamento de Física, Universidad de Buenos Aires, Buenos Aires; Argentina.
- ³¹California State University, CA; United States of America.

- ³²Cavendish Laboratory, University of Cambridge, Cambridge; United Kingdom.
- ^{33(a)}Department of Physics, University of Cape Town, Cape Town;^(b)iThemba Labs, Western Cape;^(c)Department of Mechanical Engineering Science, University of Johannesburg, Johannesburg;^(d)University of South Africa, Department of Physics, Pretoria;^(e)School of Physics, University of the Witwatersrand, Johannesburg; South Africa.
- ³⁴Department of Physics, Carleton University, Ottawa ON; Canada.
- ^{35(a)}Faculté des Sciences Ain Chock, Réseau Universitaire de Physique des Hautes Energies - Université Hassan II, Casablanca;^(b)Faculté des Sciences, Université Ibn-Tofail, Kénitra;^(c)Faculté des Sciences Semlalia, Université Cadi Ayyad, LPHEA-Marrakech;^(d)Faculté des Sciences, Université Mohamed Premier and LPTPM, Oujda;^(e)Faculté des sciences, Université Mohammed V, Rabat; Morocco.
- ³⁶CERN, Geneva; Switzerland.
- ³⁷Enrico Fermi Institute, University of Chicago, Chicago IL; United States of America.
- ³⁸LPC, Université Clermont Auvergne, CNRS/IN2P3, Clermont-Ferrand; France.
- ³⁹Nevis Laboratory, Columbia University, Irvington NY; United States of America.
- ⁴⁰Niels Bohr Institute, University of Copenhagen, Copenhagen; Denmark.
- ^{41(a)}Dipartimento di Fisica, Università della Calabria, Rende;^(b)INFN Gruppo Collegato di Cosenza, Laboratori Nazionali di Frascati; Italy.
- ⁴²Physics Department, Southern Methodist University, Dallas TX; United States of America.
- ⁴³Physics Department, University of Texas at Dallas, Richardson TX; United States of America.
- ⁴⁴National Centre for Scientific Research "Demokritos", Agia Paraskevi; Greece.
- ^{45(a)}Department of Physics, Stockholm University;^(b)Oskar Klein Centre, Stockholm; Sweden.
- ⁴⁶Deutsches Elektronen-Synchrotron DESY, Hamburg and Zeuthen; Germany.
- ⁴⁷Lehrstuhl für Experimentelle Physik IV, Technische Universität Dortmund, Dortmund; Germany.
- ⁴⁸Institut für Kern- und Teilchenphysik, Technische Universität Dresden, Dresden; Germany.
- ⁴⁹Department of Physics, Duke University, Durham NC; United States of America.
- ⁵⁰SUPA - School of Physics and Astronomy, University of Edinburgh, Edinburgh; United Kingdom.
- ⁵¹INFN e Laboratori Nazionali di Frascati, Frascati; Italy.
- ⁵²Physikalisch Institut, Albert-Ludwigs-Universität Freiburg, Freiburg; Germany.
- ⁵³II. Physikalisch Institut, Georg-August-Universität Göttingen, Göttingen; Germany.
- ⁵⁴Département de Physique Nucléaire et Corpusculaire, Université de Genève, Genève; Switzerland.
- ^{55(a)}Dipartimento di Fisica, Università di Genova, Genova;^(b)INFN Sezione di Genova; Italy.
- ⁵⁶II. Physikalisch Institut, Justus-Liebig-Universität Giessen, Giessen; Germany.
- ⁵⁷SUPA - School of Physics and Astronomy, University of Glasgow, Glasgow; United Kingdom.
- ⁵⁸LPSC, Université Grenoble Alpes, CNRS/IN2P3, Grenoble INP, Grenoble; France.
- ⁵⁹Laboratory for Particle Physics and Cosmology, Harvard University, Cambridge MA; United States of America.
- ^{60(a)}Department of Modern Physics and State Key Laboratory of Particle Detection and Electronics, University of Science and Technology of China, Hefei;^(b)Institute of Frontier and Interdisciplinary Science and Key Laboratory of Particle Physics and Particle Irradiation (MOE), Shandong University, Qingdao;^(c)School of Physics and Astronomy, Shanghai Jiao Tong University, KLPPAC-MoE, SKLPPC, Shanghai;^(d)Tsung-Dao Lee Institute, Shanghai; China.
- ^{61(a)}Kirchhoff-Institut für Physik, Ruprecht-Karls-Universität Heidelberg, Heidelberg;^(b)Physikalisches Institut, Ruprecht-Karls-Universität Heidelberg, Heidelberg; Germany.
- ⁶²Faculty of Applied Information Science, Hiroshima Institute of Technology, Hiroshima; Japan.
- ^{63(a)}Department of Physics, Chinese University of Hong Kong, Shatin, N.T., Hong Kong;^(b)Department of Physics, University of Hong Kong, Hong Kong;^(c)Department of Physics and Institute for Advanced Study, Hong Kong University of Science and Technology, Clear Water Bay, Kowloon, Hong Kong; China.

- ⁶⁴Department of Physics, National Tsing Hua University, Hsinchu; Taiwan.
- ⁶⁵IJCLab, Université Paris-Saclay, CNRS/IN2P3, 91405, Orsay; France.
- ⁶⁶Department of Physics, Indiana University, Bloomington IN; United States of America.
- ^{67(a)}INFN Gruppo Collegato di Udine, Sezione di Trieste, Udine;^(b)ICTP, Trieste;^(c)Dipartimento Politecnico di Ingegneria e Architettura, Università di Udine, Udine; Italy.
- ^{68(a)}INFN Sezione di Lecce;^(b)Dipartimento di Matematica e Fisica, Università del Salento, Lecce; Italy.
- ^{69(a)}INFN Sezione di Milano;^(b)Dipartimento di Fisica, Università di Milano, Milano; Italy.
- ^{70(a)}INFN Sezione di Napoli;^(b)Dipartimento di Fisica, Università di Napoli, Napoli; Italy.
- ^{71(a)}INFN Sezione di Pavia;^(b)Dipartimento di Fisica, Università di Pavia, Pavia; Italy.
- ^{72(a)}INFN Sezione di Pisa;^(b)Dipartimento di Fisica E. Fermi, Università di Pisa, Pisa; Italy.
- ^{73(a)}INFN Sezione di Roma;^(b)Dipartimento di Fisica, Sapienza Università di Roma, Roma; Italy.
- ^{74(a)}INFN Sezione di Roma Tor Vergata;^(b)Dipartimento di Fisica, Università di Roma Tor Vergata, Roma; Italy.
- ^{75(a)}INFN Sezione di Roma Tre;^(b)Dipartimento di Matematica e Fisica, Università Roma Tre, Roma; Italy.
- ^{76(a)}INFN-TIFPA;^(b)Università degli Studi di Trento, Trento; Italy.
- ⁷⁷Institut für Astro- und Teilchenphysik, Leopold-Franzens-Universität, Innsbruck; Austria.
- ⁷⁸University of Iowa, Iowa City IA; United States of America.
- ⁷⁹Department of Physics and Astronomy, Iowa State University, Ames IA; United States of America.
- ⁸⁰Joint Institute for Nuclear Research, Dubna; Russia.
- ^{81(a)}Departamento de Engenharia Elétrica, Universidade Federal de Juiz de Fora (UFJF), Juiz de Fora;^(b)Universidade Federal do Rio De Janeiro COPPE/EE/IF, Rio de Janeiro;^(c)Universidade Federal de São João del Rei (UFSJ), São João del Rei;^(d)Instituto de Física, Universidade de São Paulo, São Paulo; Brazil.
- ⁸²KEK, High Energy Accelerator Research Organization, Tsukuba; Japan.
- ⁸³Graduate School of Science, Kobe University, Kobe; Japan.
- ^{84(a)}AGH University of Science and Technology, Faculty of Physics and Applied Computer Science, Krakow;^(b)Marian Smoluchowski Institute of Physics, Jagiellonian University, Krakow; Poland.
- ⁸⁵Institute of Nuclear Physics Polish Academy of Sciences, Krakow; Poland.
- ⁸⁶Faculty of Science, Kyoto University, Kyoto; Japan.
- ⁸⁷Kyoto University of Education, Kyoto; Japan.
- ⁸⁸Research Center for Advanced Particle Physics and Department of Physics, Kyushu University, Fukuoka ; Japan.
- ⁸⁹Instituto de Física La Plata, Universidad Nacional de La Plata and CONICET, La Plata; Argentina.
- ⁹⁰Physics Department, Lancaster University, Lancaster; United Kingdom.
- ⁹¹Oliver Lodge Laboratory, University of Liverpool, Liverpool; United Kingdom.
- ⁹²Department of Experimental Particle Physics, Jožef Stefan Institute and Department of Physics, University of Ljubljana, Ljubljana; Slovenia.
- ⁹³School of Physics and Astronomy, Queen Mary University of London, London; United Kingdom.
- ⁹⁴Department of Physics, Royal Holloway University of London, Egham; United Kingdom.
- ⁹⁵Department of Physics and Astronomy, University College London, London; United Kingdom.
- ⁹⁶Louisiana Tech University, Ruston LA; United States of America.
- ⁹⁷Fysiska institutionen, Lunds universitet, Lund; Sweden.
- ⁹⁸Centre de Calcul de l’Institut National de Physique Nucléaire et de Physique des Particules (IN2P3), Villeurbanne; France.
- ⁹⁹Departamento de Física Teorica C-15 and CIAFF, Universidad Autónoma de Madrid, Madrid; Spain.
- ¹⁰⁰Institut für Physik, Universität Mainz, Mainz; Germany.
- ¹⁰¹School of Physics and Astronomy, University of Manchester, Manchester; United Kingdom.

- ¹⁰²CPPM, Aix-Marseille Université, CNRS/IN2P3, Marseille; France.
- ¹⁰³Department of Physics, University of Massachusetts, Amherst MA; United States of America.
- ¹⁰⁴Department of Physics, McGill University, Montreal QC; Canada.
- ¹⁰⁵School of Physics, University of Melbourne, Victoria; Australia.
- ¹⁰⁶Department of Physics, University of Michigan, Ann Arbor MI; United States of America.
- ¹⁰⁷Department of Physics and Astronomy, Michigan State University, East Lansing MI; United States of America.
- ¹⁰⁸B.I. Stepanov Institute of Physics, National Academy of Sciences of Belarus, Minsk; Belarus.
- ¹⁰⁹Research Institute for Nuclear Problems of Byelorussian State University, Minsk; Belarus.
- ¹¹⁰Group of Particle Physics, University of Montreal, Montreal QC; Canada.
- ¹¹¹P.N. Lebedev Physical Institute of the Russian Academy of Sciences, Moscow; Russia.
- ¹¹²National Research Nuclear University MEPhI, Moscow; Russia.
- ¹¹³D.V. Skobeltsyn Institute of Nuclear Physics, M.V. Lomonosov Moscow State University, Moscow; Russia.
- ¹¹⁴Fakultät für Physik, Ludwig-Maximilians-Universität München, München; Germany.
- ¹¹⁵Max-Planck-Institut für Physik (Werner-Heisenberg-Institut), München; Germany.
- ¹¹⁶Nagasaki Institute of Applied Science, Nagasaki; Japan.
- ¹¹⁷Graduate School of Science and Kobayashi-Maskawa Institute, Nagoya University, Nagoya; Japan.
- ¹¹⁸Department of Physics and Astronomy, University of New Mexico, Albuquerque NM; United States of America.
- ¹¹⁹Institute for Mathematics, Astrophysics and Particle Physics, Radboud University Nijmegen/Nikhef, Nijmegen; Netherlands.
- ¹²⁰Nikhef National Institute for Subatomic Physics and University of Amsterdam, Amsterdam; Netherlands.
- ¹²¹Department of Physics, Northern Illinois University, DeKalb IL; United States of America.
- ¹²²(^a)Budker Institute of Nuclear Physics and NSU, SB RAS, Novosibirsk; (^b)Novosibirsk State University Novosibirsk; Russia.
- ¹²³Institute for High Energy Physics of the National Research Centre Kurchatov Institute, Protvino; Russia.
- ¹²⁴Institute for Theoretical and Experimental Physics named by A.I. Alikhanov of National Research Centre "Kurchatov Institute", Moscow; Russia.
- ¹²⁵Department of Physics, New York University, New York NY; United States of America.
- ¹²⁶Ochanomizu University, Otsuka, Bunkyo-ku, Tokyo; Japan.
- ¹²⁷Ohio State University, Columbus OH; United States of America.
- ¹²⁸Faculty of Science, Okayama University, Okayama; Japan.
- ¹²⁹Homer L. Dodge Department of Physics and Astronomy, University of Oklahoma, Norman OK; United States of America.
- ¹³⁰Department of Physics, Oklahoma State University, Stillwater OK; United States of America.
- ¹³¹Palacký University, RCPTM, Joint Laboratory of Optics, Olomouc; Czech Republic.
- ¹³²Institute for Fundamental Science, University of Oregon, Eugene, OR; United States of America.
- ¹³³Graduate School of Science, Osaka University, Osaka; Japan.
- ¹³⁴Department of Physics, University of Oslo, Oslo; Norway.
- ¹³⁵Department of Physics, Oxford University, Oxford; United Kingdom.
- ¹³⁶LPNHE, Sorbonne Université, Université de Paris, CNRS/IN2P3, Paris; France.
- ¹³⁷Department of Physics, University of Pennsylvania, Philadelphia PA; United States of America.
- ¹³⁸Konstantinov Nuclear Physics Institute of National Research Centre "Kurchatov Institute", PNPI, St. Petersburg; Russia.
- ¹³⁹Department of Physics and Astronomy, University of Pittsburgh, Pittsburgh PA; United States of

America.

¹⁴⁰(^a)Laboratório de Instrumentação e Física Experimental de Partículas - LIP, Lisboa;(^b)Departamento de Física, Faculdade de Ciências, Universidade de Lisboa, Lisboa;(^c)Departamento de Física, Universidade de Coimbra, Coimbra;(^d)Centro de Física Nuclear da Universidade de Lisboa, Lisboa;(^e)Departamento de Física, Universidade do Minho, Braga;(^f)Departamento de Física Teórica y del Cosmos, Universidad de Granada, Granada (Spain);(^g)Dep Física and CEFITEC of Faculdade de Ciências e Tecnologia, Universidade Nova de Lisboa, Caparica;(^h)Instituto Superior Técnico, Universidade de Lisboa, Lisboa; Portugal.

¹⁴¹Institute of Physics of the Czech Academy of Sciences, Prague; Czech Republic.

¹⁴²Czech Technical University in Prague, Prague; Czech Republic.

¹⁴³Charles University, Faculty of Mathematics and Physics, Prague; Czech Republic.

¹⁴⁴Particle Physics Department, Rutherford Appleton Laboratory, Didcot; United Kingdom.

¹⁴⁵IRFU, CEA, Université Paris-Saclay, Gif-sur-Yvette; France.

¹⁴⁶Santa Cruz Institute for Particle Physics, University of California Santa Cruz, Santa Cruz CA; United States of America.

¹⁴⁷(^a)Departamento de Física, Pontificia Universidad Católica de Chile, Santiago;(^b)Universidad Andres Bello, Department of Physics, Santiago;(^c)Instituto de Alta Investigación, Universidad de Tarapacá;(^d)Departamento de Física, Universidad Técnica Federico Santa María, Valparaíso; Chile.

¹⁴⁸Department of Physics, University of Washington, Seattle WA; United States of America.

¹⁴⁹Department of Physics and Astronomy, University of Sheffield, Sheffield; United Kingdom.

¹⁵⁰Department of Physics, Shinshu University, Nagano; Japan.

¹⁵¹Department Physik, Universität Siegen, Siegen; Germany.

¹⁵²Department of Physics, Simon Fraser University, Burnaby BC; Canada.

¹⁵³SLAC National Accelerator Laboratory, Stanford CA; United States of America.

¹⁵⁴Physics Department, Royal Institute of Technology, Stockholm; Sweden.

¹⁵⁵Departments of Physics and Astronomy, Stony Brook University, Stony Brook NY; United States of America.

¹⁵⁶Department of Physics and Astronomy, University of Sussex, Brighton; United Kingdom.

¹⁵⁷School of Physics, University of Sydney, Sydney; Australia.

¹⁵⁸Institute of Physics, Academia Sinica, Taipei; Taiwan.

¹⁵⁹(^a)E. Andronikashvili Institute of Physics, Iv. Javakhishvili Tbilisi State University, Tbilisi;(^b)High Energy Physics Institute, Tbilisi State University, Tbilisi; Georgia.

¹⁶⁰Department of Physics, Technion, Israel Institute of Technology, Haifa; Israel.

¹⁶¹Raymond and Beverly Sackler School of Physics and Astronomy, Tel Aviv University, Tel Aviv; Israel.

¹⁶²Department of Physics, Aristotle University of Thessaloniki, Thessaloniki; Greece.

¹⁶³International Center for Elementary Particle Physics and Department of Physics, University of Tokyo, Tokyo; Japan.

¹⁶⁴Graduate School of Science and Technology, Tokyo Metropolitan University, Tokyo; Japan.

¹⁶⁵Department of Physics, Tokyo Institute of Technology, Tokyo; Japan.

¹⁶⁶Tomsk State University, Tomsk; Russia.

¹⁶⁷Department of Physics, University of Toronto, Toronto ON; Canada.

¹⁶⁸(^a)TRIUMF, Vancouver BC;(^b)Department of Physics and Astronomy, York University, Toronto ON; Canada.

¹⁶⁹Division of Physics and Tomonaga Center for the History of the Universe, Faculty of Pure and Applied Sciences, University of Tsukuba, Tsukuba; Japan.

¹⁷⁰Department of Physics and Astronomy, Tufts University, Medford MA; United States of America.

¹⁷¹Department of Physics and Astronomy, University of California Irvine, Irvine CA; United States of

America.

¹⁷²Department of Physics and Astronomy, University of Uppsala, Uppsala; Sweden.

¹⁷³Department of Physics, University of Illinois, Urbana IL; United States of America.

¹⁷⁴Instituto de Física Corpuscular (IFIC), Centro Mixto Universidad de Valencia - CSIC, Valencia; Spain.

¹⁷⁵Department of Physics, University of British Columbia, Vancouver BC; Canada.

¹⁷⁶Department of Physics and Astronomy, University of Victoria, Victoria BC; Canada.

¹⁷⁷Fakultät für Physik und Astronomie, Julius-Maximilians-Universität Würzburg, Würzburg; Germany.

¹⁷⁸Department of Physics, University of Warwick, Coventry; United Kingdom.

¹⁷⁹Waseda University, Tokyo; Japan.

¹⁸⁰Department of Particle Physics, Weizmann Institute of Science, Rehovot; Israel.

¹⁸¹Department of Physics, University of Wisconsin, Madison WI; United States of America.

¹⁸²Fakultät für Mathematik und Naturwissenschaften, Fachgruppe Physik, Bergische Universität Wuppertal, Wuppertal; Germany.

¹⁸³Department of Physics, Yale University, New Haven CT; United States of America.

¹⁸⁴Yerevan Physics Institute, Yerevan; Armenia.

^a Also at Borough of Manhattan Community College, City University of New York, New York NY; United States of America.

^b Also at CERN, Geneva; Switzerland.

^c Also at CPPM, Aix-Marseille Université, CNRS/IN2P3, Marseille; France.

^d Also at Département de Physique Nucléaire et Corpusculaire, Université de Genève, Genève; Switzerland.

^e Also at Departament de Fisica de la Universitat Autònoma de Barcelona, Barcelona; Spain.

^f Also at Departamento de Física, Instituto Superior Técnico, Universidade de Lisboa, Lisboa; Portugal.

^g Also at Department of Applied Physics and Astronomy, University of Sharjah, Sharjah; United Arab Emirates.

^h Also at Department of Financial and Management Engineering, University of the Aegean, Chios; Greece.

ⁱ Also at Department of Physics and Astronomy, Michigan State University, East Lansing MI; United States of America.

^j Also at Department of Physics and Astronomy, University of Louisville, Louisville, KY; United States of America.

^k Also at Department of Physics, Ben Gurion University of the Negev, Beer Sheva; Israel.

^l Also at Department of Physics, California State University, East Bay; United States of America.

^m Also at Department of Physics, California State University, Fresno; United States of America.

ⁿ Also at Department of Physics, California State University, Sacramento; United States of America.

^o Also at Department of Physics, King's College London, London; United Kingdom.

^p Also at Department of Physics, St. Petersburg State Polytechnical University, St. Petersburg; Russia.

^q Also at Department of Physics, Stanford University, Stanford CA; United States of America.

^r Also at Department of Physics, University of Adelaide, Adelaide; Australia.

^s Also at Department of Physics, University of Fribourg, Fribourg; Switzerland.

^t Also at Department of Physics, University of Michigan, Ann Arbor MI; United States of America.

^u Also at Dipartimento di Matematica, Informatica e Fisica, Università di Udine, Udine; Italy.

^v Also at Faculty of Physics, M.V. Lomonosov Moscow State University, Moscow; Russia.

^w Also at Giresun University, Faculty of Engineering, Giresun; Turkey.

^x Also at Graduate School of Science, Osaka University, Osaka; Japan.

^y Also at Hellenic Open University, Patras; Greece.

^z Also at IJCLab, Université Paris-Saclay, CNRS/IN2P3, 91405, Orsay; France.

^{aa} Also at Institutio Catalana de Recerca i Estudis Avancats, ICREA, Barcelona; Spain.

- ab* Also at Institut für Experimentalphysik, Universität Hamburg, Hamburg; Germany.
- ac* Also at Institute for Mathematics, Astrophysics and Particle Physics, Radboud University Nijmegen/Nikhef, Nijmegen; Netherlands.
- ad* Also at Institute for Nuclear Research and Nuclear Energy (INRNE) of the Bulgarian Academy of Sciences, Sofia; Bulgaria.
- ae* Also at Institute for Particle and Nuclear Physics, Wigner Research Centre for Physics, Budapest; Hungary.
- af* Also at Institute of Particle Physics (IPP), Vancouver; Canada.
- ag* Also at Institute of Physics, Academia Sinica, Taipei; Taiwan.
- ah* Also at Institute of Physics, Azerbaijan Academy of Sciences, Baku; Azerbaijan.
- ai* Also at Institute of Theoretical Physics, Ilia State University, Tbilisi; Georgia.
- aj* Also at Instituto de Fisica Teorica, IFT-UAM/CSIC, Madrid; Spain.
- ak* Also at Joint Institute for Nuclear Research, Dubna; Russia.
- al* Also at Louisiana Tech University, Ruston LA; United States of America.
- am* Also at LPNHE, Sorbonne Université, Université de Paris, CNRS/IN2P3, Paris; France.
- an* Also at Manhattan College, New York NY; United States of America.
- ao* Also at Moscow Institute of Physics and Technology State University, Dolgoprudny; Russia.
- ap* Also at National Research Nuclear University MEPhI, Moscow; Russia.
- aq* Also at Physics Department, An-Najah National University, Nablus; Palestine.
- ar* Also at Physics Dept, University of South Africa, Pretoria; South Africa.
- as* Also at Physikalisches Institut, Albert-Ludwigs-Universität Freiburg, Freiburg; Germany.
- at* Also at School of Physics, Sun Yat-sen University, Guangzhou; China.
- au* Also at The City College of New York, New York NY; United States of America.
- av* Also at The Collaborative Innovation Center of Quantum Matter (CICQM), Beijing; China.
- aw* Also at TRIUMF, Vancouver BC; Canada.
- ax* Also at Universita di Napoli Parthenope, Napoli; Italy.

* Deceased